

# CHAPTER 9

---

## Ultraviolet Radiation at the Earth's Surface

**Lead Authors:**

J.R. Herman  
R.L. McKenzie

**Coauthors:**

S.B. Diaz  
J.B. Kerr  
S. Madronich  
G. Seckmeyer

**Contributors:**

G. Bernhard  
M. Blumthaler  
B. Bodhaine  
C.R. Booth  
E. Celarier  
P. Forster  
N. Krotkov  
J. Lenoble  
K. Leszczynski  
C.S. Long  
B. Mayer  
F. Mims  
P. Neale  
R. Piacentini  
K. Ryan  
H. Slaper  
J. Slusser  
R. Wooldridge  
C.S. Zerefos

# CHAPTER 9

## ULTRAVIOLET RADIATION AT THE EARTH'S SURFACE

### Contents

SCIENTIFIC SUMMARY .....	9.1
9.1 INTRODUCTION .....	9.3
9.2 GROUND-BASED OBSERVATIONS OF UV .....	9.3
9.2.1 Broadband and Multi-Channel Filter Instruments .....	9.3
9.2.2 Spectroradiometers .....	9.4
9.2.3 Instrument Deployment and Data Archival .....	9.4
9.2.4 Relationship between Ozone and UV .....	9.6
9.2.5 Instrument Calibration and Measurement Uncertainties .....	9.8
9.2.5.1 Radiometric Calibration .....	9.9
9.2.5.2 Stray-Light Rejection .....	9.9
9.2.5.3 Spectral Response .....	9.9
9.2.5.4 Cosine Response .....	9.10
9.2.5.5 Wavelength Calibration .....	9.10
9.2.6 Instrument Intercomparisons .....	9.11
9.2.7 UV-Irradiance Trends from Ground-Based Measurements .....	9.12
9.3 SATELLITE ESTIMATIONS OF UV IRRADIANCE .....	9.17
9.3.1 Extraterrestrial UV Irradiance .....	9.18
9.3.2 UV Irradiance at the Earth's Surface .....	9.18
9.3.3 UV Extinction by Aerosols .....	9.21
9.3.4 Trends in UV Irradiance .....	9.23
9.3.5 Other Methods of Inferring Historical UV Irradiances .....	9.24
9.4 UV IRRADIANCE VARIABILITIES NOT RELATED TO TRENDS IN STRATOSPHERIC OZONE .....	9.24
9.4.1 Ozone and Other Trace Gases .....	9.25
9.4.2 Clouds .....	9.25
9.4.3 Altitude .....	9.26
9.4.4 Aerosols .....	9.27
9.4.5 Surface Albedo Variations (Snow) .....	9.28
9.5 GEOGRAPHIC DIFFERENCES IN UV IRRADIANCES .....	9.29
9.5.1 Mid and Low Latitude .....	9.29
9.5.2 High Latitude (North and South) .....	9.31
9.5.3 Antarctica .....	9.31
9.6 COMPARISON OF CALCULATIONS WITH OBSERVATIONS .....	9.32
9.6.1 Intercomparison of Radiative Transfer Models .....	9.32
9.6.2 Clear-Sky Comparisons with Observations .....	9.33
9.6.3 General Comparisons with Observations .....	9.34
9.7 LOCAL PREDICTABILITY AND FORECASTING .....	9.35

REFERENCES .....	9.36
APPENDIX: INTERNET ADDRESSES FOR UV SITES .....	9.45
Internet Sites with General UV Information .....	9.45
Internet Sites with UV Index Information .....	9.45
Internet Sites with UV Information, by Country .....	9.46
Internet Sites for International UV Projects .....	9.46

## SCIENTIFIC SUMMARY

The advances and new findings that have occurred in the ultraviolet (UV) radiation field since the publication of the previous Assessment (WMO, 1995) include the following:

- The inverse relationship between decreasing ozone amount and increasing UV-B radiation has been reconfirmed and firmly established in both theory and measurements. The measured effects of ozone, albedo, altitude, clouds and aerosols, and geographic differences are much better understood.
- The number, distribution, and quality of UV-irradiance (energy per unit area per unit time) instruments have greatly improved throughout the world. However, there are still regions of sparse coverage.
- Well-calibrated UV-irradiance spectral time series are now available at some ground sites for periods of up to 9 years, where changes in UV-B irradiance have been detected (e.g., 1.5% per year at 300 nm, 0.8% per year at 305 nm) at midlatitudes (near 40°) that are consistent with expected changes from the decreasing amounts of ozone. However, the long-term stability needed for trend estimates has been demonstrated for only a few ground-based UV instruments. Either the records are not long enough or the instrument stability is insufficient to reliably determine decadal change at most midlatitude sites. Other factors limiting the detection of long-term trends are that clouds, albedo, aerosols, and short-term ozone changes produce local daily, monthly, and interannual changes that are larger than the long-term trend. It is important for long-term trend detection that both UV-A and UV-B be measured separately along with ancillary data (e.g., ozone and aerosols).
- The anomalous UV-trend estimates from the Robertson-Berger (RB) meter network located in the United States are now understood. Corrections have been applied to the data, which now show no significant trends for the latitude range of the instruments' locations. It was concluded that the data from the U.S. RB network alone are unsuitable for trend detection.
- Increases in UV-B irradiance in the Northern Hemisphere at high latitudes have been attributed to the low ozone amounts in the winter and spring of 1995, 1996, and 1997.
- New types of filter instruments have been developed, using narrower band pass at a few selected wavelengths and greater filter stability specifications than previous broadband instruments. These simpler instruments may yield results with accuracy comparable to that of grating spectroradiometers (5 to 10%) and should permit a wider geographical distribution of measuring sites for UV irradiance. This is especially important to address the lack of sufficient observing sites in some regions.
- New satellite estimates of global (latitude  $\pm 65^\circ$ ) UV irradiance, which now include cloud, surface albedo, and aerosol effects, are available using radiative transfer models and measured radiances from Total Ozone Mapping Spectrometer (TOMS) instruments. The satellite-estimated UV irradiances have been compared with ground-based measurements at a single site, Toronto. The weekly-average results agree to within 5% for snow-free conditions. Further comparisons at other sites are necessary to validate the accuracy and applicability of the techniques over a wide range of observing conditions. This may be especially important when accounting for local aerosol extinctions.
- TOMS satellite data have been used to estimate long-term decadal changes in zonally averaged global and seasonal patterns in UV irradiance from 1979 to 1992. The results showed that the UV-B irradiances increased (see table below), while UV-A irradiances remained unchanged. At individual sites, changes in UV-A irradiances have occurred because of changes in local cloudiness and aerosol amounts.

## SURFACE ULTRAVIOLET RADIATION

### Zonal Average UV-Erythemal Trends (Percent Increase per Decade) 1979 to 1992.

Latitude	January	April	July	October	Annual $\pm 2\sigma$
50° to 65°N	6	4	2	4	3.7 $\pm$ 3
35° to 50°N	3	3	2	2	3 $\pm$ 2.8
30°S to 30°N	0	0	0	0	0 $\pm$ 2
35° to 50°S	4	2	2	6	3.6 $\pm$ 2
50° to 65°S	4	5	8	14	9 $\pm$ 6

- Zonally averaged UV-irradiance trend determinations from satellite data that include cloud effects yield numbers nearly identical to those from clear-sky estimates. However, the currently estimated UV trends are slightly lower than the clear-sky values in the 1994 Assessment because of the new TOMS ozone algorithm (see Chapter 4).
- Measurements at several ground sites have indicated differences between UV irradiances in the Northern and Southern Hemispheres that are larger than explained by the known differences in ozone amount and Sun-Earth separation. This may indicate that other factors such as aerosols could be involved. Satellite estimates show smaller irradiance differences between the hemispheres than do ground-based measurements.
- Several intercomparisons of UV-irradiance instruments of different types have been conducted in various countries. These have helped identify instrument capabilities and limitations. Currently, the best intercomparisons of different instruments at the same location are within  $\pm 5\%$  absolute accuracy. However, this “best” accuracy estimate does not represent the general level of agreement between geographically distributed networks of similar and different instruments over extended periods of time. Significant improvements have been made to reduce errors in the cosine response, stray light rejection, and wavelength alignment.
- Expansion of the World Ozone and Ultraviolet Radiation Data Centre (WOUDC) in Canada and the European database, Scientific UV Data Management/UV Radiation in the Arctic; Past, Present, and Future (SUVDAMA/UVRAPPF), has significantly improved the availability and distribution of data to researchers studying the effects and behavior of UV-B radiation. Extensive sources of UV information have become available on the Internet.
- Significant improvements have been made in calibration of ground-based instruments. This has been achieved through instrument intercomparisons and the use of newly developed central calibration facilities, although additional calibration facilities would continue to meet needs. After validation, satellite estimations of UV irradiance may serve as a comparison standard between widely separated ground-based instruments in a manner similar to that used for the ground-based ozone network.
- Different classes of radiative transfer models have been intercompared and found to agree within 1% for irradiances. However, for some radiative transfer approximations (e.g., delta-Eddington) the gains in computational speed are offset by losses in accuracy. Two-stream models have accuracies on the order of 5% for moderate optical depths and can have errors exceeding 10% for large optical depths (small irradiances).
- Public interest related to UV exposure has been addressed by establishing a standardized UV index in many countries, based on estimates of ozone and, in some cases, cloud cover and surface albedo, to provide daily information about the intensity of UV radiation.

## 9.1 INTRODUCTION

The ultraviolet (UV) region (200-400 nm) of the solar radiation spectrum accounts for a small fraction of the total radiant energy that reaches the Earth's surface. Wavelengths shorter than 280 nm (UV-C) are important for atmospheric photochemistry, but they are completely absorbed in the atmosphere by ozone (O<sub>3</sub>), molecular oxygen (O<sub>2</sub>), and other minor atmospheric species, and do not reach the ground. The remaining UV spectral region is arbitrarily subdivided into two subregions: UV-B and UV-A. The UV-B component (280-315 nm) is of particular interest because it is strongly absorbed by ozone, and it increases when the atmospheric ozone amount decreases. This spectral region has significant impact on important biomolecules, such as deoxyribonucleic acid (DNA) and proteins, and therefore, on living organisms. The UV-A region (315-400 nm) is largely unaffected by ozone. Although the photons are somewhat less energetic than those in the UV-B range, they still have important biological effects (e.g., sunburn). Both UV-A and UV-B radiation have important impacts on various materials and chemical processes on the Earth's surface and in the atmosphere. Although the internationally agreed boundary between the UV-A and UV-B is at 315 nm, some authors whose work is cited in this document prefer to use a boundary at 320 nm, because there is still significant ozone absorption between 315 and 320 nm.

Since the last evaluation, there has been extensive publication of new results in the field of UV research. More emphasis has been put into ground-based spectral measurements, satellite-derived estimates (combining backscattered radiance data and a radiative transfer model) of UV-irradiance (energy per unit area per unit time) reaching the Earth's surface, and radiative transfer studies.

This chapter reviews progress made since the previous Assessment (WMO, 1995, Chapter 9) in our understanding of UV radiation that reaches the Earth's surface. In addition, this review identifies some of the most important outstanding problems in the quantitative determination of UV irradiances. The impacts of UV irradiance increases (e.g., effects on the biosphere, including human health and materials) are outside the scope of this report and are discussed in the United Nations Environment Programme (UNEP) "Effects Panel" reports (UNEP 1991, 1994, 1998). Impacts on

tropospheric chemistry that may result from changes in UV radiation fields are discussed in Chapter 10 of this report and are also found in UNEP (1998); predicted effects of future changes in UV are discussed in Chapter 11 (UNEP, 1998).

## 9.2 GROUND-BASED OBSERVATIONS OF UV

The majority of UV-A and UV-B instruments fall into the following classes:

1. broadband radiometers (e.g., to match the erythema, or "sunburning," action spectrum (McKinlay and Diffey, 1987)),
2. multi-channel medium-spectral-resolution (2-10 nm resolution) instruments, or
3. high-resolution spectrometers (0.5-1 nm resolution).

The multi-channel instruments sample irradiance at a number of fixed wavelength bands determined by the transmission of individual filters. The spectrometers usually sample at a uniform wavelength interval comparable with or smaller than their resolution (typically 0.5 nm or better). Most UV-A and UV-B instruments are designed to measure the amount of radiation falling on a horizontal surface (direct plus diffuse irradiance, known as global irradiance).

In recent years there have been developments in new types of instrumentation to measure actinic UV radiation (multi-directional radiances), rather than downwelling irradiance alone (e.g., McElroy, 1995; Shetter and Müller, 1998). Such measurements are useful in studies of atmospheric photochemical processes.

### 9.2.1 Broadband and Multi-Channel Filter Instruments

Broadband radiometers have provided an important source of UV-irradiance information over wide geographic areas and over long time periods. Compared with multi-channel spectroradiometers, their low cost and rapidity of measurement make them very attractive for monitoring UV irradiances. Considerable efforts in quality control and assurance are required to produce scientifically useful information. Changes in their spectral response or sensitivity can lead to errors that are difficult to detect. Multi-channel filter instruments have an advantage in making nearly simultaneous measurements at many wavelengths, compared with

## SURFACE ULTRAVIOLET RADIATION

grating spectroradiometers, which typically require several minutes to complete a wavelength scan. Simultaneous wavelength measurements are useful for separating cloud and aerosol effects from ozone effects.

There has been continuing strong interest in the historical record for broadband instruments, particularly in the much-discussed work of Scotto *et al.* (1988), which showed a decline in annually integrated UV irradiance measured by eight Robertson-Berger (RB) meters in the continental United States between 1974 and 1985. The average trend based on the eight stations was -0.7% per year, while the statistically significant values for individual stations varied from -0.5 to -1.0% per year. DeLuisi and Barnett (1992) uncovered a potential shift in calibration of the RB-meter network in 1980 that could remove the downward trend found by Scotto *et al.* (1988). A reanalysis of the RB-meter data (Weatherhead *et al.*, 1997), with an extension through 1991 but without including a term in the time series analysis to account for “mean level shifts,” showed a UV-irradiance decrease of 0.6% per year, in agreement with the original work by Scotto *et al.* (1988). However, when corrections are made for mean level shifts, which may be due to calibration changes and other instrument-related problems, the resulting overall trend is found by Weatherhead *et al.* to be +0.2% per year (not statistically significant). In many cases Weatherhead *et al.* found that the adjustments to the instruments were not traceable to physical causes in the log records. This makes the use of the U.S. RB-meter network unsuitable for detecting long-term trends. The small rate of increase is also in agreement with recent analysis of UV-irradiance trends estimated from Total Ozone Mapping Spectrometer (TOMS) satellite data (J.R. Herman *et al.*, 1996) for the same geographical region.

### 9.2.2 Spectroradiometers

Spectroradiometers consist of medium- and high-spectral-resolution filter and grating instruments. These cover the entire UV-A and UV-B range of wavelengths with the purpose of both measuring the amount of UV irradiance and determining the atmospheric processes that contribute to UV-irradiance attenuation (e.g., ozone, sulfur dioxide (SO<sub>2</sub>), aerosols) and variability (e.g., ozone, clouds). Their increased cost and maintenance are offset by the increase of spectral detail available, their ability to independently determine ozone and aerosol amounts, and their ability to estimate the extraterres-

trial UV flux. Changes in ozone amount produce a clear spectral signature that is quite different from UV-irradiance changes produced by aerosols, clouds, and surface reflectivity. Unlike broadband instruments, spectroradiometers can separate ozone effects from the variability produced by clouds by using the longer UV-A wavelengths that are not absorbed by ozone.

The number and quality of spectroradiometers used for studies of UV radiation at the surface have improved significantly since the last Assessment. Generally, the time period of observations is still too short to determine UV-irradiance trends unambiguously with these instruments. However, they have been used to demonstrate the spectrally resolved effects of changes in ozone amount, cloud cover, surface albedo, and observing altitude.

### 9.2.3 Instrument Deployment and Data Archival

Although there has been a significant increase in the number of instruments deployed and in the effort to calibrate these instruments, many problems remain. The addition of several calibration facilities or regional instrumental quality assurance centers should help to reduce the problems in future years. Examples are the National Oceanic and Atmospheric Administration (NOAA) calibration facilities in Boulder, Colorado, to calibrate broadband and spectral instruments; the Atmospheric Environment Service, Toronto, of Environment Canada; the Radiation and Nuclear Safety Authority, Helsinki, Finland (STUK); and the German reference instrument center in Garmisch-Partenkirchen.

Assessing the impact of ultraviolet radiation on biological processes requires accurate and sustained monitoring of UV irradiances over the entire globe from both ground (e.g., Kerr and McElroy, 1993) and satellite instruments (J.R. Herman *et al.*, 1996), if short-term changes or coincidental biological phenomena are to be distinguished from those caused by long-term UV-irradiance changes. The ground-based instruments are necessary to understand the effects of clouds, aerosols, and local terrain on UV radiation reaching the ground, whereas only the satellite estimation of UV radiation can give the global and regional perspective necessary for understanding the overall effects of UV radiation at the Earth's surface.

Many parts of the world now maintain large networks of ground-based UV-irradiance instruments of

## WMO Coordinated UV Monitoring

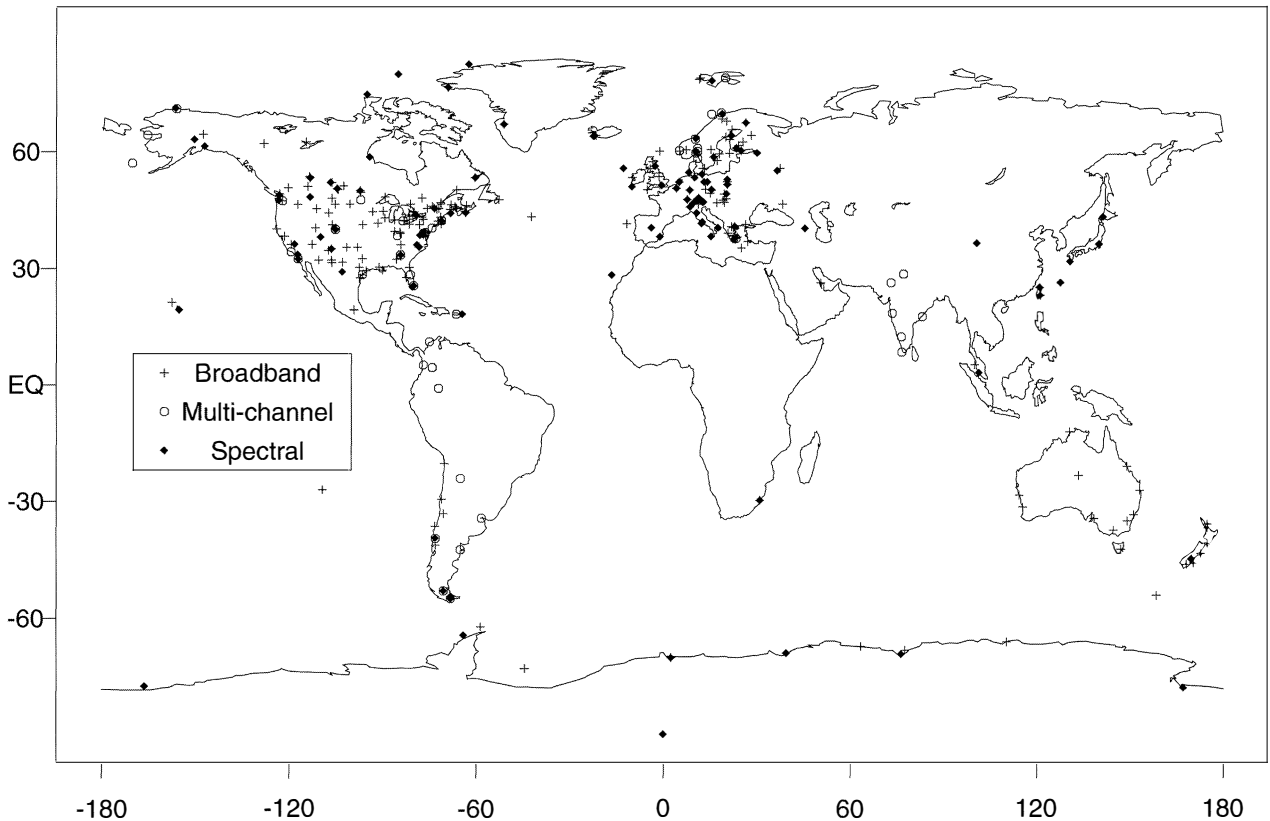


**Figure 9-1.** Map showing the global distribution of surface-based instruments monitoring UV radiation. (Updated from Weatherhead and Webb, 1997.)

various types. Most prominent among these are the networks operating in Canada, the United States, Japan, and Europe. For the Southern Hemisphere, one important installation is in Lauder, New Zealand. In South America and the Antarctic Peninsula, several new UV-irradiance instruments have been installed and are collecting data. In this network project, involving scientists from Chile, Argentina, and various other countries, the disparate networks are brought together within a centralized data processing and quality control facility in Ushuaia, Argentina. This South American network is based on a model of the U.S. network, where a collection of smaller UV-irradiance networks (e.g., the U.S. Department of Agriculture (USDA), U.S. National Science Foundation (NSF), U.S. Environmental Protection Agency (EPA), U.S. National Oceanic and Atmospheric Administration (NOAA), and universities), comprised of different

instruments, is linked by standardized protocols, inter-comparisons, and calibrations. A map of prominent ozone and UV monitoring sites is shown in Figure 9-1.

Progress has also been made in standardizing the archival of UV-irradiance data. The primary archive of spectral UV-irradiance data is at the World Ozone and Ultraviolet Radiation Data Centre (WOUDC) in Toronto (Wardle *et al.*, 1997). The WOUDC database consists of more than 600,000 spectra representing more than 120 station-years from 23 sites. There are plans to make the database available on compact disk-read only memory (CD-ROM) media. Other datasets are recently available from individual groups (e.g., Gardiner *et al.*, 1993; McKenzie *et al.*, 1993) and from the emerging European database, Scientific UV Data Management/UV Radiation in the Arctic: Past, Present, and Future (SUVDAMA/UVRAPPF). An additional repository of UV-irradiance

## SURFACE ULTRAVIOLET RADIATION

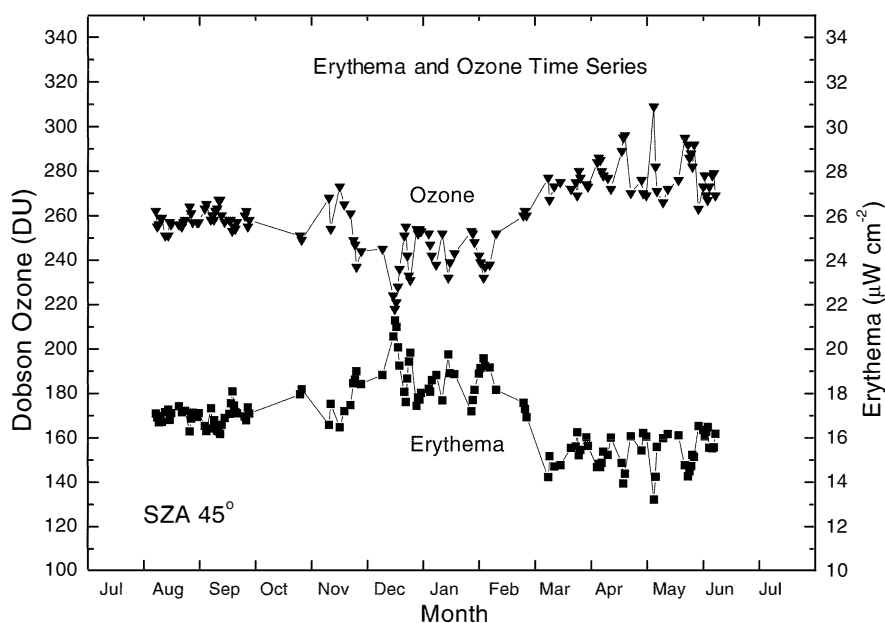


**Figure 9-2.** Measured erythemal irradiances (lower curve) from an ultraviolet spectroradiometer at SZA 45° compared with total ozone (upper curve) for 132 clear mornings during July 1995 to July 1996 at Mauna Loa Observatory (19.5°N, 155.6°W, 3.4 km), showing the inverse relationship between erythemal UV and ozone amount. (From Bodhaine *et al.*, 1997.)

data from 26 European stations has been established in the Finnish Meteorological Institute, Helsinki, Finland (Scientific Data Management, SUVDAMA/UVRAPPF), which is planned to have close links with WOUDC. Radiative transfer studies using the archived data have already provided experimental corroboration of the modeled relationship between ozone and UV irradiance (WMO, 1992, 1995).

Multi-year spectral and broadband data are also available from networks of instruments operated by the National Science Foundation on CD-ROM (Booth *et al.*, 1994), from the U.S. Department of Agriculture UV-B monitoring program operated by Colorado State University (Bigelow *et al.*, 1998), from the NOAA Integrated Surface Irradiance Study (Hicks *et al.*, 1996), and from several other groups (e.g., the Japan Meteorological Agency, the U.S. Environmental Protection Agency) (Gardiner *et al.*, 1993; McKenzie *et al.*, 1993; Kerr and McElroy, 1993; Ito *et al.*, 1994).

### 9.2.4 Relationship between Ozone and UV

There is excellent experimental evidence that UV-irradiance increases at the Earth's surface are directly

correlated with ozone decreases in the atmosphere (Kerr and McElroy, 1993; Madronich *et al.*, 1995; Varotsos and Kondratyev, 1995; Bodhaine *et al.*, 1996, 1997). The model-predicted effect of decreasing atmospheric ozone content on surface-UV irradiance has been confirmed by process studies from ground-based instrumentation (WMO, 1992, 1995).

The anticorrelation is most clearly seen when measurements are filtered to remove the effects of the meteorological factors discussed in Section 9.4. For example, measurements from the high-altitude Mauna Loa Observatory (MLO, 3.4 km), which is relatively cloud free and pollution free, show strong anticorrelations (see Figure 9-2) between ozone and erythemally weighted UV irradiance over a full year of measurements at fixed solar zenith angle (SZA) (Bodhaine *et al.*, 1996, 1997).

The same spectra have been used to calculate the wavelength-dependent sensitivity of UV to ozone changes. Figure 9-3 shows that the measured sensitivity increases strongly toward shorter wavelengths and demonstrates that a 1% reduction in ozone causes a 7% increase in UV irradiance at 295 nm (SZA = 45°, ozone = 265 Dobson units (DU)). The increasing sensitivity of

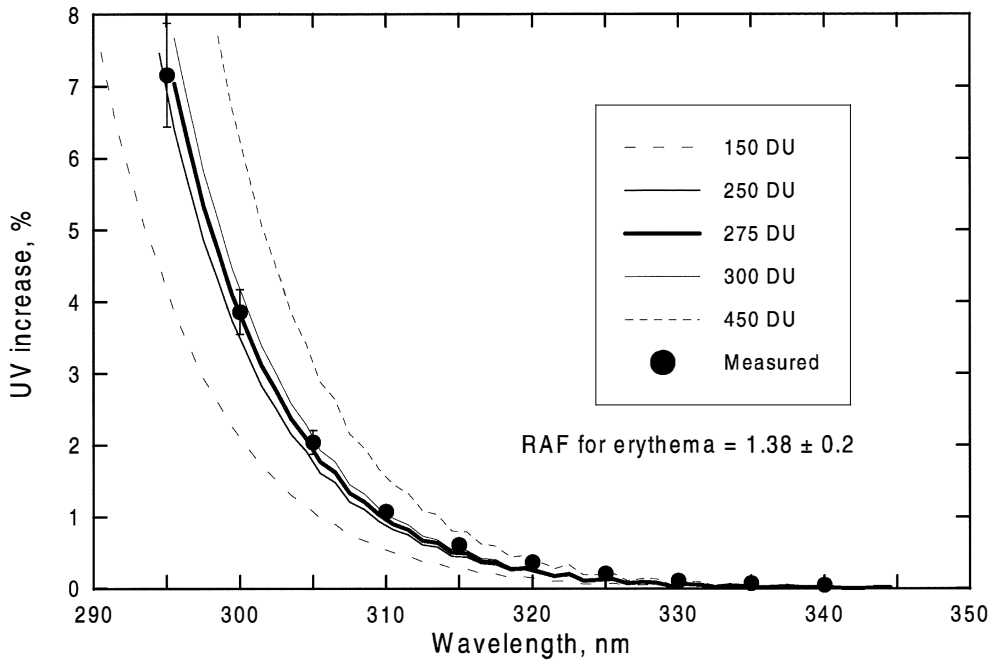


**Figure 9-3.** The measured wavelength-dependent sensitivity of UV to a 1% decrease in ozone at SZA 45° for 132 clear days during July 1995 to July 1996 at Mauna Loa Observatory. The curves show the calculated sensitivity for several assumed ozone amounts. (Based on Bodhaine *et al.*, 1997.)

UV irradiance for a given SZA to changes in ozone amount at shorter wavelengths is as predicted based on larger ozone absorption coefficients. The deduced radiation amplification factor (RAF) for erythema from this dataset is in agreement within the experimental uncertainty.

For most conditions, the RAF (see below) can be derived using Equations (9-1) and (9-2), without the need for a full radiative transfer calculation, from  $\alpha\Omega\sec(\theta)$ , where  $\theta = \text{SZA} < 50^\circ$  is the solar zenith angle:

$$\frac{dF}{F} \approx -\alpha\Omega \frac{d\Omega}{\Omega} \sec(\theta) \quad (9-1)$$

where  $\alpha$  is the ozone absorption coefficient;  $\Omega$  is the ozone column amount; and  $F$  is the irradiance.

The sensitivity of UV to small changes in ozone may be expressed as a radiation amplification factor, defined as

$$\text{RAF} \equiv -\frac{dF/F}{d\Omega/\Omega} \equiv \alpha\Omega \sec(\theta) \quad (9-2a)$$

Equation (9-2b) is a modified form of Equation (9-2a) that was proposed by Madronich (1994) as more suitable for estimating the RAF when the changes  $\Omega - \Omega^*$  and  $F - F^*$  are large (Madronich and deGruijl, 1994):

$$\text{RAF} = -\frac{\ln \frac{F^*}{F}}{\ln \frac{\Omega^*}{\Omega}} \quad (9-2b)$$

For many biologically weighted action spectra, the RAF is approximately constant over a wide range of ozone and SZA (Madronich *et al.*, 1995).

For larger SZA (greater than 50°) and high ozone amounts, deviations from Equation (9-2a) can occur because of the Umkehr effect (Mateer, 1965), which occurs when most of the direct solar UV radiation at high SZA (near the horizon) is absorbed by ozone along the large slant path to the observer’s site. In this case, the global radiation (scattered plus direct) consists of mainly diffuse radiation that scatters high in the atmosphere above the observer’s site. These scattered photons have a shorter optical path through the ozone than do the

## SURFACE ULTRAVIOLET RADIATION

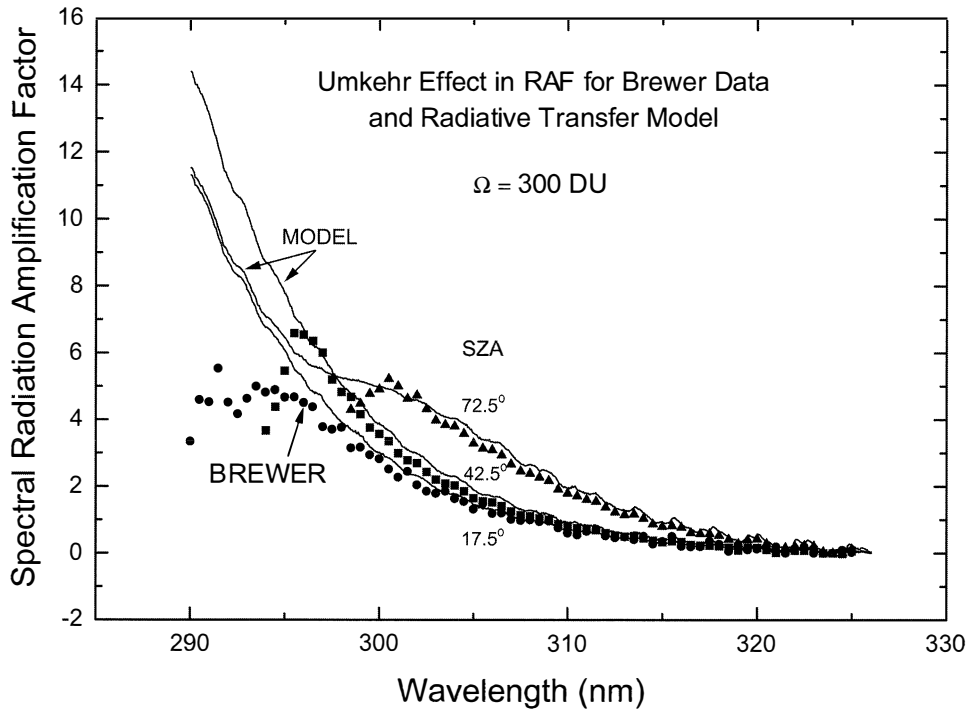


**Figure 9-4.** A comparison of the measured and calculated sensitivities to a 1% ozone reduction, for ozone amount = 300 DU. The model results (solid lines) show the onset of the Umkehr effect for solar zenith angle 72.5°. The measured values, obtained from a Brewer instrument (single monochromator), diverge from the model at shorter wavelengths. (From Fioletov *et al.*, 1997.)

photons in the direction of the direct beam, and therefore a reduced RAF compared with the prediction of Equation (9-2a) (Brühl and Crutzen, 1989). Under such conditions (see Figure 9-4), the sensitivity of UV to changes in ozone decreases toward shorter wavelengths, relative to predictions from Equation (9-2a) (Fioletov *et al.*, 1997). These conditions are usually unimportant from a biological point of view, because the irradiances are small compared to noon conditions (except in the polar spring and autumn).

An extensive analysis of UV-B irradiance and its dependence on total ozone is reported by Fioletov *et al.* (1997). About 300,000 spectra made by Brewer spectrophotometers at seven stations in Canada and Japan between 1989 and 1995 were used to establish a statistical relationship. Irradiance values at wavelengths between 300 and 325 nm were normalized to the value at 324 nm, where the effects of ozone absorption are nearly negligible. The dependence of these normalized spectra on SZA, and the nearly simultaneous measurements of total ozone, were determined for solar zenith angles

between 27.5° and 87.5°. The analysis provides an empirical wavelength-by-wavelength measure of the increase of UV-B irradiance for a 1% decrease of total ozone. These values were found to be essentially the same for clear and cloudy conditions (except for very heavy clouds) and are in good agreement with model results for longer wavelengths and moderate SZA (see Figure 9-4).

### 9.2.5 Instrument Calibration and Measurement Uncertainties

All types of UV-radiation instruments share some common problems related to the accuracy of the data obtained. Many of these are related to the steep slope of the irradiance spectrum in the UV-B region caused by the increasing ozone-absorption coefficient with decreasing wavelength (320 to 250 nm).

Other problems are related to the instrumentation. These include errors resulting from (1) calibration-lamp accuracy (radiometric calibration), (2) stray-light

problems, (3) slit-function or spectral-response characterization, (4) diffuser cosine corrections for irradiance instruments, and (5) wavelength calibration for spectroradiometers and narrowband filter instruments. These error sources are discussed in detail in the following subsections. The combined effect of these and other error sources leads to overall accuracies of  $\pm 5\%$  to  $\pm 15\%$ .

The requirements to achieve the necessary long-term repeatability have been considered by the Network for the Detection of Stratospheric Change (NDSC) as well as by the World Meteorological Organization (WMO) (e.g., McKenzie *et al.*, 1997b).

#### 9.2.5.1 RADIOMETRIC CALIBRATION

One source of uncertainty concerns tracing the absolute calibration to a common standard, such as maintained by the U.S. National Institute of Standards and Technology (NIST), the German Physikalisch Technische Bundesanstalt (PTB), and the British National Physical Laboratories (NPL). Standard lamps used by national standards laboratories can disagree by more than  $\pm 2\%$  in the UV-B region (Walker *et al.*, 1991). Also, there is evidence indicating that individual lamps behave differently with regard to stability, both in the short term (calibration to calibration) and long term (drift over several years).

One investigation into the use of the Langley method as an alternative to lamp calibrations has been conducted at two sites (Table Mountain, Colorado, and Mauna Loa, Hawaii) of the 25-site network of UV Multi-Filter Rotating Shadowband Radiometers (UV-MFRSRs, 2-nm spectral resolution, full-width half-maximum (FWHM)) by the USDA UV-B Monitoring Program (Bigelow *et al.*, 1998). Preliminary results of the application of this method (Bigelow *et al.*, 1998) show good agreement between radiative transfer estimates of the irradiances and measurements from the UV-MFRSR instruments, but disagreement with measurements made at Table Mountain with a Brewer spectroradiometer.

An alternative calibration approach is a variation of the Langley method (a method of measured radiances at different sun angles extrapolated to zero-air mass (Schmid and Wehrli, 1995)), which uses the measured extraterrestrial solar irradiance as an absolute reference (Wilson and Forgan, 1995; Schmid *et al.*, 1998). This

method has the potential to avoid problems of lamp variabilities, although it cannot be used for UV-B wavelengths at sites where diurnal variations of total ozone often occur (Kerr and McElroy, 1993; Kohler, 1986; Kerr, 1998) and at sites with changing aerosol conditions.

#### 9.2.5.2 STRAY-LIGHT REJECTION

Another consideration for UV measurements is the effect of stray light. It is often the case that stray light from wavelengths with a relatively high radiation amount adds significantly to the signal being registered at nearby wavelengths that are several orders of magnitude less. This is particularly important for wavelengths less than 305 nm, because the radiation at the ground increases by several orders of magnitude from 290 nm to 325 nm. The direct method to overcome this problem is to use double monochromators that typically have out-of-band contributions of about 1 part in  $10^6$  to  $10^8$  compared to 1 part in  $10^3$  to  $10^4$  for a single monochromator. The recent deployment of double-monochromator Brewer instruments to reduce stray-light problems has improved accuracy at short wavelengths compared to widely deployed single-monochromator versions (Bais *et al.*, 1996). However, it is possible to partially correct data from single-monochromator instruments, provided the details of the stray-light spectrum are known. Some of the data from single monochromators currently archived in the WOUDC (see Section 9.2.3) have had a stray-light correction applied. The use of band-pass filters with sharp wavelength cutoffs can improve the performance of single monochromators.

#### 9.2.5.3 SPECTRAL RESPONSE

An important part of the UV-irradiance calibration process is the accurate determination of the spectral response of an instrument. For a filter instrument (either broad or medium band), the combined spectral transmission of the filter and the spectral alignment of the sensor must be known. Accurate knowledge of the spectral response function is necessary for comparing with radiative transfer models and with other instruments. The filter transmission and sensor response can be measured either separately or together. The wavelength response of spectroradiometers is often determined by using spectral scans of lamps with emission lines at known wavelengths.

## SURFACE ULTRAVIOLET RADIATION

### 9.2.5.4 COSINE RESPONSE

In practice, it is difficult to make an instrument with a true cosine response. Uncorrected deviation of the angular response from the ideal cosine function is a significant source of uncertainty in UV spectroradiometry. For most instruments, the deviation from true cosine response increases with increasing angle from normal incidence, and falls below the true cosine response function (Seckmeyer and Bernhard, 1993; Ireland and Sacher, 1996; Bernhard and Seckmeyer, 1997). Many instruments tend to underestimate the UV irradiance incident on a horizontal surface usually by 6 to 10%, and sometimes by as much as 15% (Bernhard and Seckmeyer, 1997). The underestimate can cause errors in measurements of both the direct and diffuse components of the global UV irradiance, which are functions of the SZA. Knowledge of the departure from a true cosine function is necessary for comparing measurements with models and intercomparing different instruments.

New designs of entrance optics are now available that reduce the cosine response function error to less than 4% (Bernhard and Seckmeyer, 1997). Although correction algorithms for cosine response function can be used (WMO, 1995, Chapter 9) for cloudless skies, with possibilities for corrections with cloudy conditions, the new designs are major improvements especially for measurements with broken clouds. New algorithms for reducing the remaining cosine errors, after the entrance-optics corrections, have also been reported (Feister *et al.*, 1997).

### 9.2.5.5 WAVELENGTH CALIBRATION

Figure 9-5 shows the calculated wavelength sensitivity of the surface irradiance at different spectral resolutions (Krotkov *et al.*, 1998) simulating the measurements taken with instruments ranging from spectroradiometers (Brewer instrument, 0.5 nm) to filter instruments (5 nm). The sharp features of the solar Fraunhofer-line spectrum in the UV-B region (see Figure 9-10) pose specific instrumental problems that must be overcome to cope with the wide dynamic range, the need to align wavelengths accurately (McKenzie *et al.*, 1992; Webb *et al.*, 1994; Slaper *et al.*, 1995), and to know the slit function for each central wavelength. Particularly for those instruments with higher resolution, wavelength

alignment is critical because of the structure of the solar spectrum and the strong wavelength dependence of the ozone absorption cross section.

The result is that small errors in wavelength alignment can complicate intercomparisons between instruments. At high spectral resolution, errors of 5-10% are possible near solar Fraunhofer lines throughout the entire UV spectral region. At low resolution, the irradiance is still sensitive to wavelength shifts in the UV-B region, because of the sharp increase in ozone absorption. Integrating the measured irradiances from a high-resolution instrument over one of the broadband action spectra, or over any extended wavelength range of 5 nm or more, reduces the effect of the wavelength alignment error.

UV-B instruments that do not resolve solar Fraunhofer lines must have the wavelength-dependent response function of the instrument determined and maintained with high accuracy (e.g., about 0.01-nm accuracy at  $305 \pm 2.5$  nm, because a wavelength error of 0.1 nm can cause a 3% error in irradiance). For erythemally weighted UV, a wavelength error of 0.1 nm results in an error of approximately 2%. In addition to problems arising from solar-line structure, the ozone absorption coefficient is a rapidly decreasing function of wavelength in the UV-B range. Because of this, even a small drift in wavelength can mask the changes in UV irradiance caused by decreasing ozone amounts.

A simple method to improve the wavelength alignment for spectrometers has been demonstrated (Slaper *et al.*, 1995) using measured high-spectral-resolution extraterrestrial irradiances (see Section 9.3.1). The method is based on minimization of the sum over wavelengths of the squared deviation of the ratio of extraterrestrial irradiances to the wavelength-shifted irradiances. Because the method is independent of the atmospheric parameters and radiative transfer calculations, it can be used to directly compare measurements with different slit functions and wavelength-alignment errors. For example, with scanning spectroradiometers in field use, any nonlinearity in the wavelength drive can change with instrument wear. Errors greater than 0.1 nm can occur on some instruments, but some misalignments are only about 0.01 to 0.02 nm. Methods to recognize and correct for wavelength nonlinearities have also been developed using scans of mercury lamps (Liley and McKenzie, 1997).

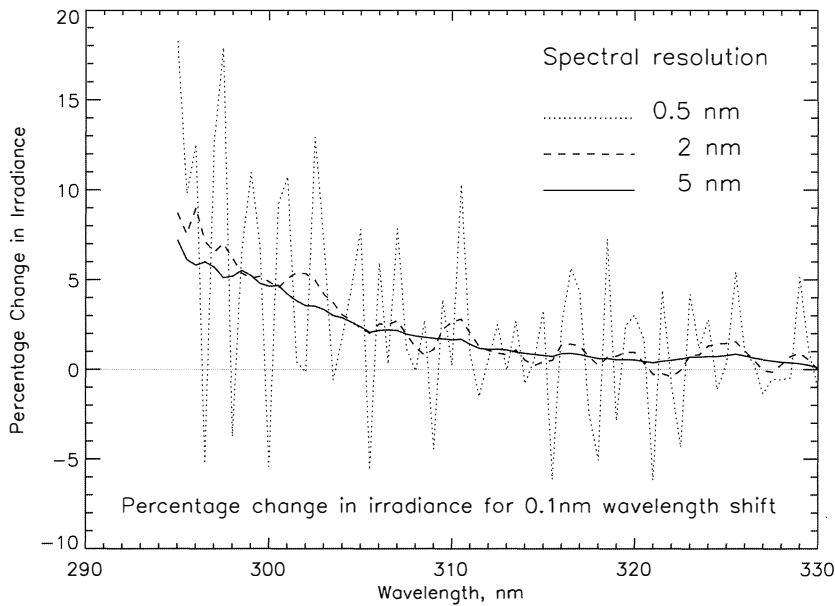


**Figure 9-5.** The UV-irradiance sensitivity to a wavelength shift of 0.1 nm at different spectral resolutions simulating measurements taken with instruments ranging from spectroradiometers (full width half maximum (FWHM) = 0.5 nm for Brewer instrument) to filter instruments (FWHM = 5 nm). (From Krotkov *et al.*, 1998.)

## 9.2.6 Instrument Intercomparisons

Field intercomparisons are important for assessing the quality of UV instruments and for assessing the expected instrumental variance for measured irradiances under identical conditions. The results can be used to suggest future improvements of their performance through investigation of the causes of the variances. Differences in the characteristics of the instruments require the development of techniques for the standardization of measured spectra, as well as for the assessment of intercomparison results (Slaper *et al.*, 1995; Webb, 1997). Even comparisons between instruments of the same type pose problems related to calibration and maintenance (Vaughan *et al.*, 1997). Since the previous Assessment (WMO, 1995) there have been several spectral instrument intercomparison campaigns in Europe (e.g., Seckmeyer *et al.*, 1994a; Koskela, 1994; Kjeldstad *et al.*, 1997) and North America (Thompson *et al.*, 1997). The results of these intercomparisons indicate that there has been continuous improvement in the agreement of absolute UV-irradiance measurements between the various instruments and instrument types. Instruments were characterized for wavelength accuracy, repeatability, bandwidth, and stray-light rejection, and were calibrated using common standard lamps for each campaign. Some of the discrepancies observed between the different groups have

been explained by differences in the calibration reference lamps. When a common reference lamp calibrates the various instruments, the “best” agreement is now within  $\pm 5\%$  for many instruments.

Since the above campaigns, a recent European comparison of 19 instruments in Nea Michaniona, Greece, was conducted during July 1997, in the framework of the European Commission (EC)-funded Standardisation of Ultraviolet Spectroradiometry in Preparation of a European Network (SUSPEN) project. The results showed that, in terms of their absolute calibration, more than half of the spectroradiometers agreed to within about  $\pm 7\%$ , at SZA less than  $85^\circ$ . The diurnal variation of most of the instruments, relative to the reference spectra, was less than  $\pm 5\%$ , and the same is true for their spectral variability. The wavelength stability of the majority of the spectroradiometers was better than 0.1 nm. A significant outcome was that many of the instruments provided results that were consistent with at least the previous two EC intercomparison campaigns held in Italy (1995) and Germany (1993). It appears that there is a core group of UV spectroradiometers that can be trusted to produce measurements close to the limits of accuracy and precision expected using existing technology.

Intercomparisons between broadband erythemal-proxy instruments, such as RB-type meters, are difficult because their spectral response functions (SRF) do not precisely match the standard erythemal response func-

## SURFACE ULTRAVIOLET RADIATION

tion (McKinlay and Diffey, 1987) used to estimate the probability of skin reddening from UV exposure. There are also differences in the weighting functions produced by different manufacturers, as well as differences in corrections required for errors in the cosine response function. Field intercomparisons of broadband measurements with spectral data have revealed the importance of the SRFs.

One such comparison, the WMO/STUK Intercomparison of Erythemally Weighted Radiometers, was undertaken by the Radiation and Nuclear Safety Authority in Helsinki, Finland, in cooperation with the University of Innsbruck and with support from the WMO (Leszczynski *et al.*, 1997, 1998). During this intercomparison, the erythemally weighted (EW) radiometers were compared with two spectroradiometers in solar radiation, and the cosine and spectral responsivities of all participating instruments were measured in the laboratory. Most of the instruments (16 of 20) involved in the intercomparison were from a single manufacturer (Solar Light Company (SLC) meters).

Based on the laboratory measurements, the correction factors required to eliminate the errors due to non-ideal characteristics were calculated as functions of SZA and ozone. Figure 9-6a demonstrates that the calculated correction factor to eliminate the error due to the deviation of the SRF from the CIE weighting function (CIE = International Lighting Commission (France)) is a strong function of total ozone content and of solar elevation.

Examples of instruments manufactured by other companies (i.e., Yankee Environmental Systems, Inc., Vital Technologies Co., and Scintec Atmosphären Messtechnik GMBH) were also included in the study. The spectral responsivity correction factor for one of these instruments is compared with the SLC meters in Figure 9-6b. The figure also shows that the conversion to the CIE-weighted UV irradiance has significant variability even between instruments from the same manufacturer, due to slight differences in SRFs. If instrument-to-instrument differences in cosine response are factored in, the correction factors show only slightly greater variability.

During the intercomparison in solar radiation in Helsinki (60.2°N, 25.0°E), the broadband instruments were calibrated using simultaneously measured CIE-weighted solar spectra as a reference. To intercompare the calibration results, the calibration factors were averaged over solar elevations higher than 35°. The wide

range of the average values, from 0.87 to 1.75, indicates that the comparability of UV monitoring can be significantly improved by centralized calibration. The uncertainty of the spectroradiometric solar measurements was estimated as  $\pm 6\%$  at its best, while the overall uncertainty of the spectroradiometric calibration of the EW radiometers under the prevailing atmospheric conditions was estimated as  $\pm 10\%$ . The study represents a useful step in the international standardization of results from these instruments. It would be useful to repeat this procedure at regular intervals, preferably at a site that allows for a greater range of solar elevations for the measurements.

An intercomparison between broadband and spectroradiometric measurements was carried out to determine correction factors during different observing conditions including cloudy skies (Mayer and Seckmeyer, 1996). When the derived correction factors were used, good agreement was obtained after correcting for spectral mismatch and for cosine errors. Bodhaine *et al.* (1998) have recently studied the ozone dependence of broadband sensors and developed a calibration strategy using irradiance data obtained at Mauna Loa, Hawaii.

### 9.2.7 UV-Irradiance Trends from Ground-Based Measurements

Because of the cloud and aerosol variability that occurs over large regions from year to year, and over longer periods of several years, it is very difficult to detect UV-B increases caused by the few percent long-term decreases in ozone amounts for latitudes between 35° and 65° in both hemispheres. Consequently, there were only a few studies demonstrating the expected upward trend in UV as ozone has declined (Basher *et al.*, 1994; WMO, 1995, Chapter 9). More recent studies are discussed below. At higher latitudes, ozone trends are much larger. The large Antarctic springtime ozone decreases (70%) and large springtime decreases in the Arctic region during the last 3 years (30%) have caused large increases in UV-B irradiance that are easily detectable (Booth *et al.*, 1998).

The long-term stability of 1 to 2% per decade, needed to detect midlatitude UV-B trends, has yet to be demonstrated. Use of shorter wavelengths (290-300 nm) to take advantage of the larger percentage UV-irradiance increases caused by ozone decreases (see Figure 9-3) reduces the stability requirements, but increases calibration and stray-light problems.

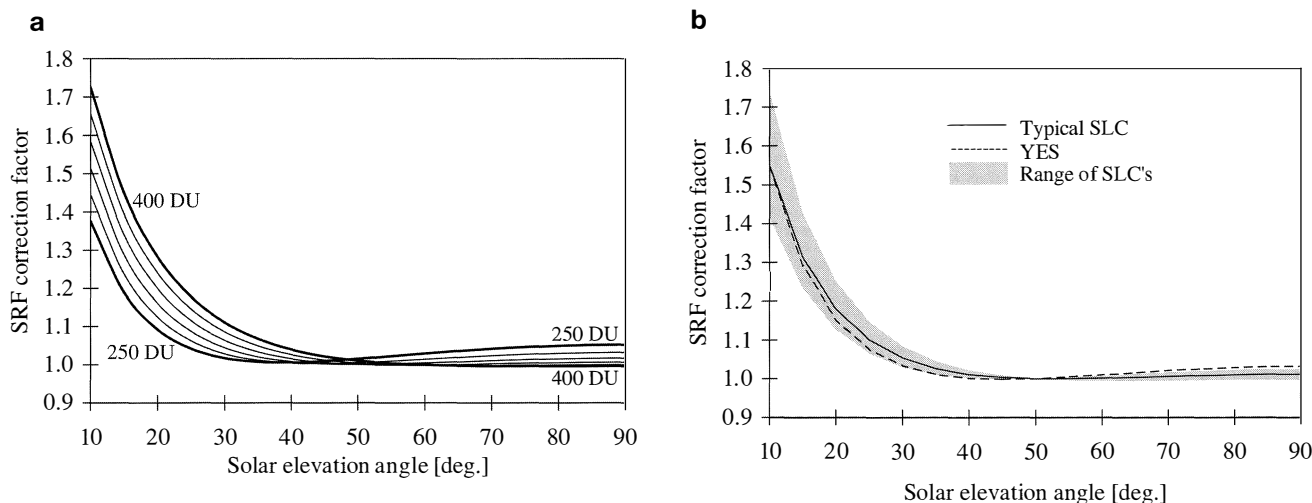


**Figure 9-6.** (a) Correction factors for eliminating errors due to non-ideal spectral response function (SRF) for a typical example of the model SL 501 V.3 radiometers, as a function of solar elevation angle, for total ozone content of 250 to 400 DU. The correction factors have been normalized to unity at an ozone content of 325 DU and solar elevation angle of 50°. (From Leszczynski *et al.*, 1997, 1998.) (b) The range of the correction factors for 16 similar instruments (model SL 501 V.3 radiometers). Correction factors for the YES UV-B-1 radiometer and the “typical” SLC radiometer have also been included for comparison. The correction factors were calculated for an ozone column of 325 DU and have been normalized to unity at a solar elevation angle of 50°. (From Leszczynski *et al.*, 1997, 1998.)

The effects of meteorological variability can be reduced by considering the ratio of irradiances at UV-B to UV-A wavelengths, as long as there are no significant wavelength-dependent instrument changes during the measurement period (Frederick *et al.*, 1993; Bais *et al.*, 1997). The use of ratios may also reduce the effect of absolute calibration errors (Vaughan *et al.*, 1997), but no conclusions can be drawn about changes in the absolute UV irradiance. Channels centered at 305 nm and 340 nm have the needed ozone sensitivity and suitability for observing cloud and haze effects, respectively.

If the absolute UV-A irradiances are monitored, the attenuation effects on UV-B and UV-A irradiance caused by clouds, aerosol haze, and ozone effects can be obtained. Using UV-A measurements and ozone amounts, the results of radiative transfer calculations, matched to a few well-calibrated measured irradiances, can be used to reconstruct the entire UV spectrum at the resolution of the most accurately measured extra-terrestrial solar irradiance (0.15 nm).

The observation period covered by well-calibrated multi-channel radiometers is still too short to reliably detect midlatitude (<55°) trends resulting from ozone

changes. Even for clear-sky data, a minimum period of about 11 years is desirable from the viewpoint of removing solar cycle and QBO (quasi-biennial oscillation) effects (Stolarski *et al.*, 1991; Herman and Larko, 1994). The interannual variation in monthly-average UV-B irradiance from meteorological causes (clouds and haze) is generally comparable to or greater than that caused by monthly-average percentage variation in overhead column-ozone content. This results in trend-determination uncertainties that are larger than the expected trends.

The effects of clouds on detecting local trends of UV-B irradiance have been studied using cloud cover estimates from co-located Earth Radiation Budget Experiment (ERBE) data and ozone data obtained from the Total Ozone Mapping Spectrometer (TOMS) (Lubin and Jensen, 1995). The paper examined how the established ozone-amount trends compare with the cloud-induced variability in UV irradiances. Lubin and Jensen (1995) found that throughout many temperate regions (large parts of continental Europe, North and South America, New Zealand, Australia, and southern Africa) the interannual variability in cloud opacity is sufficiently small that by the end of the century, biologically

## SURFACE ULTRAVIOLET RADIATION

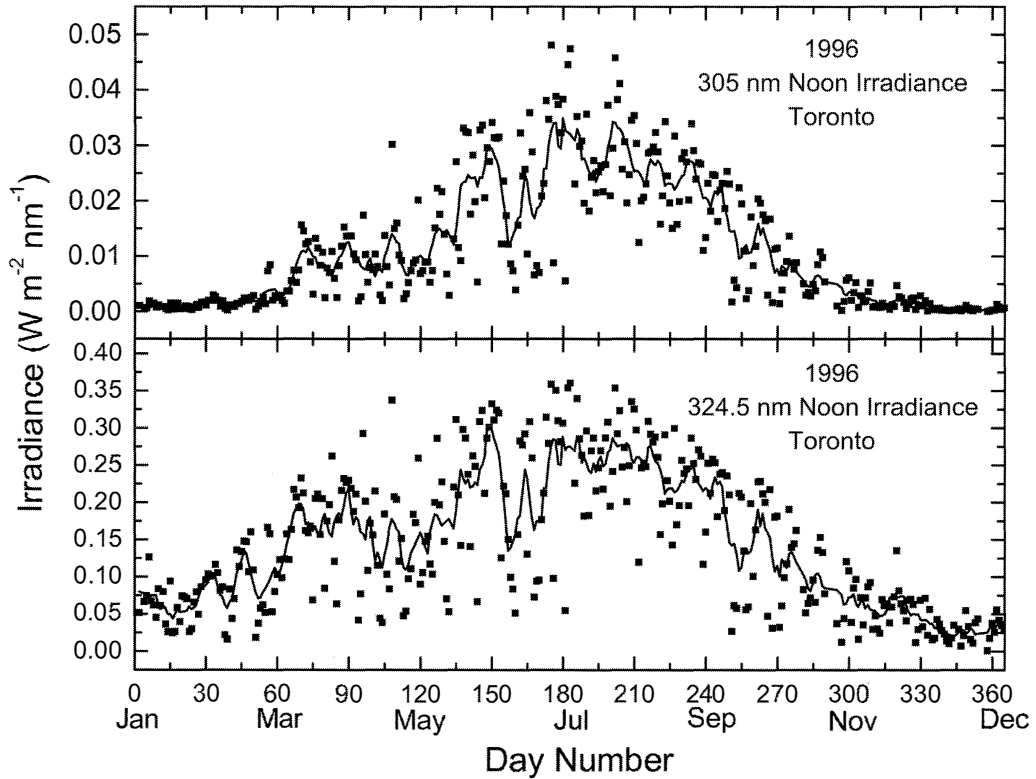


**Figure 9-7.** Local UV variability throughout 1996 due to clouds, SZA, aerosols, and ozone using ground-based UV-irradiance measurements at 305 nm (top panel) and 324.5 nm (bottom panel) from Toronto Brewer #14 (single monochromator at 42°N). Points are daily averages from  $\pm 1$  hour of noon. The solid lines are weekly running averages. (From J.B. Kerr, WOUDC database; see Section 9.2.3.)

significant trends in UV-B should be observable from ground-based instruments even with the cloud-induced variability. This analysis, made in 1994, appears to be optimistic from the vantage point of the current Assessment (1998).

The problem of extracting small UV-irradiance trends from data obtained on clear and cloudy days is illustrated in Figure 9-7. This figure shows the variability of noontime irradiances obtained at Toronto during 1996. The 305-nm irradiances (top panel) have the effects of seasonal changes in SZA, day-to-day changes in cloud cover, and daily changes in ozone. At this wavelength there is an approximate  $100 \frac{dF}{F} = 2 \sec(\theta)$  percent increase in irradiance for every 1% decrease in ozone amount (see Equations (9-1) and (9-2)). Changing SZA and clouds causes the variations seen at 324.5 nm (bottom panel). The variations at 305 nm caused by ozone are much smaller than those due to clouds. Integrating over longer periods (e.g., 1 day) can reduce some of the effects of cloud variability.

The first measured effects of ozone depletion on integrated daily UV-B at midlatitudes, including cloudy conditions, was the Toronto study by Kerr and McElroy (1993, 1995), as reported in the previous Assessment. Extension of the dataset to 1996 shows that the upward trends in UV irradiance, over the 4-year period to August 1993, continued, but at a much slower rate (Wardle *et al.*, 1997). Much of the earlier change is now attributed to the anomalously low ozone during the 1992-1993 period following the eruption of Mt. Pinatubo (Herman and Larko, 1994). By 1994, ozone and UV-B measurements had reverted to levels similar to those seen prior to 1992 (unpublished data from WOUDC; see Figure 9-8), showing that the UV-irradiance increases in 1992-1993 are better described as a perturbation, rather than a trend. The anticorrelations of ozone and UV-B radiation during this short-term perturbation quantitatively illustrate the link between ozone depletion and increases in UV-B radiation.

Long-term irradiance changes estimated from

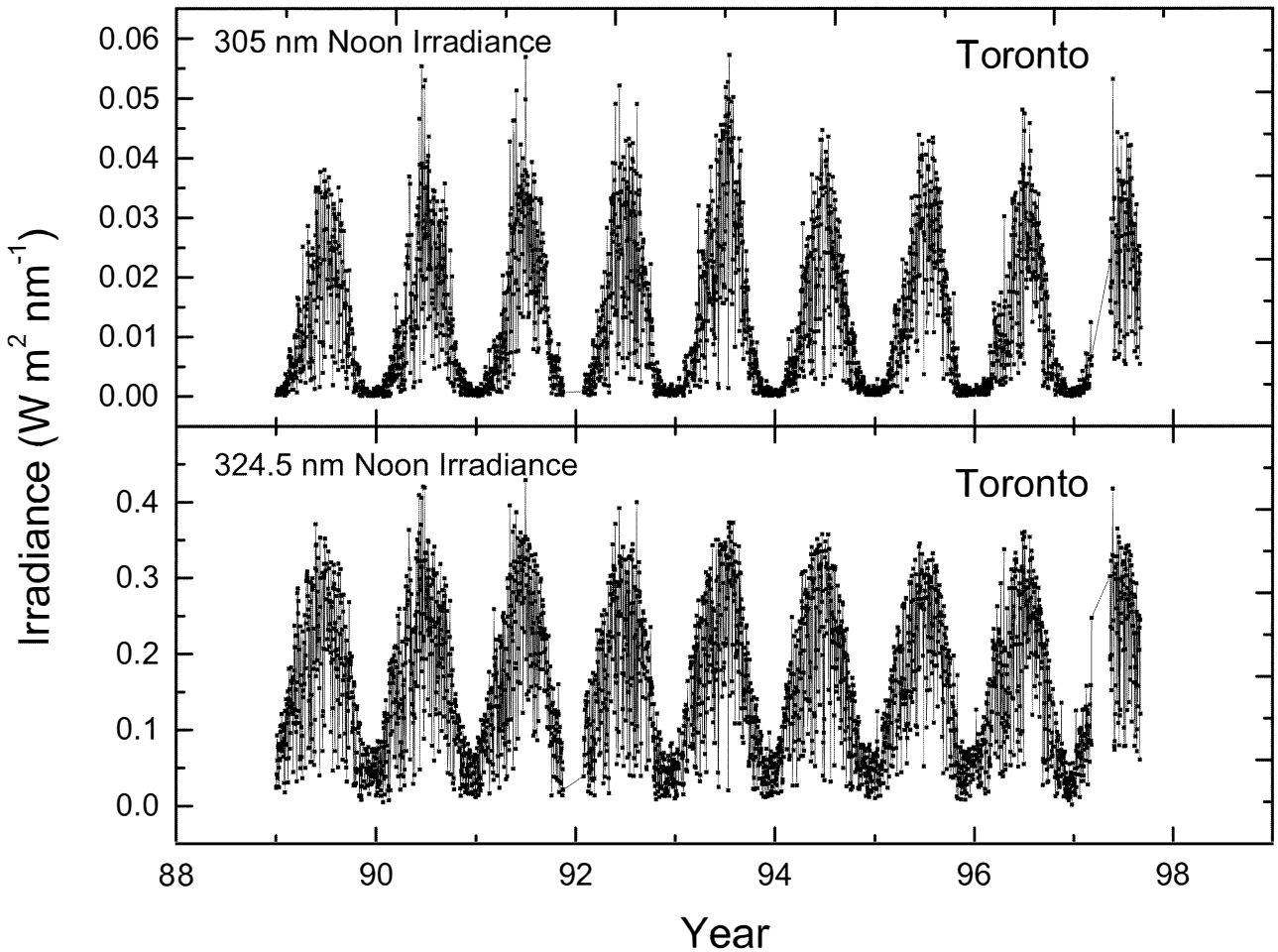


**Figure 9-8.** Interannual variability of UV irradiances at Toronto for the years 1989 to 1997, illustrated using daily noon values at wavelengths  $305 \pm 0.25$  nm (top panel) and  $324.5 \pm 0.3$  nm (bottom panel). The data were obtained by Brewer #14 (single monochromator) and are not corrected for instrumental cosine-function errors.

average integrated daily irradiances at Toronto between May and August from 1989 to 1997 are about 1.5% per year at 300 nm, 0.8 to 1% per year at 305 nm, and 0% per year at 324 nm (negligible ozone absorption). Using the RAF, this corresponds to the summer average ozone amount declining by 0.43% per year, consistent with the results discussed in Chapter 4 and consistent with the changes estimated from satellite data (J.R. Herman *et al.*, 1996). However, the combination of instrumental uncertainties and irradiance variance causes linear-trend error estimates comparable to the measured change. Several other studies investigating longer-term changes have appeared in the literature since the

previous Assessment.

Longer-term changes are more clearly seen when irradiance data are filtered for clouds and SZA dependence. A 7-year time series at Thessaloniki, Greece, shows the expected anticorrelation between 305-nm irradiance and ozone (Zerefos *et al.*, 1995a,b, 1997). Corresponding measurements at 325 nm show only a steady increase caused by reduced aerosol extinction, as deduced from collocated ancillary data. After aerosols and SO<sub>2</sub> effects are taken into account, a long-term increase in 305-nm irradiance caused by the ozone decrease for this period is detectable (see Figure 9-9). Shorter time series from three other sites in Europe

## SURFACE ULTRAVIOLET RADIATION

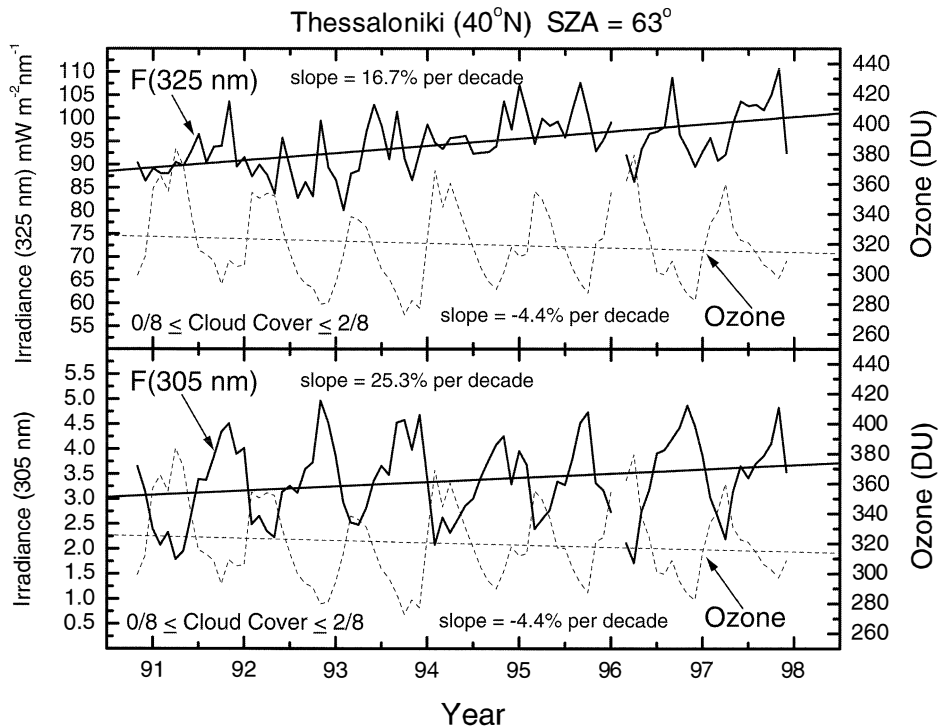


**Figure 9-9.** Time series of monthly mean values of solar UV irradiance (solid lines) at 325 nm (top panel) and at 305 nm (bottom panel) measured at  $63^\circ$  SZA under clear-sky conditions, and total ozone (dashed lines), at Thessaloniki, Greece ( $40^\circ\text{N}$ ), during the period from November 1990 to December 1997. Cloud fraction numbers can range from 0/8 (entirely clear skies) to 8/8 (entirely overcast). Straight lines represent linear regressions on the monthly mean data from November 1990 to November 1997. (Updated from Zerefos *et al.*, 1997.)

(Bruxelles-Uccle, Garmisch-Partenkirchen, and Reykjavik) show similar anticorrelations with ozone. The authors point out that the estimated slopes from the linear least-squares fits to the data vary strongly with the length of the irradiance time series and so should not be taken as an estimate of irradiance trends until much longer time series are available.

A study using RB meters (1976-1992) and a 501 Biometer (1993-1994) located at Belsk, Poland ( $52^\circ\text{N}$ ), found increases in UV irradiance of  $1.9 \pm 2.8\%$  per decade for the April to October period and  $3.2 \pm 3.1\%$  per decade for the November to March period (1-standard deviation error estimates). These UV-irradiance changes include local cloud-cover increases that partially offset UV-irradiance increases due to stratospheric ozone decreases (Krzyscin, 1996; Nemeth *et al.*, 1996). While the trends appear to indicate a seasonal difference, the variances in the data are sufficiently large that neither of the seasonal trends is statistically different from zero.

Large apparent increases in UV-B were reported by Gurney (1998) at Barrow, Alaska ( $71.2^\circ\text{N}$ ,  $159^\circ\text{W}$ ), over a 5-year period (1991 to 1995). The data appear to show absolute irradiance decreases at both 305 and 340 nm, but the irradiance ratio  $F(305)/F(340)$  showed an increase. The results implied an increase of 15-50% over the study period for all months except June, the month of maximum UV irradiance, which showed a decrease. However, the study period included the anomalous period of low ozone in 1992-1993. Furthermore, for most months the increases were not statistically significant. Available concurrent ozone measurements were not considered in the study.

The increasing frequency of extreme events (ozone amounts outside the envelope of values from the years 1979 to 1990) may be another indicator of long-term atmospheric change (Seckmeyer *et al.*, 1994b). Very low ozone has been reported over Canada (spring 1997) associated with extremely low stratospheric

temperatures, and with ice-crystal formation in the troposphere and lower stratosphere, within an unusually stable north-polar vortex region. Other enhancements in UV irradiance, caused by short-term ozone decreases, have been reported recently in Europe (Seckmeyer *et al.*, 1997) and Hawaii (Hofmann *et al.*, 1996).

Because of the difficulty of detecting small, systematic long-term changes hidden in the large dynamic range of daily and seasonal changes (see Figures 9-7 and 9-8), the long-term stability of UV-B instrumentation must be improved and maintained over decadal time scales. Unlike the satellite measurements that can remove much of the local variability by geographic averaging, the ground-based measurements must also deal with local meteorological effects (clouds and haze, and, in some regions, possible changes in surface albedo) that show systematic multi-year changes. Systematic differences and variable calibration drifts between different instruments in a network may partly negate the benefits of ground-based geographical averaging. The calculated UV irradiance results from satellite observations of ozone amounts, scene reflectivity (clouds), surface reflectivity, and aerosol amounts over the entire globe may prove useful in the future for checking consistency with the conclusions drawn from local ground-based studies.

Although measurements from polluted sites will be of interest to epidemiologists and for process studies, instruments designed to monitor trends due to ozone depletion should generally be located at remote sites where tropospheric changes from local pollution effects are minimized (Grant, 1988).

### 9.3 SATELLITE ESTIMATIONS OF UV IRRADIANCE

Satellite estimations of UV have recently become available from TOMS (Total Ozone Mapping Spectrometer, November 1978 to May 1993, August 1991 to December 1994, August 1996 to present) satellite instruments. The estimated UV irradiances form a global daily image of the spectral and geographic distribution of UV irradiance over the UV-A and UV-B range. The TOMS UV-irradiance estimates are calculated using derived values of ozone amounts, cloud reflectivities, aerosol amounts, and scene reflectivity, from measured backscattered radiances and extraterrestrial solar flux (Cebula *et al.*, 1994, 1996). Surface UV irradiances have

also been estimated from the Earth Radiation Satellite-2 (ERS-2) Global Ozone Monitoring Experiment (GOME) and the National Oceanic and Atmospheric Administration (NOAA) Advanced Very High Resolution Radiometer (AVHRR) satellite instruments (Meerkotter *et al.*, 1997).

Satellite estimates of UV irradiance at the Earth's surface can give regional and global views of its variation and long-term trends. Estimates are not sensitive to the stratospheric ozone profile shape except at very high SZA ( $>70^\circ$ ), but are slightly sensitive to variations in the tropospheric distribution of ozone because of multiple scattering effects. A 10% perturbation in the amount of tropospheric ozone would produce less than a 2% change in the diffuse component of the global irradiance (diffuse + direct) at 300 nm, and smaller changes at longer wavelengths. The direct component is not affected by profile shape. At  $30^\circ$  SZA the 300-nm diffuse component is less than half of the global irradiance, and the fraction decreases gradually with increasing wavelength. Therefore, a profile shape error in the troposphere would produce less than a 1% perturbation in the global irradiance for the same amount of total column ozone. This error estimate applies to both the Northern and Southern Hemispheres even though there may be less tropospheric ozone in the south than in the north at comparable latitudes.

The TOMS satellite instruments have obtained contiguous global coverage of ozone, aerosol, and scene-reflectivity (cloud) measurements since November 1978, which have been converted into estimates of the UV irradiance. On the basis of the 1979-1994 TOMS satellite data record, ozone changes are statistically significant at latitudes larger than  $35^\circ\text{N}$  or  $35^\circ\text{S}$  (McPeters *et al.*, 1996) and have been observed by the distributed network of ground-based UV-Dobson instruments with a sufficiently long record. Because TOMS data showed that there has been no trend in zonally averaged cloud reflectivity (J.R. Herman *et al.*, 1996), a zonally distributed network of UV-B sensitive instruments should also detect the UV-irradiance changes caused by the ozone trend. For example, at latitudes between  $35^\circ$  and  $40^\circ$  the zonal average ozone change is about 2 to 3% per decade and produces a corresponding 2.5 to 3.5% per decade change in UV irradiance at  $310 \pm 0.5$  nm or in the spectrally weighted erythemal irradiance range between 290 and 400 nm. Larger percentage changes occur at shorter wavelengths (about 7 to 11% at 300 nm). From satellite data, the zonally averaged decadal trend in erythemal

## SURFACE ULTRAVIOLET RADIATION

irradiance is  $2.9 \pm 3\%$  per decade (2 standard deviations) in the latitude bands between  $35^\circ$  and  $45^\circ$  in both hemispheres (J.R. Herman *et al.*, 1996).

Current TOMS data (August 1996 to the present) can be used to extend the daily UV-irradiance record. However, UV trend estimates cannot be made until a longer continuous data record is available and the intercalibration differences between TOMS instruments discussed in Chapter 4 have been fully resolved. If cloud amounts observed from other satellites can be quantitatively related to TOMS reflectivity measurements, then it may be possible to bridge the TOMS data gap (from January 1995 to July 1996).

The satellite-derived UV irradiances compare well with ground-based measurements at a single site, Toronto (Eck *et al.*, 1995). However, extensive intercomparisons with other ground-based instruments are still required.

### 9.3.1 Extraterrestrial UV Irradiance

Satellite estimations of UV irradiance at the surface require the use of independently measured extraterrestrial solar fluxes over the 280- to 400-nm range. These values are also useful for comparison with derived extraterrestrial solar fluxes from ground-based instruments. Under clear-sky conditions, the comparison can be used as a validation for ground-based spectroradiometer data, under the assumption that the extraterrestrial flux is invariant in time for 280 to 400 nm.

Daily flux measurements have been made since October 1991 by two UV solar spectrometers, the Solar-Stellar Irradiance Comparison Experiment (SOLSTICE) (Rottman *et al.*, 1993) and the Solar Ultraviolet Spectral Irradiance Monitor (SUSIM) (Brueckner *et al.*, 1993) on the Upper Atmosphere Research Satellite (UARS). The measurement period includes most of the decrease from solar maximum to solar minimum and part of the recovery. Daily UV solar spectral irradiance measurements were also made by the Solar Backscatter Ultraviolet/model 2 (SBUV/2) instrument on board the NOAA-11 satellite between February 1989 and October 1994 (DeLand and Cebula, 1998a,b; Cebula and DeLand, 1998). These three independent instruments have shown that the natural variability of the solar flux in the 280- to 400-nm wavelength range is less than 1% over 11-year and 27-day cycles in solar activity. Lean *et al.* (1997) estimated that the long-term (solar cycle maximum to minimum) change in UV solar radiance is about 1.1% (200 to 300

nm) and 0.25% (300 to 400 nm) based on sunspot and facular records. In addition, they concluded that present measurements in the 300- to 400-nm range do not have the required level of precision to detect such changes.

The absolute accuracy of these measurements is maintained through internal calibrations and dataset intercomparisons (of SOLSTICE, SUSIM, and SBUV/2 instruments). The agreement between the UARS SUSIM and SOLSTICE instruments has been estimated to be  $\pm 5\%$  (Cebula *et al.*, 1994, 1996). The measurements made by the two UARS instruments were compared with same-day measurements by three other solar instruments (the Solar Spectrum (SOLSPEC), the Shuttle Solar Backscatter Ultraviolet (SSBUV), and the Shuttle SUSIM instruments) during the Atmospheric Laboratory for Applications and Science (ATLAS)-1 and ATLAS-2 Space Shuttle missions in March 1992 and April 1993, respectively (Cebula *et al.*, 1996; Woods *et al.*, 1996), and ATLAS-3 in November 1994. In the 280- to 400-nm wavelength region, at 5-nm spectral resolution, the difference between the various datasets is less than  $\pm 3\%$  and is wavelength dependent.

The ATLAS-3 SUSIM data (110 to 410 nm with 0.15-nm resolution) and the SOLSTICE data are both available on the Internet (see Appendix). The ATLAS-3 SUSIM instrument was modified to be more accurate than the ATLAS-1, ATLAS-2, and UARS versions of SUSIM. A general error analysis for the ATLAS-3 data is not currently available, but for the previously measured spectrum (ATLAS-2 SUSIM), the accuracy was specified to be 4-8% (Woods *et al.*, 1996). Examples of the SOLSTICE and higher-resolution ATLAS-3 SUSIM data in Figure 9-10 show good agreement. For the examples shown in Figure 9-10 the agreement is about 2% when the SUSIM data are degraded to SOLSTICE resolution. Either the 1992 SOLSTICE data or the 1994 SUSIM data can be used, because at the wavelengths of interest, 280-400 nm, the solar flux is invariant to within the precision of the measurements.

### 9.3.2 UV Irradiance at the Earth's Surface

UV irradiances at the Earth's surface can be estimated by combining satellite measurements of ozone amounts, clouds, aerosols, ground reflectivity, and the extraterrestrial solar-flux spectrum using a Mie and Raleigh scattering radiative transfer equation (Green, 1983; Grant *et al.*, 1996; J.R. Herman *et al.*, 1996;

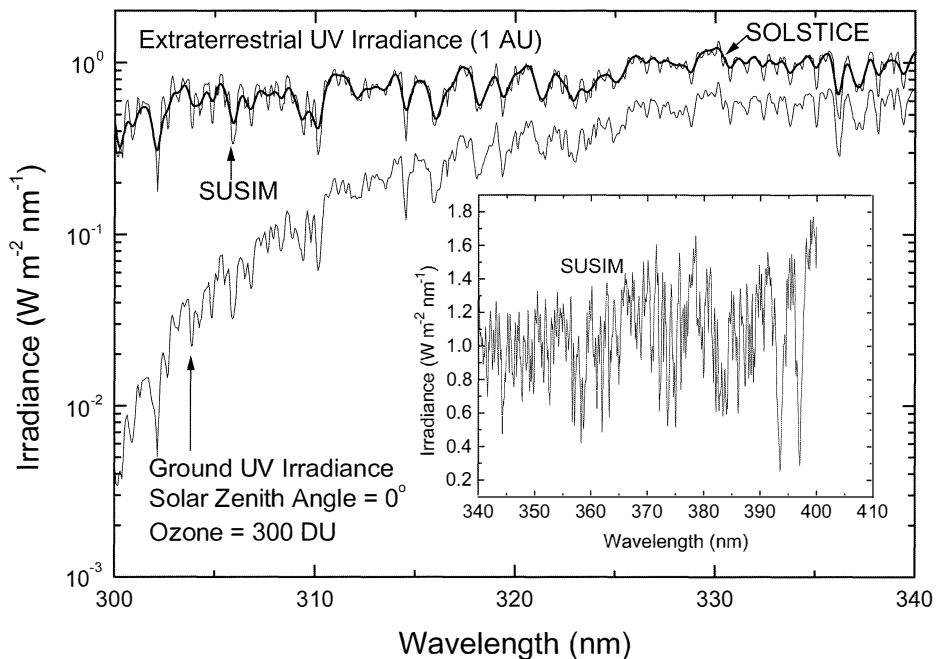


**Figure 9-10.** The extraterrestrial solar spectrum (280-400 nm) obtained from SUSIM at 0.15-nm resolution (November 1994, Shuttle ATLAS-3 mission) and, at lower spectral resolution, from SOLSTICE (March 1992, UARS) satellite-borne instruments plus the calculated UV irradiance at the ground for overhead sun with clear sky and 300 DU of ozone. Wavelengths are in vacuum.

Krotkov *et al.*, 1998). Other input parameters (e.g., surface pressure, temperature profiles, absorption, and scattering coefficients) are obtained from standard data compilations. Additional minor atmospheric species that absorb UV radiance (e.g.,  $\text{SO}_2$ ) are not ordinarily significant in determining surface UV irradiance (Bais *et al.*, 1993; Fioletov *et al.*, 1998). If zonal averaging is used to minimize local variability of cloudiness, satellite determination of UV irradiances at the Earth's surface is well suited for detecting changes caused by variations in the amount of atmospheric ozone. The major advantages of TOMS satellite data are the use of a single instrument that was wavelength and radiometrically calibrated while in flight over a long period of time (1978 to 1993), nearly complete global coverage, and uniform spectral accuracy. The accuracy of the estimated UV irradiance depends on knowledge of the ozone absorption coefficients, errors in the measured extraterrestrial solar flux, the relationship of average cloud and nonabsorbing aerosol (mainly sulfates) transmissivity over the satellite footprint to the measured reflectivity, and the knowledge of possible absorbing aerosols (e.g., smoke or dust) in the satellite's field of view. The disadvantages are the

coarse spatial resolution ( $100 \times 100 \text{ km}^2$  on average), a single measurement per day, the inability to independently separate low-altitude (below about 1.5 km) absorbing aerosols from sub-pixel clouds (clouds smaller than the TOMS field of view) or nonabsorbing aerosols, and the inability to accurately compare with daily ground-based measurements under broken-cloud conditions. Except for the low-altitude absorbing aerosol discrimination problem, the above disadvantages can be mostly overcome by considering weekly, or longer, averages for comparison with ground-based data obtained within  $\pm 1$  hour of the satellite overpass time. Recently, the effect of clouds on irradiance combining data from the Earth Radiation Budget Experiment (ERBE) instrument and TOMS data has been studied by Lubin *et al.* (1998) and used to produce a UV climatology.

Figure 9-11 shows the seasonal and geographic variability of the erythemally weighted monthly exposure estimated from TOMS data for 1997. The exposure is obtained from integrals of the hourly irradiance for each month based on a single daily near-noon measurement of backscattered radiances at six wavelengths. The estimation includes the effects of ozone absorption,

## SURFACE ULTRAVIOLET RADIATION

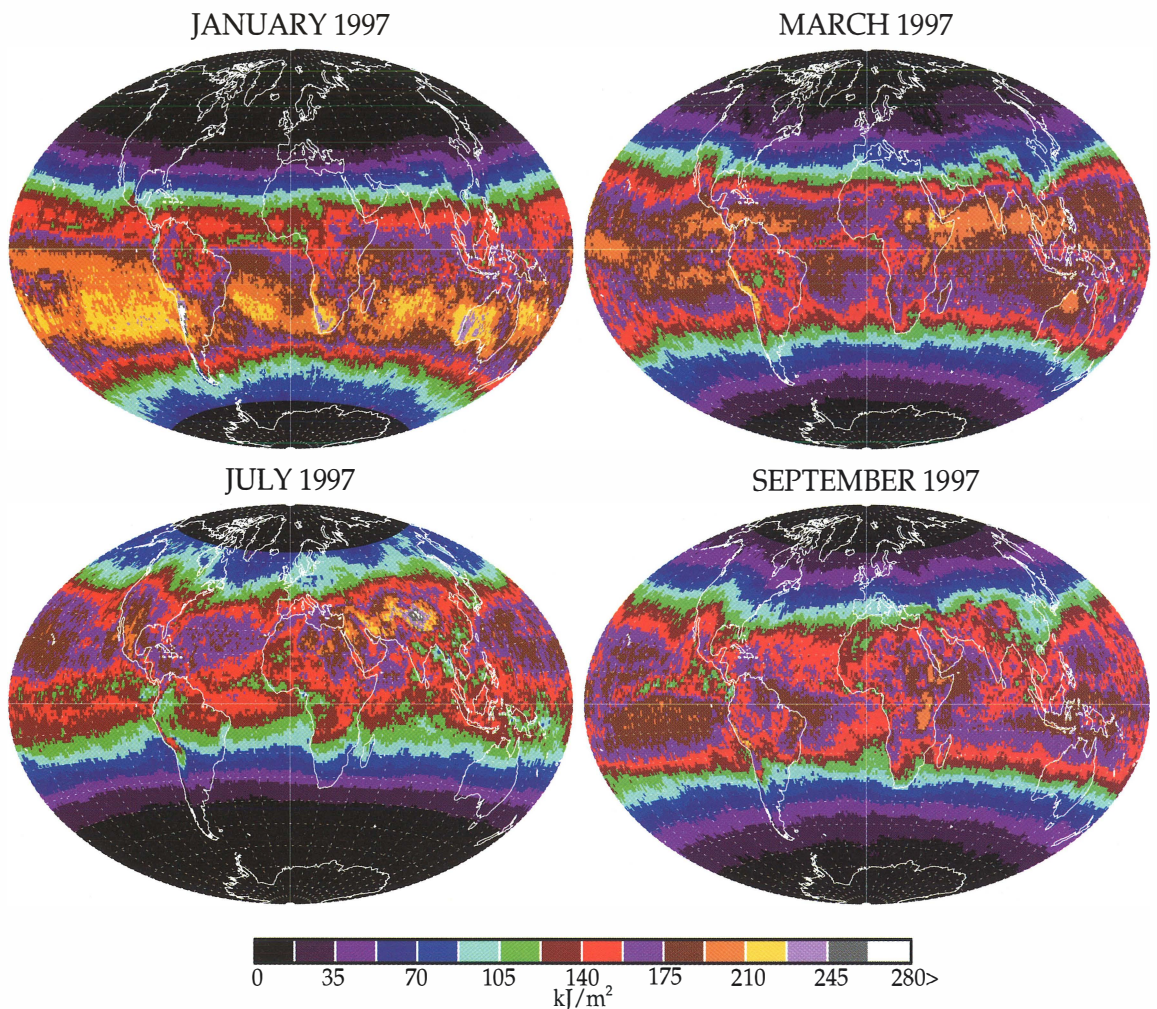


**Figure 9-11.** Global maps from TOMS-estimated irradiances of the monthly erythemal exposure for January, March, July, and September, including the effects of ozone, clouds, aerosols, and surface reflectivity. (Updated from J.R. Herman *et al.*, 1996, 1997; Krotkov *et al.*, 1998.)

cloud transmissivity, and surface albedo determined from TOMS data on a  $1^\circ$  by  $1^\circ$  grid (McPeters *et al.*, 1996; J.R. Herman *et al.*, 1996; Herman and Celarier, 1997; Krotkov *et al.*, 1998), and includes the decreases in UV irradiance caused by absorbing and nonabsorbing aerosols based on the attenuation calculations contained in Krotkov *et al.* (1998) and the global distributions of aerosols in Herman *et al.* (1997). Terrain height tables are used in addition to TOMS data. For most locations, only a single near-noon measurement is made each day for atmospheric and surface properties. Although the reductions in UV irradiance by absorbing aerosols are only estimates, because of the assumed height of the

absorbing aerosol plumes at 3 km (see discussion below) (Torres *et al.*, 1998), the aerosol dataset used is the only one currently available over both land and oceans.

As expected, the highest values of exposure are near the seasonal sub-solar points (SZA  $\sim 0^\circ$ ) between  $\pm 23^\circ$  latitude, in regions of elevated altitude (e.g., Andes Mountains), and in regions that are relatively free of clouds for the given month (e.g., South Africa and Australia in January and in large regions over the oceans). In July, during the Northern Hemisphere summer, very high exposures are estimated over the Sahara, Saudi Arabia, the southwestern United States, and the Himalayan mountain regions in northern India

and southern China. The equinox at March produces high exposure values throughout equatorial Africa, the southern part of the Arabian Peninsula, southern India, Malaysia, and Indonesia. Even though the SZAs in September are nearly the same as in March, the increased number of cloudy days produces lower exposures during September.

A measurement-modeling comparison between TOMS-measured ozone and reflectivity as inputs into a radiative transfer calculation (Dave, 1964; Eck *et al.*, 1995) and the Toronto Brewer instrument (Kerr and McElroy, 1993) showed very good agreement over a wide range of seasonal and cloud conditions. Recent studies using a larger sample of data show a seasonal difference, with the largest differences occurring in the winter months (G. Labow, Raytheon STX, United States, personal communication, 1998; V. Fioletov, Atmospheric Environment Service, Canada, personal communication, 1998). A new UV CD-ROM for erythral exposure will be available from the National Aeronautics and Space Administration (NASA) Goddard Space Flight Center (GSFC), based on the TOMS ozone and 380-nm radiance data for Nimbus/TOMS (1979 to May 1993) and on 360-nm reflectivity for Earth Probe/TOMS (since August 1996). The 1996 version of the TOMS UV CD-ROM used an incorrect version of the erythral action spectrum given in Booth *et al.* (1993).

It should be emphasized that satellite-borne sensors do not directly measure surface UV irradiances or any other atmospheric characteristic. All quantitative satellite measurements infer Earth surface or atmospheric properties using radiative transfer calculations. The major uncertainties in satellite UV-irradiance estimation are due to possible undetected variability in small-scale (sub-pixel) boundary layer extinctions from aerosols, tropospheric ozone, and clouds. The coarse spatial resolution can also be a useful feature, compared with the localized measurements of ground-based instruments, because the satellite-borne measurements estimate the average irradiance striking the geographic area covered by the instrument's field of view (26 to 100 km for Earth Probe/TOMS, 50 to 200 km for Nimbus-7/TOMS), including the average transmissivity of the cloud and aerosol fields from measurements of their backscattered radiances over the TOMS field of view. The transmissivity is essentially an energy balance estimate assuming a Lambertian equivalent reflectivity over the field of view.

The spatial resolution of the current satellite UV-

radiance instruments does not resolve the effects of broken clouds or small-scale cloud structure. A simple example is when the direct sun is observed through broken clouds from the ground. Even for rather large fractional cloud cover, it has been shown that if the sun is not obscured, the UV irradiance measured at the surface remains close to the clear-sky value (e.g., Blumthaler *et al.*, 1994) or can exceed it for some cloud conditions. Conversely, for small fractional cloud cover in the TOMS field of view, the ground-based observation may have the sun obscured by clouds and measure a smaller radiance than estimated from the TOMS data. This means that daily comparisons of satellite data with ground-based measurements may disagree substantially even though weekly or monthly averages may agree quite well (Eck *et al.*, 1995). This will not be true if there is a systematic cloud amount bias at the ground site compared to adjacent areas.

Observations at higher spatial resolution, of about 1 km at near-UV wavelengths (412 nm), have been made by the SEAWIFS (Sea-viewing Wide Field-of-view Sensor) satellite instrument. These observations may be of use for estimating the effects of broken clouds on the larger pixels used by TOMS ( $26 \times 26 \text{ km}^2$  to  $100 \times 150 \text{ km}^2$ ). Finally, the frequency of satellite overpasses is such that the modeled diurnal variations arising from cloud or aerosol effects are not realistic (see discussion in Section 9.6.3). Well-maintained, strategically located ground-based instruments are needed to verify the applicability of satellite-derived estimations of surface UV radiation.

### 9.3.3 UV Extinction by Aerosols

Of the major factors affecting surface UV, only ozone has a known widespread long-term change (decrease), and only for latitudes between  $35^\circ$  and the poles. For major sources of UV-absorbing aerosols (dust and smoke), only the biomass-burning smoke over South America shows a systematic increase since 1979 (Herman *et al.*, 1997). An analysis of zonal-average reflectivity, based on the 1979-1993 TOMS backscattered radiance data, indicates that the global- and zonal-average UV transmission by clouds (of all types combined) plus nonabsorbing aerosol (all Mie-scattering aerosols of size 0.07 microns ( $\mu\text{m}$ ) or greater) has not changed significantly (J.R. Herman *et al.*, 1996). Scattering from particulates smaller than about 0.07  $\mu\text{m}$  is not easily distinguished from the Rayleigh scattering background

## N7/TOMS, Estimated Aerosol Attenuation for 09/03/87

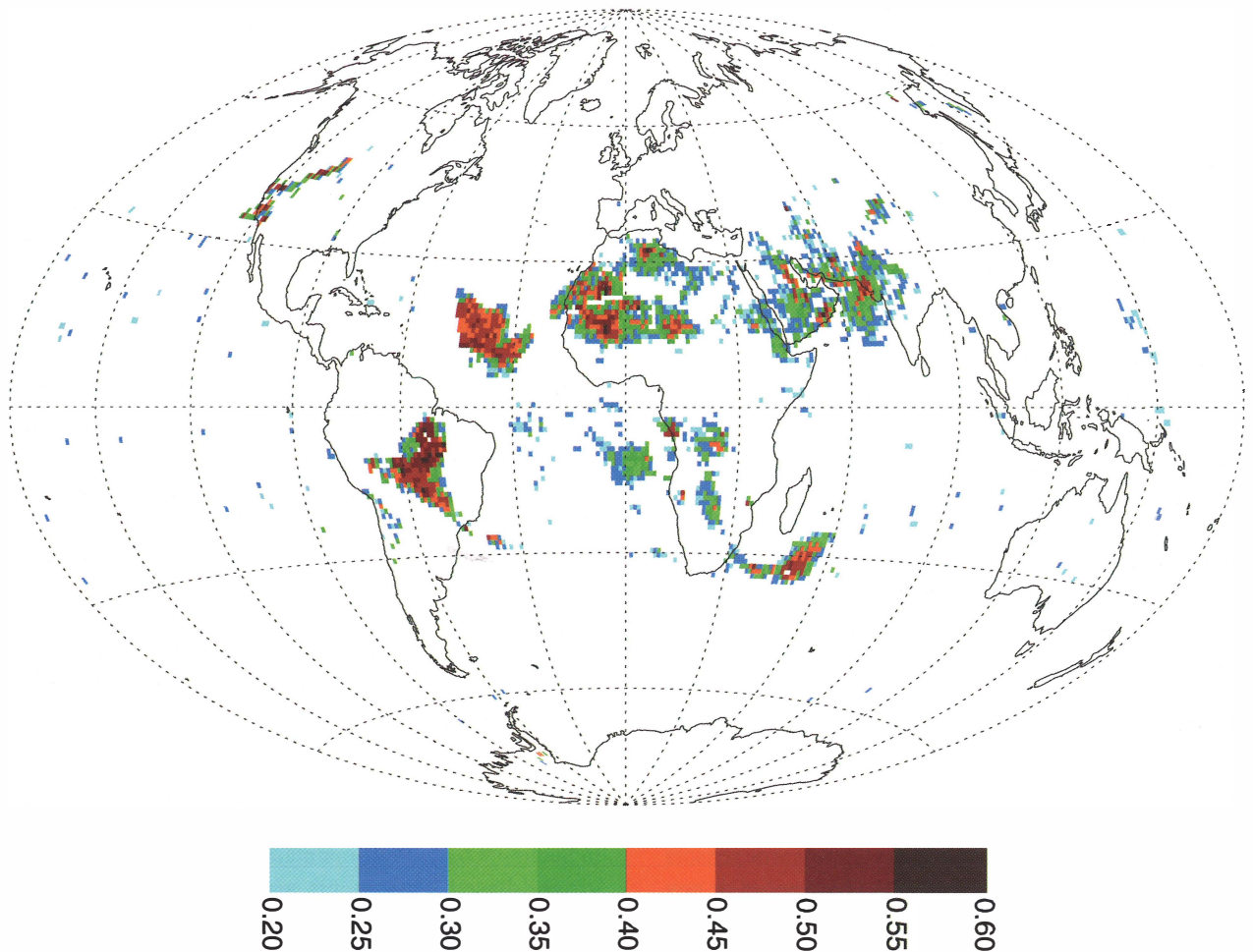


**Figure 9-12.** Map of the percentage of UV-irradiance reduction relative to clear-sky irradiance, on 3 September 1987, using an assumed aerosol plume height of 2.9 km, showing the effect of Saharan desert dust and biomass burning in South America, southern Africa, and California. The estimated errors are 7.5% for smoke and 11% for dust for a  $\pm 0.5$ -km error in assumed height. The irradiance reduction method is not sensitive to absorbing aerosols below about 1.5 km. (From Krotkov *et al.*, 1998.)

at the observing wavelengths of TOMS (360 or 380 nm). However, regional changes in cloud or aerosol cover may have changed UV doses at ground level (Liepert *et al.*, 1994; Seckmeyer *et al.*, 1994b).

TOMS estimations of aerosol amount (Herman *et al.*, 1997; Torres *et al.*, 1998; Krotkov *et al.*, 1998) can be used to calculate the aerosol attenuation of UV irradiance for the Earth's surface between  $\pm 65^\circ$ . The sample UV-irradiance attenuation map shown in Figure 9-12 was derived assuming that the height of the aerosol layer was known. In this case, the altitude was assumed to be uniform at 2.9 km. Comparisons of derived optical

depths with sunphotometer optical depths (Torres *et al.*, 1998) show that 2.9 km is a good average first-order approximation. Using a constant altitude neglects some seasonal changes such as the increase in height over the Sahara during the summer months. TOMS is unable to distinguish absorbing aerosols from sub-pixel clouds or nonabsorbing aerosols when their optical depths are less than 0.1 or if they are below about 1.5 km in altitude. This means that it is unlikely that TOMS, by itself, will be able to detect weakly absorbing aerosols near the surface, often found in urban atmospheres.

The map in Figure 9-12 shows that aerosol absorption can produce very large reductions in UV irradiance ( $\sim 50 \pm 12\%$ ) in certain parts of the world. One sees the effects of smoke from a west-coast Canadian forest fire that is moving in the southwesterly direction, biomass burning in South America and Africa, and desert dust blowing both east and west from the Saharan region of Africa. These estimates are consistent with ground-based sunphotometer observations (Torres *et al.*, 1998) showing agreement in optical depths that are equivalent to observing a 50% or more reduction in surface UV radiation due to smoke from widespread biomass burning in the Brazilian rain forest. The data shown in the map have been truncated so as not to show lower amounts of absorbing aerosol (optical depth less than 0.4) that appear to be more widely distributed away from the sources of biomass burning and dust. If validated, these plumes with lower optical depth would result in a 5 to 10% reduction in UV radiation. The recent Indonesian fires had dense smoke plumes that were observed by TOMS, AVHRR, GOME, and SEAWIFS satellite instruments. On the basis of the TOMS observations, optical depths greater than 5 occurred, which resulted in estimated reductions in UV irradiance of 90%.

**9.3.4 Trends in UV Irradiance**

The satellite determinations of changes in zonally averaged, decadal global UV exposure are summarized in Figure 9-13 as a function of latitude (J.R. Herman *et al.*, 1996). The exposure changes are computed for three different action spectra: (1) erythema (McKinlay and Diffey, 1987), (2) DNA damage (Setlow, 1974), and (3) plant damage (Caldwell *et al.*, 1986). The UV-irradiance changes are based on the TOMS reflectivity and ozone amounts from 1979 to 1992. The results include both ozone changes in the stratosphere and troposphere, and the effect of clouds and non-absorbing aerosols, but did not include the effect of absorbing aerosols (dust and smoke).

The results show that no statistically significant changes have occurred for latitudes equatorward of  $35^\circ$ , but that increases in UV-irradiance between  $40^\circ$  and  $65^\circ$  have been substantial for any of the standard action spectra (Madronich and de Gruijl, 1994; J.R. Herman *et al.*, 1996; Weatherhead *et al.*, 1997). In the Northern Hemisphere the UV-irradiance increases have occurred over the densely populated regions of Europe, Canada, and Russia, while in the Southern Hemisphere, the

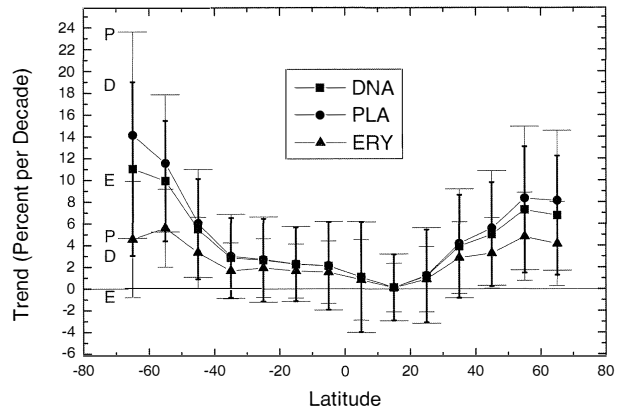


**Figure 9-13.** The percentage change per decade in action-spectra-weighted annual UV exposure as a function of latitude estimated from TOMS data (1979-1992) including cloud effects. The error bars indicate uncertainties of 2 standard deviations (from combined instrument error and variability in the UV-irradiance data). The symbols P and PLA stand for the plant damage action spectrum, D and DNA stand for the DNA damage action spectrum, and E and ERY stand for the erythemal action spectrum (J.R. Herman *et al.*, 1996).

largest increases are over the southern portions of Argentina and Chile. The large statistical-uncertainty bars in the calculated linear fits to the UV-exposure changes are caused largely by the interannual variability in ozone amount at all latitudes, and to a smaller extent by the annual variability of zonally averaged cloudiness. As part of the study of UV-irradiance changes since 1979, it was determined that there has been no statistically significant change in zonal average reflectivity (a surrogate for effective cloudiness, or cloud fraction combined with optical depth) for latitudes between  $\pm 65^\circ$ , even though there have been changes in regional reflectivities or cloud amounts.

TOMS-derived UV trends after 1992 cannot easily be estimated at present, because the continuous Nimbus-7/TOMS (November 1978 to May 1993) data record was broken in May 1993. The non-sun-synchronous (212-day orbital-precession period) Meteor-3/TOMS (August 1991 to December 1994) overlapped Nimbus-7/TOMS for over a year. After sufficient operating time, Earth Probe/TOMS (August 1996 to present) data may be used, in conjunction with other satellite and ground-based data, to fill in the data gap and to extend the trends.

## SURFACE ULTRAVIOLET RADIATION

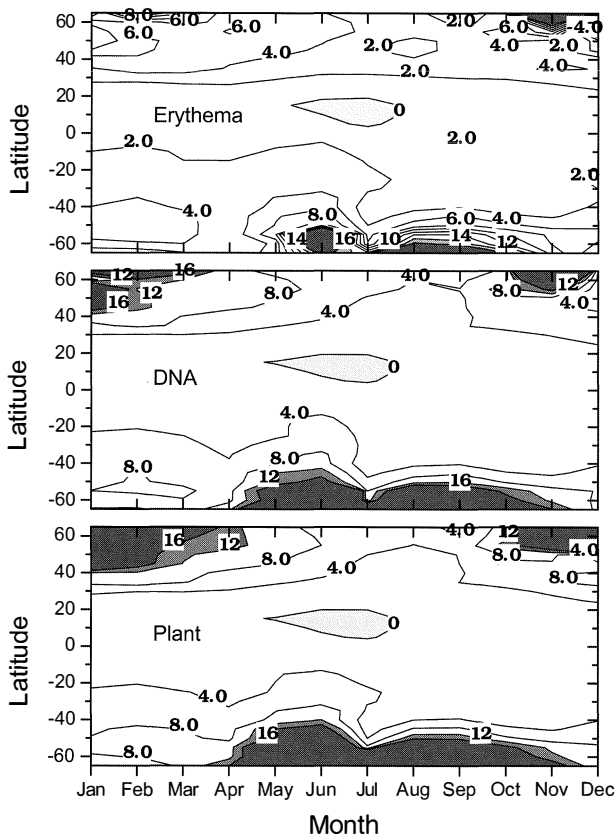


**Figure 9-14.** Percentage change per decade in UV exposure weighted by erythemal (top panel), DNA (middle panel), and plant damage (bottom panel) action spectra, as a function of latitude and month, estimated from TOMS satellite data from 1979 to 1992. The regions of statistically significant erythemal changes have a lower bound given by the 2% per decade contour line (J.R. Herman *et al.*, 1996).

Similar analyses of zonally averaged UV exposures for each month (1979 to 1992) show that the largest increases of UV irradiance have occurred at higher latitudes in the spring months corresponding to the largest decreases in stratospheric ozone (see Figure 9-14). The erythemal UV-irradiance changes shown in Figure 9-14 are statistically different from zero at about the 2% per decade contour line and larger. The computed UV-irradiance changes do not include the effects of the recently observed low ozone amounts at high latitudes in the Northern Hemisphere.

### 9.3.5 Other Methods of Inferring Historical UV Irradiances

The method described above is currently the only feasible means to estimate the global distribution of UV irradiance in near-real time. However, for the reconstruction of past records of UV, some alternative approaches show promise.

One approach to estimating past UV irradiances uses historical ozone data and current data from ground-based pyranometers, as first attempted by Ito *et al.* (1994). For this, it is first necessary to establish the relationship between pyranometer data and surface UV irradiance (Bodeker and McKenzie, 1996). Long-term global changes in UV irradiances are not known prior to the start of the TOMS satellite data in 1979. However, there is a good record of ozone measurements prior to 1979 from the Dobson network (Bojkov and Fioletov, 1995a) that could be used to estimate UV irradiances, at least at sites where ozone measurements are available.

Changes over even longer time scales have been investigated by Sabziparvar *et al.* (1998), who attempted to simulate changes in UV radiation since preindustrial times. They started with a four-season climatology of daily doses of UV irradiance based on satellite-derived ozone fields (TOMS) and satellite-derived cloud distributions (International Satellite Cloud Climatology Project, ISCCP) (Rossow and Garder, 1993). The changes in UV radiation were estimated from the combined effects of decreasing stratospheric ozone (from TOMS and Dobson data) and increases in tropospheric ozone (from a chemical transport model). The theory indicates that reductions in UV irradiance may have occurred at low latitudes; however, the accuracy of such estimates is unknown.

### 9.4 UV IRRADIANCE VARIABILITIES NOT RELATED TO TRENDS IN STRATOSPHERIC OZONE

The most critical parameter controlling clear-sky UV irradiance at the surface is the solar zenith angle (SZA). At a given location and at fixed SZA, the sources of UV-irradiance variability include clouds, aerosols, local changes in ground albedo, and short-term changes in ozone amount (Blumthaler *et al.*, 1994; Balachandran and Rind, 1995; Bordewijk *et al.*, 1995; Frederick and Steele, 1995; Huber *et al.*, 1995; Bernhard *et al.*, 1996; Kerr 1997, 1998).

### 9.4.1 Ozone and Other Trace Gases

Examples of the large variability in day-to-day changes and year-to-year changes are given by Zerefos *et al.* (1995a,b, 1997) for UV irradiances observed over Central Europe. They show that the erythemally weighted daily dose rate varies by a factor of 5 during the month of maximum exposure and the annual dose varies by about 20% for the 3 years 1994 to 1996. The variability of ozone and SO<sub>2</sub> can account for 50% and 26%, respectively, of the erythemal irradiance changes over Greece. A survey of 13 locations in Canada and Japan indicated only two sites where SO<sub>2</sub> was important for the reduction of UV irradiance (Fioletov *et al.*, 1998). These were Kagoshima, Japan (32°N, 131°E), located 10 km from a volcano (Sakurajima) with 236 days having SO<sub>2</sub> > 10 DU, and Toronto, Canada (44°N, 79°W), with 26 days having SO<sub>2</sub> > 10 DU from local pollution sources. For example, with an SO<sub>2</sub> amount of 10 DU the exposure to erythemally weighted irradiance is reduced by about 5% at midlatitudes (ozone amount about 330 DU and SZA = 40°).

At all latitudes, except near Antarctica (and recently the Arctic), day-to-day fluctuations in stratospheric ozone, tropospheric ozone, and interannual ozone variability cause short-term UV-B fluctuations in the long-term ozone decline. Even at lower latitudes (less than 30°), such fluctuations in ozone are observed to cause easily detectable UV-B changes. For example, during years when strong incursions of ozone-poor tropical air flow into temperate latitudes during spring and summer, UV-B at the surface can become significantly higher than normal (Mims *et al.*, 1995). At a given location, or on a zonal average basis, the approximately 2.3-year period QBO effect can cause a 3 to 5% interannual change in total column ozone amount at equatorial latitudes ( $\pm 10^\circ$ ) and at higher latitudes ( $> 20^\circ$ ) (Ziemke *et al.*, 1997).

In addition to ozone and SO<sub>2</sub>, several other pollutant trace gases can absorb significantly in the UV-B range. These include nitrogen dioxide (NO<sub>2</sub>), nitric acid (HNO<sub>3</sub>), formaldehyde (CH<sub>2</sub>O), and others. However, under normal condition their effects are below the detection threshold of UV spectroradiometers.

### 9.4.2 Clouds

Clouds (and nonabsorbing aerosols) reduce the UV irradiance at the ground by Mie backscattering at

all wavelengths. Plane-parallel modeling of cloud transmittance shows the reductions are wavelength dependent (Seckmeyer *et al.*, 1996; Kylling *et al.*, 1997; Frederick and Erlick, 1997; Krotkov *et al.*, 1998), even when the wavelength dependence of the cloud or aerosol scattering is ignored. When the models assume cloud characteristics that do not vary with wavelength, embedded in a Rayleigh atmosphere over a spectrally gray surface, the calculated wavelength dependence for cloud transmission to the surface is due to the interactions with Rayleigh scattering and ozone absorption. An example of the spectral variation of cloud transmittance was observed by Seckmeyer *et al.* (1996) and further analyzed by Kylling *et al.* (1997). For this case, the transmittance (as a fraction of clear-sky transmittance) was about 45% in the UV-A and 60% in the UV-B, a 15% difference.

Figure 9-15 shows the variations in the spectral dependence of the cloud factor (CF), the ratio of cloudy-sky irradiance to clear-sky irradiance (day 213) that can occur on different days as conditions change. The clear-sky irradiances were measured on day 213 ( $\Omega = 308$ ,  $R_{\text{TOMS}} = 6\%$ ). The data points are from spectroradiometric measurements made at Barrow, Alaska, August 1991 (available on CD-ROM; Booth *et al.*, 1993, 1998). Ozone values ( $\Omega$ ) and scene reflectivities ( $R_{\text{TOMS}}$ ) were determined from overpass data measured by Nimbus-7/TOMS. On the lightly clouded day 212 ( $R_{\text{TOMS}} = 22\%$ ), CF shows almost no longer-wavelength spectral dependence. The decrease of CF for the shorter wavelengths on day 212 (31 July 1991) is due to the greater column ozone ( $\Omega = 322$  DU) compared with day 213 ( $\Omega = 308$  DU). On the moderately clouded day 215 ( $R_{\text{TOMS}} = 61\%$ ) the spectral influence of the clouds and that of the difference in total ozone ( $\Omega = 321$ ) combine to give the short-wavelength decrease, while the long-wavelength behavior is due to the influence of the clouds alone. On day 216 ( $R_{\text{TOMS}} = 77\%$ ), which was heavily clouded, the spectral variation of CF is the greatest ( $> 25\%$ ) even though the ozone amount is nearly the same as the reference case (day 213).

Systematic changes in UV have also been related to changes in clouds, as shown from multi-year data taken since 1968 at the Meteorological Observatory of Moscow University (Nezval, 1996). Local changes in UV-A surface irradiances taken at 5-minute intervals from an elevated relatively clear site were complemented by simultaneous hourly visual observations of clouds (cloud types, layers, and fraction). This dataset was used to

## SURFACE ULTRAVIOLET RADIATION

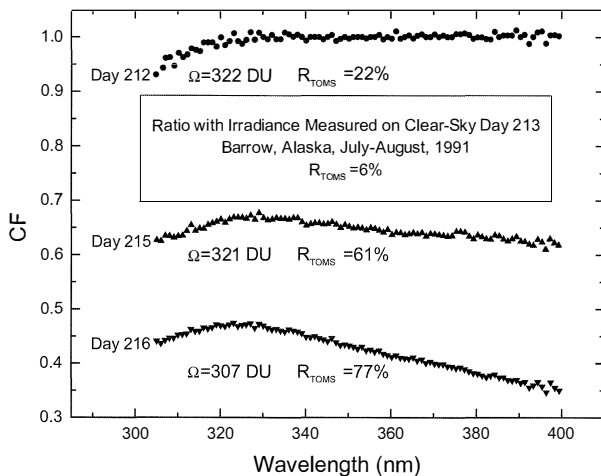


**Figure 9-15.** Wavelength dependence of cloud transmittance in a Rayleigh-scattering atmosphere for different ozone amounts ( $\Omega$ ) and cloud amounts (reflectivities,  $R$ ). The cloud factor (CF) is from measurements made by spectroradiometer at Barrow, Alaska, July-August 1991; CF = ratio of cloudy-sky irradiance to clear-sky irradiance (day 213,  $R_{\text{TOMS}} = 6\%$ ). (CD-ROM data from Booth *et al.*, 1993, 1998.)

show that the average UV irradiance for the period 1968-1992 has decreased at Moscow by 15-20% (with some seasonal dependence). At the same time, the average cloud fraction has increased significantly (for lower layer clouds by 27% and for all cloud layers by 14%).

Measurements at Raleigh, North Carolina (Estupinan *et al.*, 1996), show the UV-irradiance attenuation for unbroken clouds (up to 99%) and haze (5 to 23%). However, for broken convective-type cumulus clouds of large vertical extent, increases of up to 27% have been observed (see also Nack and Green, 1974; Seckmeyer *et al.*, 1996; Frederick and Steele, 1995). Additional measurements of UV-B under partially cloudy conditions using a Brewer spectrometer in North Carolina show increases over clear-sky values of as much as 11% (Schafer *et al.*, 1996). According to Estupinan *et al.* (1996), broken cloud fields of types with small vertical extent show no excess of UV irradiance over clear-sky values. Additional validation studies at different locations are needed to further quantify the enhancements found in these studies.

Analysis of data from the Canadian Brewer network indicates that the effects of thin clouds, which reduce irradiance by up to 50%, are nearly the same for

wavelengths between 280 and 325 nm (Fioletov *et al.*, 1997; Wardle *et al.*, 1997). The effect of cloud cover on reducing global irradiance has little dependence on zenith angle. However, large convective clouds that reduce irradiance values to less than 10% of clear-sky values show enhanced ozone absorption effects that are likely caused by increased multiple scattering within the cloud and in the regions above and below the cloud. Recent measurements have been conducted of the angular distribution of diffuse radiation underneath overcast skies (Grant *et al.*, 1997). They show that the ratio of measured irradiance under overcast skies was not correlated with cloud-base height, opaque cloud fraction, or solar zenith angle. Grant and Heisler (1997) found that the rate of change  $N_r$  (or relative distribution) of both UV-A and UV-B radiances with SZA ( $\theta$ ) for solar-obscured overcast skies can be modeled as

$$N_r = 0.426 \frac{1 + 1.23 \cos(\theta)}{1 + 1.23} \quad (9-3)$$

### 9.4.3 Altitude

As has been shown from numerous radiative transfer studies, UV irradiances change with the observing altitude because of changes in scattering and absorption. The altitude dependence varies with both SZA and wavelength. Therefore, it is not possible to describe the change with altitude by a single number in percent per kilometer (Duguay, 1995; Seckmeyer *et al.*, 1997; Krotkov *et al.*; 1998). For example, Seckmeyer *et al.* (1997) found that the monthly erythemally weighted irradiation is between 25% and 90% higher on the Zugspitze (3-km altitude) than at the lower site in Garmisch-Partenkirchen (0.73 km) within a 5-month period. The variability in the differences indicates that they are caused by a combination of several factors, including Rayleigh scattering, cloud effects, air pollutants (e.g., tropospheric ozone), aerosols, and surface albedo. These results show that data from a single site are not sufficient to determine the altitude effect for UV irradiance at sites other than the measurement site.

Regional differences in the altitude dependence of UV irradiance have also been reported by Blumthaler *et al.* (1997) based on measurements made at Jungfraujoeh, Switzerland (3.576-km altitude), and Innsbruck, Austria (0.577-km altitude), where daily clear-sky erythemal doses have been compared. The paper showed an increase of 8% per km for total irradiance, 9% per km

for UV-A, and 18% per km for erythemal effective irradiance during the summer. It also showed that the altitude dependence of the direct radiance is larger than that of the global radiance at all wavelengths.

A study of the altitude dependence of UV irradiance in clean, dry air in South America showed much smaller altitude gradients than in Europe and in more polluted regions of the continent than reported in the previous Assessment (WMO, 1995). The gradients that were determined for global irradiances, as well as the direct and diffuse components separately, depended on wavelength and on SZA (Piazena, 1996). As expected, global and direct irradiances increased with altitude, whereas the diffuse component decreased. In the UV-B range, global irradiances generally increased by 8-10% per km for SZA > 70°, which is still a somewhat larger increase than predicted for clear sky.

High-altitude results (3.4 km) from an ultraviolet spectroradiometer installed at Mauna Loa Observatory (MLO) in Hawaii have been reported by Bodhaine *et al.* (1996, 1997). For observations at SZA = 45°, the erythemally weighted UV irradiance at MLO can exceed 0.21 Wm<sup>-2</sup>, which is approximately 15-20% greater than that seen at clean-air sites near sea level (e.g., Lauder, New Zealand) for similar ozone amounts. For overhead sun conditions at MLO, the largest value of erythemal UV irradiance was 0.51 Wm<sup>-2</sup>. For now, this is probably the highest recorded value of erythemal irradiance anywhere on the Earth's surface, as would be expected for these conditions.

#### 9.4.4 Aerosols

Changing aerosol (and cloud) conditions can lead to increases or decreases in UV irradiance (Justus and Murphey, 1994; Mims and Frederick, 1994; Forster and Shine, 1995; Dahlback, 1996; Zerefos *et al.*, 1994; Olmo and Alados-Arboledas, 1995). In general, the backscatter from volcanic aerosol decreases the erythemal UV irradiance by about 5% (Tsitas and Yung, 1996). At high SZA, when there is a thin aerosol layer at an altitude where the direct solar beam is still a significant component of the total irradiance, the amount of UV-B at the surface can be increased while at the same time the amount of UV-A is decreased (e.g., Forster and Shine, 1995). This is because of the reduced average optical path through the ozone layer for scattered radiation compared to the direct beam. The short-wavelength portions of UV-B (<300 nm) are absorbed sufficiently

by ozone so that its surface irradiance is increased by the presence of additional high-altitude scattering, while UV-A is reduced by the additional amount scattered back to the top of the atmosphere (Tsitas and Yung, 1996). This effect is especially important at high latitudes where the proportion of scattered irradiance to direct-beam irradiance is larger due to higher SZA (Taalas *et al.*, 1997).

Atmospheric aerosols affect the amount of global irradiance received at the Earth's surface after scattering and absorption. The largest aerosol reductions in UV irradiance are associated with the major sources of dust and smoke in Africa and South America (Herman *et al.*, 1997). The reductions in these regions frequently exceed 50% of the clear-sky value. The amount of UV-irradiance reduction depends strongly on the absorption properties of the aerosols. Most of the aerosols in the Northern Hemisphere are sulfates or other industrial pollutants whose Mie scattering reduces the surface UV irradiance by about 10% (Krotkov *et al.*, 1998).

There are relatively small plumes of UV-absorbing aerosols that strongly reduce surface UV irradiance over urban areas such as Los Angeles, Mexico City, Beijing, or Berlin, or downwind from regions of seasonal forest fires (e.g., Canada, California, and Russia). Smaller UV-irradiance reductions of 10 to 20% also occur under the widespread nonabsorbing aerosols prevalent in the Northern Hemisphere (Seckmeyer *et al.*, 1994b; Krotkov *et al.*, 1998) and in small regions of the Southern Hemisphere (see also Ryan *et al.*, 1996).

In localized regions where there are increased atmospheric pollutants from anthropogenic activities, the reduction of pollutants for health reasons may have the effect of increasing UV radiation at the ground closer to preindustrial levels for the region. In addition to pollution, long-term increases of cloudiness may have significantly decreased UV irradiation in Central Europe since the 1950s, and may be partly masking an upward trend of UV irradiances caused by ozone depletion (Seckmeyer *et al.*, 1994b; Nezval, 1996; Varotsos *et al.*, 1995; Zerefos *et al.*, 1997). Observations by Feister and Grewe (1995) showed UV-irradiance enhancements arising from decreases in the ozone amount and changes in the average amount of cloudiness over middle Europe (52°N) for the years 1992 and 1993.

The effect of aerosols on UV-B irradiances was quantified using data from clear days over a 3-year period (1989-1991) at Toronto (Kerr, 1998). Results of this analysis show that for the aerosols present over this site,

## SURFACE ULTRAVIOLET RADIATION

reductions in global irradiance are about 20-30% of the reductions in direct irradiance. That is, if aerosols were to reduce the direct irradiance by 10%, the global irradiance would be reduced by 2-3%. The reduction has little wavelength dependence and is in reasonable agreement with radiative transfer models results for aerosols that are nearly nonabsorbing (single scattering albedo  $> 0.95$ ; Krotkov *et al.*, 1998). The residual variability, after considering the effects of ozone absorption and aerosol scattering, was between 2 and 5% over the 3-year period.

### 9.4.5 Surface Albedo Variations (Snow)

For most conditions at non-polar latitudes, the surface reflectivity at UV wavelengths is less than 10% for ground without snow or for water (Herman and Celarier, 1997). The snow-free surface reflectivities (Lambert equivalent reflectivities) estimated from the TOMS radiance data range from a minimum of about 2% over vegetation-covered land to about 8% over some portions of the Sahara desert and over large areas of the ocean that are relatively free from UV-absorbing phytoplankton. There is a small seasonal dependence in the estimated surface reflectivity, but the reflectivity always stays below about 8% except in regions where there is snow or ice cover. All the TOMS estimates of surface irradiance use the estimated UV-reflectivity climatology generated from 14 years of Nimbus-7/TOMS data.

The occurrence of snow on the ground is the main factor that causes large surface albedo changes in the UV. Results of a study reported in Wardle *et al.* (1997) summarize the effects of snow on UV irradiance at seven sites in Canada. The irradiance at 324 nm was used as an indicator, because ozone has negligible absorption at this wavelength. The variation due to zenith angle was removed by normalizing the observed irradiance at 324 nm to that expected under a clear sky at the same zenith angle. A comparison of observations taken with snow on the ground and those taken without snow shows an enhancement in the normalized 324-nm irradiance ranging from 8% (Halifax) to 39% (Churchill). When there was no snow on the ground, the normalized 324-nm irradiance was nearly constant for all seven stations. Snow has significantly different enhancements at different stations, likely because of terrain or snow quality differences. For example, the enhancements in the Arctic (Resolute, 35%, and Churchill, 39%), with flat and "white" terrain, are larger than those seen at urban

sites (Toronto, 12%, and Halifax, 8%).

Even if the snow/ice surface reflectivity does not depend on wavelength, the reflectivity-amplification of UV irradiance is not neutral, but has a strong maximum of about 0.5 near 320 nm for a surface reflectivity of 0.8 (Lenoble, 1998; Krotkov *et al.*, 1998; Chubarova, 1993, 1998) (see Figure 9-16). This maximum occurs for both clear-sky and cloudy-sky cases. However, for cloudy skies the slope from 320 nm to 400 nm is very small compared with the clear-sky case, because of the nearly wavelength-independent reflection from the clouds. Increased atmospheric Rayleigh scattering back to the surface at shorter wavelengths causes the increasing effect of changes in surface reflectivity with wavelength (from 400 nm to 320 nm). The small structure seen starting at about 330 nm is caused by ozone absorption. For wavelengths shorter than 320 nm the increasing ozone absorption dominates the increasing Rayleigh scattering, or cloud reflection, and results in a smaller UV-irradiance increase relative to 320 nm. The formal solution for the results presented in Figure 9-16 is given (in percent) as

$$\frac{dF}{F} = 100 \frac{S_b}{1 - R_s S_b} \frac{dR_s}{R_s} \quad (9-4)$$

Here  $S_b$  is the wavelength-dependent fraction of radiation backscattered from the atmosphere back to the surface.  $S_b(320 \text{ nm})$  is frequently greater than 0.6 for clouds and about 0.4 for clear sky.  $R_s$  is the surface reflectivity;  $R_s \approx 0.05$  for ground and  $R_s > 0.8$  for fresh snow.  $F$  is the irradiance at the Earth's surface.

Figure 9-16 also shows the effect on modeled UV irradiances of an uncertainty in knowledge of the surface reflectivity. For clear skies the errors in the irradiances are roughly 0.5% for each percent uncertainty in the surface reflectivity. The presence of significant cloud cover, and particularly cloud cover over snow, can lead to large errors in estimated UV irradiances from model calculations that assume a constant albedo. Errors in surface reflectivity affect the estimate of UV irradiances from satellite data and affect the derivation of atmospheric parameters (e.g., ozone and aerosol amounts) from ground-based measurements using global solar irradiance (direct + diffuse), but not those using the direct solar component alone. These results have not been validated against ground-based measurements.

Away from snow and ice, the reflection problems for satellite retrievals of UV are minimized because of

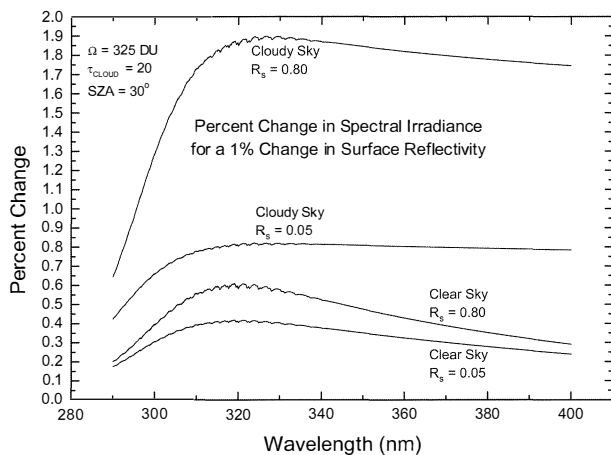


**Figure 9-16.** Reflectivity amplification of UV irradiances as a function of wavelengths for ground reflectivity ( $R_s = 0.05$ ) and fresh-snow/ice conditions ( $R_s = 0.80$ ) for clear and cloudy ( $\tau_{\text{cloud}} = 20$ ) skies with column ozone amount 325 DU, SZA =  $30^\circ$ , and  $dR_s = 0.01$ . (Adapted from Lenoble, 1998.)

the low values of reflectivity in the UV of 4 to 8% (Eck *et al.*, 1987; Herman and Celarier, 1997) over both land and water. Even lower values of about 1% in the UV-B, 2% at 400 nm, and 4.5% at 450 nm have been measured over long grass in New Zealand (McKenzie *et al.*, 1996). There the albedos tend to increase at large SZAs, implying that the surface is not strictly Lambertian. Because of the low reflectivities and large amount of scattering in the boundary layer, moderate percentage errors in assumed surface reflectivity have little effect on the UV irradiance. There are also problems with realistically representing boundary layer scattering because of the difficulties in haze characterization for each particular case (Schwander *et al.*, 1997).

## 9.5 GEOGRAPHIC DIFFERENCES IN UV IRRADIANCES

The major causes of geographic differences in peak summer or annually integrated UV irradiances are differences in latitude (i.e., SZA); regional differences in cloud, ozone, and aerosol amounts; differences in terrain height; and a larger Sun-Earth separation during the summer in the Northern Hemisphere compared with the austral summer.

### 9.5.1 Mid and Low Latitude

While low-latitude regions ( $\pm 20^\circ$ ) have not experienced any significant long-term declines in ozone amounts, these regions receive the highest amounts of daily UV irradiance except for a few locations at extremely high elevations. Because of the very dense populations in and near this latitude region, it is important to understand UV exposure and any possible increases. Measurements of surface UV irradiance in Penang, Malaysia ( $5.5^\circ\text{N}$ ,  $100^\circ\text{E}$ ), have been made to establish the diurnal and seasonal dependence. It was shown that the surface irradiance routinely reaches the extreme zone (UV index  $> 9$ ; see Section 9.7) for about 5 hours each day. Because ozone is nearly constant with the seasons, the modulation of UV irradiance is mainly by clouds. An extension to these data (M. Ilyas, University of Science-Malaysia, personal communication, 1998) shows that the amount of UV irradiance reaching the surface was reduced substantially during haze events from Indonesian biomass burning during 1997 and 1998.

Investigations of geographic differences based on measurements from the same instrument (Seckmeyer and McKenzie, 1992; Bernhard and Seckmeyer, 1997) have shown that for clear-sky observing conditions and similar SZA, UV irradiances measured in New Zealand are much higher than in Central Europe. For example, the DNA and erythemal action-spectra-weighted irradiances are larger in New Zealand by factors of 1.81 and 1.44, respectively. The average difference in total column ozone between the two sites is 53 DU (New Zealand has less ozone). The ozone difference contributes to an increase in DNA action-spectra-weighted UV irradiance by a factor of  $1.58 \pm 0.1$ . The corresponding factor for erythemal action-spectra-weighted irradiance is  $1.28 \pm 0.1$ . Although stratospheric ozone is the dominant factor, a part of the differences arises from Sun-Earth separation differences, and changes in tropospheric pollution (ozone, aerosols), which has increased in Central Europe (Stahelin and Schmid, 1991; Seckmeyer and McKenzie, 1992) compared with the relatively clean Southern Hemisphere atmosphere.

In a study that also considered clouds, geographical differences in erythemally weighted UV irradiance were investigated on the basis of measurements of five spectroradiometers and several broadband UV-irradiance meters (Seckmeyer *et al.*, 1995) from four different groups (Garmisch-Partenkirchen, the National Institute of Water & Atmospheric Research (NIWA), the

## SURFACE ULTRAVIOLET RADIATION

Australian Radiation Laboratory (ARL), and the U.S. National Science Foundation (NSF)). Before the survey, the spectroradiometers were brought together for an intercomparison campaign. Based on the results of this examination, adjustments were made to correct for systematic calibration differences seen in the spectroradiometric data in order to achieve consistency between four different groups of instruments. The broadband UV-irradiance meters were calibrated in the field against the spectroradiometers.

Data from 12 locations, ranging from the South Pole to Barrow, Alaska, were analyzed to study geographic differences in UV. For each site, daily integrals of erythemal irradiance measured during summer months, maxima, and monthly means of the daily integrals were compared. Data from 1991 were used at Australian sites. At other sites, data were from 1993-1994. At low latitudes, these irradiances appear to be similar in both hemispheres. However, for mid and high latitudes, it was found that geographic differences in UV irradiance clearly exceed the measurement uncertainties (less than  $\pm 10\%$ ). The latitudinal variations seen in the summer months are shown in Figure 9-17a. Observed latitudinal gradients of UV irradiance in the Southern Hemisphere were much smaller than in the north, with mid-southern latitudes receiving approximately 40-50% more UV irradiance than corresponding sites in the Northern Hemisphere. An example is the difference observed between Lauder, New Zealand ( $45.05^{\circ}\text{S}$ ,  $169.67^{\circ}\text{E}$ ), and Neuherberg, Germany ( $50^{\circ}\text{N}$ ,  $6.95^{\circ}\text{E}$ ), for similar seasonal conditions, but very different ozone amounts (266 DU in Lauder and 352 DU in Neuherberg,  $\sim 30\%$  difference) (Seckmeyer and McKenzie, 1992). In the Seckmeyer *et al.* (1995) study, hemispheric differences are most pronounced at high latitudes, consistent with the results of the previous study by Seckmeyer and McKenzie (1992), where only clear-sky conditions were investigated. In summer months the daily UV doses at high southern latitudes, and at the South Pole, are greater than at midlatitudes in the Northern Hemisphere. The largest maximum daily dose for all sites considered was for Palmer Station, Antarctica (Figure 9-17b). The measurements were considered as a first step to estimate geographic differences in UV. These latitudinal differences are much larger than those shown by the satellite retrievals from the summer of 1997 (Figure 9-11). Further studies are required to understand these discrepancies and to determine whether the differences are representative of zonal means.

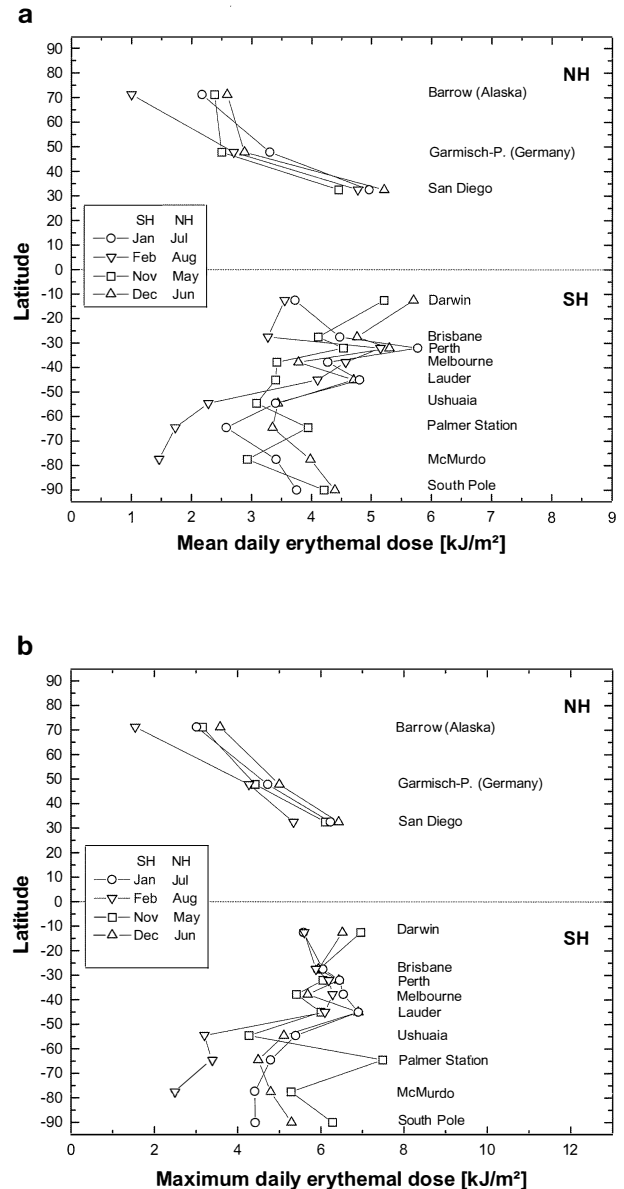


**Figure 9-17.** Measured monthly mean (a) and maximum (b) of the daily integrals of erythemal UV irradiance during the summer months in the Northern Hemisphere (NH) and Southern Hemisphere (SH) as a function of latitude, including effects of aerosols, cloud, altitude, and ground albedo (from Seckmeyer *et al.*, 1995).

Latitudinal variability of UV irradiance has also been investigated using a mobile spectroradiometer and comparisons with a radiative transfer model. Bernhard *et al.* (1997) measured the difference in solar UV irradiances between Southern Germany (47.5°N) and tropical Australia (19°S). The data from Australia are from a 1-month campaign during the austral summer of 1995-1996. The maximum values of erythemally weighted irradiance on clear-sky days were 372 mW m<sup>-2</sup> (Australia) and 234 mW m<sup>-2</sup> (Germany), which gives a difference of about 60%. For cloudless days there was good agreement with radiative transfer model calculations, with the differences explained by the smaller SZA and lower ozone amounts in Australia.

### 9.5.2 High Latitude (North and South)

The maximum variability of UV-B caused by ozone changes, on time scales of daily to yearly, occurs at high latitudes (above 50°) in both hemispheres. However, year-to-year differences in cloudiness are generally the largest source of interannual variability in monthly integrated UV irradiance measured at the ground (Frederick *et al.*, 1993; Diaz *et al.*, 1994; Frederick *et al.*, 1994). This can vary from one location to the next, depending on the timing and severity of ozone depletions. At the NSF site in Ushuaia, Argentina (54.6°S), the lowest ozone column amounts (1988-1997) were in the years 1995 to 1997. The highest UV irradiances occurred whenever the ozone-hole region (220 DU contour) elongated into an elliptical shape that rotated over South America and the cloud cover was minimal. The highest 24-hour integrated irradiance (exposure) occurred during the coincidental occurrence of cloud-free days with small ozone depletion (less than 10%) during the longer days of mid-summer, rather than during the much more severe ozone depletions in early spring (Diaz *et al.*, 1994).

TOMS observations of ozone amounts over Ushuaia show a steady decline since 1980 on top of large day-to-day variability (Bojkov and Fioletov, 1995a; Bojkov *et al.*, 1995a; Diaz *et al.*, 1994, 1996). Using ground-based measurements from an NSF high-resolution spectroradiometer, the modeled increase in UV irradiance for 1989-1993 relative to the 1979-1983 period was estimated to be 80% at 300 nm and 35% at 305 nm for a 15% ozone decrease (about 345 DU to 300 DU). Bojkov *et al.* (1995a) state that the 300-nm irradiance observed during the spring (October) is as high as it is 4 months later during the summer. The char-

acteristic spectral shape of the percentage change demonstrates that the increase in UV irradiance is caused by ozone decreases. Kirchhoff *et al.* (1997) found similar results, where measurements were made using a Brewer (single monochromator) spectroradiometer at Punta Arenas, Chile. The research shows significant enhancements in UV-B during the days when ozone-poor Antarctic air passes over portions of South America. Results from a cruise originating in Punta Arenas, Chile (53°S), near the tip of South America, and traveling to 71°S near Palmer station showed that the average UV-B radiation (280-330 nm) inside the Antarctic ozone hole was double the average measured outside the region. At the same time, UV-A irradiances were not affected (Wendler and Quackenbush, 1996).

Increased UV-B radiation has occurred over the Arctic and high-latitude regions surrounding the Arctic (e.g., northern Canada and Russia), corresponding to more frequent occurrences of low ozone amounts during the spring (Bojkov *et al.*, 1995b; Bojkov and Fioletov, 1997; Gurney, 1998). For example, with clear-sky conditions, the percentage increases in UV irradiance at 300 nm, 305 nm, and 310 nm are expected to be 65%, 33%, and 17%, respectively, from an average 10% springtime ozone decrease near 50°N. Data from Canada during 1996 and 1997 showed even lower ozone values than found by Bojkov *et al.* (1995b) and correspondingly high UV-B irradiances (Fioletov *et al.*, 1997). Some of the ozone decrease, and therefore UV irradiance increase, is associated with colder stratospheric temperatures in recent years (e.g., Ramaswamy *et al.*, 1996).

### 9.5.3 Antarctica

At the South Pole (~90°S) the only solar angle variation comes from the seasonal cycle, with the solar elevation angles ranging from 23° (summer) to angles below the horizon. The dominant features in the Antarctic are the high surface reflectivity for UV irradiance from ice and snow and the large SZA. Both of these features increase the amount of diffuse irradiance at the surface relative to the direct irradiance. Grenfell *et al.* (1994) measured variations in snow albedo at Amundsen-Scott South Pole Station and the Vostok Station, finding a nearly uniform high value (0.96-0.98) across the visible and UV spectrum (300-400 nm), nearly independent of snow grain size and SZA. Under clear skies Grenfell *et al.* (1994) found that significant errors in apparent albedo can result if the instrument's cosine

## SURFACE ULTRAVIOLET RADIATION

response collector plate is not made parallel to the local surface instead of the horizon. Perturbations by clouds are relatively small at this site, because of the high surface albedo and the extremely cold temperatures that keep clouds from becoming optically thick. As is normal for Antarctica, the highest instantaneous UV irradiances (erythema, or UV-B) do not occur at the time of the greatest ozone depletion, but at a time closer to the summer solstice, combining the effects of higher SZAs with relatively low ozone. Although the relative seasonal increases are large, the absolute monthly UV exposures at this site are less than summer values at mid or low latitudes, but exceed values in the Northern Hemisphere with comparable SZA.

### 9.6 COMPARISON OF CALCULATIONS WITH OBSERVATIONS

The problem of successfully comparing different measurements of UV irradiances at the Earth's surface is tied directly to accurate modeling using radiative transfer calculations and the availability of relevant input data. Most published radiative transfer calculations are essentially plane-parallel multiple-scattering methods, with some having spherical geometry included for the primary and first-order scattering (pseudo-spherical). Some methods of calculation are more suitable for certain situations related to large optical depths (variations of doubling methods) and some are more suitable for including complex aerosol-scattering phase functions (variations on Gauss-Seidel methods).

The Gauss-Seidel method (Herman and Browning, 1965) has been used for radiative transfer calculations ranging from the UV to the IR. This method can handle such conditions as a non-Lambertian reflecting surface (Ahmad and Fraser, 1982), polarization, all orders of multiple scattering, thick aerosol clouds (Herman *et al.*, 1980), a mixture of particle compositions with different vertical distributions (i.e., aerosols and water droplets), scattering by large particles, scattering by non-spherical particles, scattering in a spherical atmosphere (B.M. Herman *et al.*, 1996), and thermal emission.

#### 9.6.1 Intercomparison of Radiative Transfer Models

One study of detailed comparisons of backscattered radiances has been made with the following codes: the TOMS Ozone Processing Team's version of the

Gauss-Seidel code (the Herman-Flittner code); the pure Rayleigh scattering code of Dave (1964) (used to create the TOMS Version 7 look-up tables); the Dave Fourier expansion Mie and Rayleigh scattering code (Dave and Gazdag, 1970) (used to analyze atmospheric aerosols and their effects on UV irradiance (Torres *et al.*, 1998; Krotkov *et al.*, 1998)); and the unpolarized version of the discrete ordinates radiative transfer method (DISORT) method (Stamnes *et al.*, 1988) with the pseudo-spherical correction added. All the comparisons show agreement in the inferred surface irradiances to better than 1% when the atmospheric model is the same. However, the differences in inferred radiances between codes including polarization (Dave, 1964; Dave and Gazdag, 1970; Herman and Browning, 1965) and those not including polarization (Stamnes *et al.*, 1988) can be as large as 10% for a pure Rayleigh atmosphere.

Recently, full spherical geometry calculations (e.g., B.M. Herman *et al.*, 1996), which are required to model UV irradiance at large SZAs, have become possible on moderately fast computers. These have been compared with much faster plane-parallel computations. For irradiances, comparisons of pseudo-spherical calculations with full spherical geometry calculations show 1% agreement to approximately 84° SZA.

Irradiance calculations can neglect polarization as a reasonable approximation. However, for calculating radiances at the Earth's surface, the models should include polarization effects. For small to moderate optical depths ( $\tau = 2$  to 5) of scattering within clouds, polarization effects are important for radiances at the Earth's surface. For larger Mie scattering optical depths ( $\tau > 10$ ), the solutions including polarization and those neglecting polarization agree to within 1%. Radiative transfer calculations suitable for large optical depths neglecting polarization are much faster computationally than methods including polarization.

For irradiance calculations with SZA < 84°, different modeling methods agree well. However, to represent the real atmosphere, there remain a number of outstanding problems. From the viewpoint of local UV irradiance and radiance, the next important problem is that of modeling cloud effects for broken cloud fields, cloud fields containing different cloud types, and multi-layer broken clouds. An additional problem is dealing with reflections from the Earth's surface, particularly over snow and ice with and without clouds (Lenoble, 1998; see also Figure 9-16). There are also remaining problems with the angular distribution of reflections

(non-Lambertian reflections) and the interactions with clouds.

Various approximate methods have been used for computational efficiency. Use of these methods may compromise the accuracy needed to compare with measurements. Forster and Shine (1995) compared the accuracy of the delta-Eddington and discrete-ordinate approximations for calculating high-wavelength-resolution UV irradiances at the Earth's surface. For certain atmospheric conditions, differences were greater than 10% in integrated UV-B between the delta-Eddington and eight-stream discrete-ordinate model.

Two-stream modeling of clear-sky and all-sky spectral irradiances during a full annual cycle (1992) were compared for Ushuaia, Argentina (55°S) (Diaz *et al.*, 1996). Measured irradiances at 340 nm were used to characterize the attenuation provided by cloudy skies. When irradiances in the range of 302.5 to 320 nm were corrected for cloud attenuation, both sets of data showed agreement, with correlation coefficients ranging from 0.97 to 0.99. At high SZA the differences are consistent with the neglect of spherical geometry in the calculated irradiances.

Model comparisons have been carried out using data from Toronto, Canada (Eck *et al.*, 1995), tropical Australia (Bernhard *et al.*, 1997), Greece (Weihs and Webb, 1997b), and southern Germany (Mayer *et al.*, 1997). The results suggest that accurate UV-A (for cloud attenuation) and ozone measurements combined with multiple-scattering radiative transfer calculations can provide the UV irradiances over the 280-400 nm range. Surface UV irradiances in the presence of broken clouds have been modeled using Monte Carlo methods (Geogdzhayev *et al.*, 1996, 1997). It should also be possible to use the approximate, but computationally faster, independent-pixel methods (Marshak *et al.*, 1998). A recent study by Loeb and Davies (1996) based on analysis of 1 year of Earth Radiation Budget Satellite (ERBS) reflectivity data between  $\pm 30^\circ$  latitude, matched on a pixel basis to plane-parallel model calculations, showed a systematic shift toward larger reflectivities with increasing SZA relative to the observations. At nadir, differences were found to be about 10% and increased to 30% at large SZA (near  $90^\circ$ ), the differences being attributed to the three-dimensional characteristics of real clouds compared with a plane-parallel simulation.

It is desirable to perform wide-ranging parameter studies on various standard radiative transfer models to eliminate computational artifacts. One such study

(Forster, 1995) examined the influence of surface albedo, ozone profile, cloud, and aerosol on the UV irradiances calculated by the discrete-ordinate model. This was done to understand the causes of the largest modeling uncertainties and to allow calculation of errors for subsequent model predictions. The study showed that at  $50^\circ\text{N}$  in midsummer, the effect on UV-B caused by a decrease in total column ozone could be partially offset by the addition of an urban-type aerosol. Weihs and Webb (1997a,b) added to the parameter space testing in Forster (1995); they give a useful discussion of how uncertainties in model input parameters translate into UV irradiance errors.

For the purposes of calculating UV-forecasting indices (see Section 9.7) it has been shown (e.g., Diaz *et al.*, 1996; Koepke *et al.*, 1998) that two-stream models are adequate.

### 9.6.2 Clear-Sky Comparisons with Observations

Blumthaler *et al.* (1996) have compared measurements taken in Europe at sites that are considered relatively clear of aerosols (Lerwick, Scotland,  $60.15^\circ\text{N}$ ,  $1.17^\circ\text{W}$ , and Esrange, Sweden,  $67.88^\circ\text{N}$ ,  $21.12^\circ\text{E}$ ) with a site with heavy pollution (Ispra, Italy,  $45.8^\circ\text{N}$ ,  $8.6^\circ\text{E}$ ). The data were compared with aerosol-free modeling results. The comparison showed a strong dependence of UV-B sky radiance on the presence of aerosol particles and a possible dependence on tropospheric ozone because of increased scattering from aerosols. The absolute disagreement with model results is considerable, but the deviation from the predicted shapes shows the aerosol effect clearly. Zeng *et al.* (1994) have compared clear-sky measurements before and after the Mt. Pinatubo eruption, and with a snow-covered surface, with the results from a discrete-ordinates radiative transfer model. Their comparison suggests that reasonable clear-sky diffuse/direct ratios can be computed if the atmospheric density, ozone amounts, surface albedo, and aerosol optical properties are known.

Clear-sky surface UV-B measurements in Greece have been compared with a discrete-ordinates model that included nonabsorbing aerosols in the first few kilometers above the ground (Wang and Lenoble, 1994). Agreement to about 6% was observed over a wide wavelength (290-350 nm) and SZA range ( $44\text{--}75^\circ$ ) for both global and direct irradiances, and it was concluded that the model output might be used as a means of

## SURFACE ULTRAVIOLET RADIATION

validating instrument calibration and long-term maintenance. The authors also suggest that the models be used to extrapolate into the short-wavelength regions for which most instruments fail to provide correct values. The agreement found is consistent with the results of an uncertainty analysis of model input parameters by Schwander *et al.* (1997).

An extensive study comparing measured and calculated UV spectral irradiances has been carried out by Mayer *et al.* (1997). Approximately 1200 clear-sky spectra obtained over a 2-year period (1994 to 1996) were used, covering the wavelength range 290-410 nm, for SZAs ranging up to 80°. The spectra represent a dynamic range of approximately  $10^6$  in irradiance. Ozone column amounts and wavelength-dependent aerosol optical depths were derived from near-simultaneous direct-sun spectra. When these were used as inputs to the radiative transfer model (pseudo-spherical version of DISORT), the modeled global irradiance showed excellent agreement with the measured irradiances over the full range of SZA and wavelengths tested. Although there were systematic differences of up to 11%, the variances were generally smaller than 2-3%, which is within the range of instrument noise. Since that paper (Mayer *et al.*, 1997) was published, the instrument data analysis procedures were improved by changing the lamp standard, correcting for small drifts in the working standard, correcting for amplifier and detector non-linearities, and improving the cosine correction. The resulting model-measurement differences were reduced significantly and are shown in Figure 9-18.

The close agreement between model and measurement over such a wide range gives confidence in both the ability of the measurements to sustain accuracy over long periods and the ability of the radiative transfer model to accurately predict the effects of future changes for clear-sky conditions. For all of these observations at Garmisch-Partenkirchen, a constant single-scattering albedo was assumed. However, a recent study (Kylling *et al.*, 1998) suggests that in more polluted conditions (e.g., Thessaloniki), variations in this parameter can also be important.

### 9.6.3 General Comparisons with Observations

Spectral measurements have been compared with discrete-ordinates radiative-transfer model results for both clear and cloudy conditions (Forster *et al.*, 1995;

Weihls and Webb, 1997b). Measurements and model agreed to within 6-10% for clear-sky UV-B irradiances, with worse agreement at short wavelengths ( $\lambda < 300$  nm). This result is consistent with earlier work of Wang and Lenoble (1994). For cloudy skies, Weihls and Webb found the agreement was worse, with deviations between measurements and calculations of  $\pm 10\%$  at two locations. The uncertainty of model input parameters was also shown to be an important contributing factor, especially measurements of the aerosol optical depth.

The uncertainties in modeled UV irradiances are

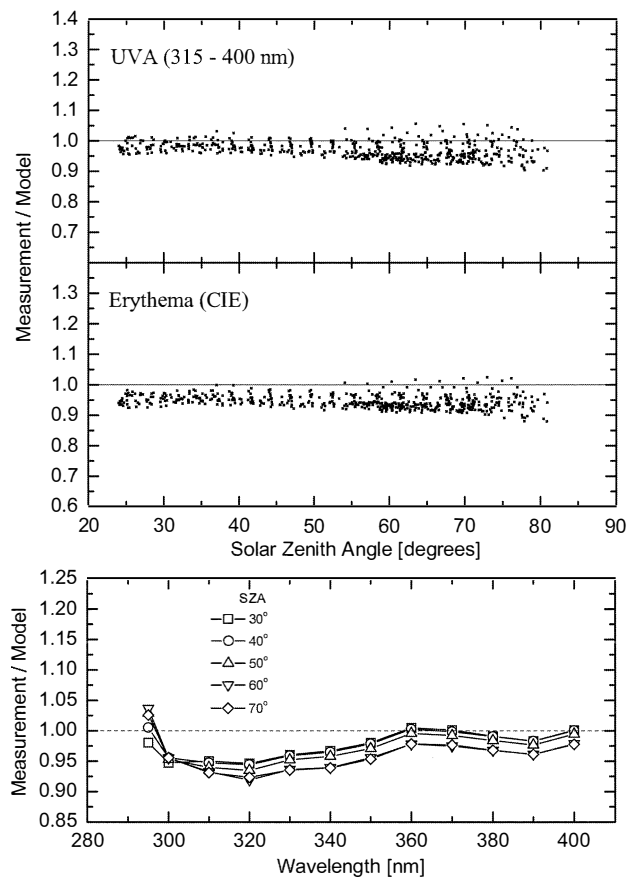


**Figure 9-18.** Comparison of measured (at Garmisch-Partenkirchen) and modeled spectral irradiances for clear skies. Top panels: Measurement/model ratios for UVA irradiance (315-400 nm) and erythemal UV irradiance as a function of SZA. Bottom panel: Measurement/model ratios of UV irradiance as a function of wavelength, for several values of SZA. (Updated from Mayer *et al.*, 1997.)

largely due to the limited accuracy and availability of input data characterizing the state of the atmosphere and the extraterrestrial irradiance. Neglecting extraterrestrial irradiance uncertainties, the best results that can be expected with model inputs of ozone, aerosol, and  $\text{SO}_2$  are about 5% uncertain (Schwander *et al.*, 1997). The authors also conclude that these results cannot be improved significantly, even when measured values of vertical profiles of all atmospheric constituents are used. If only observed visibility is used instead of measured aerosol properties, then uncertainty is about 10-15%. In addition to atmospheric uncertainties, part of the difficulty in comparing model calculations of absolute irradiance is with the input solar irradiances (see Figure 9-10). In the UV-B region, satellite instruments differ at the 5% level (Cebula *et al.*, 1996), giving a fundamental uncertainty between model results and ground-based measurements.

Results from the Dave (1964) multiple-scattering code for a pure Rayleigh atmosphere containing a cloud correction term were compared (Eck *et al.*, 1995) with measurements from the Brewer #14 instrument in Toronto (Kerr and McElroy, 1993). The model was adjusted to the data by using independently measured cloud reflectivities ( $R$ ) and ozone amounts from TOMS to determine the amount of UV-irradiance reduction in the 300- to 325-nm range. It was found that the simple cloud attenuation model  $(1 - (R - 0.05)/0.95)$  gave an estimate of the observed irradiance as a function of wavelength and as a function of the day of the year to better than 10%. Daily values could differ by much more than 10% because of the difference between the field of view of the spectroradiometer and the TOMS satellite that might contain different amounts of cloud and aerosol cover.

A sample comparison between the Toronto Brewer data and UV irradiance calculated using TOMS data for a single day (8 August 1996) is shown in Figure 9-19. The clear-sky curve uses the TOMS-measured ozone amount of 290 DU and a surface reflectivity of 4%. The same calculation was made using the estimated cloud cover ( $\tau_{\text{CLOUD}} = 40.4$ ) from the TOMS-measured backscattered radiances at 360 nm. The results show an apparent good instantaneous agreement between the Toronto Brewer measurement at the time of the TOMS overpass. However, it also shows the large difference that can occur if the time of the TOMS overpass is shifted by a few minutes relative to the Brewer measurement time or if the local cloud cover changes. Figure 9-19

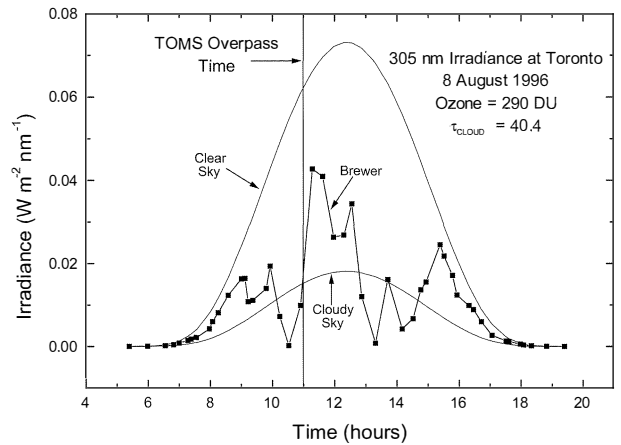


**Figure 9-19.** UV irradiances derived from radiative transfer results (smooth curves) for clear and cloudy skies compared with corresponding ground-based measurements (squares) for 8 August 1996 at Toronto Canada (43.5°N, 79.3°W). The vertical straight line marks the time of the Earth-Probe/TOMS overpass of Toronto (from WOUDC database).

also shows the error that can occur if the TOMS data are used to estimate daily UV exposure unless the UV irradiance from enough days (at least 1 week) are combined to average out different daily cloud and aerosol amounts in the instruments' fields of view.

## 9.7 LOCAL PREDICTABILITY AND FORECASTING

Since the 1994 Assessment report (WMO, 1995, Chapter 9), an international agreement has been reached on defining a UV-irradiance index for the dissemination of UV exposure information to the public (WMO, 1994). The UV index has been used in daily weather reports and in forecasts used by the media in several countries (see Appendix). In Canada, where the UV index was developed and first used, and in the United States, predictions of the UV index include advection effects of measured ozone fields and estimates of cloud attenuation (Long, 1996; Burrows, 1997). In Canada, the ozone measurements are from the network of Brewer instruments, whereas in the United States, satellite measurements of ozone and cloud-amount predictions are used.

## SURFACE ULTRAVIOLET RADIATION

Similar products involving the UV index are available in other countries (e.g., Australia; Rikus, 1997). The UV index gives a regional prediction of the amount of UV irradiance expected on a scale that is essentially a danger index for human exposure, but is intended to be applicable to other processes involving UV damage as well. It is based on incidence on a horizontal surface only and can underestimate the risk for surfaces in other orientations, such as surfaces that are oriented toward the sun (McKenzie *et al.*, 1997a). The NOAA method of ozone-amount estimation used in UV-irradiance forecasting (Long, 1996; Long *et al.*, 1996) has been compared with a statistical approach using the global ozone maps from TOMS instead of the nadir views of SBUV/2, which are widely separated in longitude (Ziemke *et al.*, 1998). The results show that a modest improvement in UV-irradiance predictability can be obtained. Although not essential for all UV forecasting purposes, the ability to accurately predict cloud fields and their effect on UV irradiance remains a challenging problem (Burrrows, 1997).

## REFERENCES

- Ahmad, Z., and R.S. Fraser, An iterative radiative transfer code for ocean-atmosphere systems, *J. Atmos. Sci.*, 39, 656-665, 1982.
- Bais, A.F., C.S. Zerefos, C. Meleti, I.C. Ziomas, and K. Tourpali, Spectral measurements of solar UVB radiation and its relations to total ozone, SO<sub>2</sub> and clouds, *J. Geophys. Res.*, 98, 5199-5204, 1993.
- Bais, A.F., C.S. Zerefos, and C.T. McElroy, Solar UVB measurements with the double- and single-monochromator Brewer ozone spectrophotometers, *Geophys. Res. Lett.*, 23, 833-836, 1996.
- Bais, A.F., M. Blumthaler, A.R. Webb, J. Groebner, P.J. Kirsch, B.G. Gardiner, C.S. Zerefos, T. Svenoe, and T.J. Martin, Spectral UV measurements over Europe within the SESAME activities, *J. Geophys. Res.*, 102, 8731-8736, 1997.
- Balachandran, N.K., and D. Rind, Modeling the effects of UV variability and the QBO on the troposphere-stratosphere system: Part I, The middle atmosphere, *J. Clim.*, 8, 2058-2079, 1995.
- Basher, R.E., X. Zheng, and S. Nichols, Ozone-related trends in solar UV-B series, *Geophys. Res. Lett.*, 21, 2713-2716, 1994.
- Bernhard, G., and G. Seckmeyer, New entrance optics for solar spectral UV measurements, *Photochem. Photobiol.*, 65, 923-930, 1997.
- Bernhard, G., B. Mayer, and G. Seckmeyer, All weather comparisons between spectral and broadband (Robertson-Berger) UV meters, *Photochem. Photobiol.*, 64, 792-799, 1996.
- Bernhard, G., B. Mayer, and G. Seckmeyer, Measurements of spectral solar UV irradiance in tropical Australia, *J. Geophys. Res.*, 102, 8719-8730, 1997.
- Bigelow, D.S., J.R. Slusser, A.F. Beaubien, and J.H. Gibson, The USDA Ultraviolet Radiation Monitoring Program, *Bull. Amer. Meteorol. Soc.*, 79, 601-615, 1998.
- Blumthaler, M., W. Ambach, and M. Salzgeber, Effects of cloudiness on global and diffuse UV irradiance in a high-mountain area, *Theor. Appl. Climatol.*, 50, 23-30, 1994.
- Blumthaler, M., J. Grobner, M. Huber, and W. Ambach, Measuring spectral and spatial variations of UVA and UVB sky radiance, *Geophys. Res. Lett.*, 23, 547-550, 1996.
- Blumthaler, M., W. Ambach, and R. Ellinger, Increases in solar UV radiation with altitude, *J. Photochem. Photobiol. B: Biol.*, 39, 130-134, 1997.
- Bodeker, G.E., and R.L. McKenzie, An algorithm for inferring surface UV irradiance including cloud effects, *J. Appl. Meteorol.*, 35, 1860-1877, 1996.
- Bodhaine, B.A., R.L. McKenzie, P.V. Johnston, D.J. Hofmann, E.G. Dutton, R.C. Schnell, J.E. Barnes, S.C. Ryan, and M. Kotkamp, New ultraviolet spectroradiometer measurements at Mauna Loa Observatory, *Geophys. Res. Lett.*, 23, 2121-2124, 1996.
- Bodhaine, B.A., E.G. Dutton, R.L. McKenzie, and P.V. Johnston, Spectral UV measurements at Mauna Loa: July 1995-July 1996, *J. Geophys. Res.*, 23, 2121-2124, 1997.
- Bodhaine, B.A., E.G. Dutton, R.L. McKenzie, and P.V. Johnston, Calibrating broadband UV instruments: Ozone and solar zenith angle dependence, *J. Atmos. Oceanic Technol.*, 15, 916-926, 1998.
- Bojkov, R.D., and V.E. Fioletov, Estimating the global ozone characteristics during the last 30 years, *J. Geophys. Res.*, 100, 16537-16551, 1995a.
- Bojkov, R.D., and V.E. Fioletov, Total ozone variations in the tropical belt: An application for quality of ground-based measurements, *Meteorol. Atmos. Phys.*, 58, 223-240, 1995b.

- Bojkov, R.D., and V.E. Fioletov, Changes in lower stratospheric ozone over Europe and Canada, *J. Geophys. Res.*, 102, 1337-1347, 1997.
- Bojkov, R.D., V.E. Fioletov, and S.B. Diaz, The relationship between solar UV irradiance and total ozone from observations over southern Argentina, *Geophys. Res. Lett.*, 22, 1249-1252, 1995a.
- Bojkov, R.D., V.E. Fioletov, D.S. Balis, C.S. Zerefos, T.V. Kadygrova, and A.M. Shalamjansky, Further ozone decline during the northern hemisphere winter-spring of 1994-1995 and the new record low over Siberia, *Geophys. Res. Lett.*, 22, 2729-2732, 1995b.
- Booth, C.R., T.B. Lucas, T. Mestechkina, J.R. Tusson IV, D.A. Neuschuler, and J.H. Morrow, *NSF Polar Programs UV Spectrometer Network 1991-1993 Operations Report*, Biospherical Instruments Inc., San Diego, Calif., 1993.
- Booth, C.R., T. Mestechkina, and J.H. Morrow, Errors in the reporting of solar irradiance using moderate bandwidth radiometers: An experimental investigation, *Proc. Soc. Photo.-Opt. Instrum. Eng.*, 2258, 654-663, 1994.
- Booth, C.R., J.C. Ebrahimian, T. Mestechkina, L.W. Cabasug, J.S. Robertson, and J.R. Tusson, *NSF Polar Programs UV Spectroradiometer Network 1995-1997 Operations Report*, 241 pp., Biospheric Instruments Inc., San Diego, Calif., 1998.
- Bordewijk, J.A., H. Slaper, H.A.J.M. Reinen, and E. Schlamann, Total solar radiation and the influence of clouds and aerosols in the biologically effective UV, *Geophys. Res. Lett.*, 22, 2151-2154, 1995.
- Brüeckner, G.E., K.L. Edlow, L.E. Floyd IV, J.L. Leon, and M.E. VanHoosier, The Solar Ultraviolet Spectral Irradiance Monitor (SUSIM) experiment on board the Upper Atmospheric Research Satellite (UARS), *J. Geophys. Res.*, 98, 10695-10711, 1993.
- Brühl, C., and P.J. Crutzen, On the disproportionate role of tropospheric ozone as a filter against solar UV-B radiation, *Geophys. Res. Lett.*, 16, 703-706, 1989.
- Burrows, W.R., CART regression models for predicting UV radiation at the ground in the presence of cloud and other environmental factors, *J. Appl. Meteorol.*, 36, 531-544, 1997.
- Caldwell, M.M., L.B. Camp, C.W. Warner, and S.D. Flint, Action spectra and their key role in assessing biological consequences of solar UV-B radiation change, in *Stratospheric Ozone Reduction, Solar Ultraviolet Radiation and Plant Life*, edited by R.C. Worrest and M.M. Caldwell, pp. 87-111, Springer-Verlag, Berlin, 1986.
- Cebula, R.P., and M.T. Deland, Comparisons of the NOAA-11 SBUV/2, UARS SOLSTICE, and UARS SUSIM Mg II solar activity proxy indexes, *Sol. Phys.*, 177, 117-132, 1998.
- Cebula, R.P., E. Hilsenrath, and M.T. Deland, Middle ultraviolet solar spectral irradiance measurements, 1985-1992, from SBUV/2 and SSBUV instruments, in *The Sun as Variable Star: Solar and Stellar Variations*, edited by J.M. Pap, C. Frolich, H.S. Hudson, and S.K. Folanki, pp. 81-88, Cambridge University Press, Cambridge, U.K., 1994.
- Cebula, R.P., G.O. Thuillier, M.E. VanHoosier, E. Hilsenrath, M. Herse, G.E. Brueckner, and P.C. Simon, Observations of the solar irradiance in the 200-350-nm interval during the ATLAS-1 mission: A comparison among three sets of measurements—SSBUV, SOLSPEC, and SUSIM, *Geophys. Res. Lett.*, 23, 2289-2292, 1996.
- Chubarova, N.E., Transmission of total UV radiation through clouds of different types, *Izv. Atmos. Oceanic Phys.*, 29, 639-645, 1993.
- Chubarova, N.E., Ultraviolet radiation under broken cloud conditions as inferred from many-year ground-based observations, *Izv. Atmos. Oceanic Phys.*, 34, 131-134, 1998.
- Dahlback, A., Measurements of biologically effective UV doses, total ozone abundance and cloud effects with multi-channel moderate bandwidth filter instruments, *Appl. Opt.*, 35, 6514-6521, 1996.
- Dave, J.V., Meaning of successive iteration of the auxiliary equation in the theory of radiative transfer, *Astrophys. J.*, 140, 1292-1303, 1964.
- Dave, J.V., and J. Gazdag, A modified Fourier transform method for multiple scattering calculations in a plane parallel Mie atmosphere, *Appl. Opt.*, 9, 1457-1466, 1970.
- DeLand, M.T., and R.P. Cebula, NOAA-11 SBUV/2 solar spectral irradiance measurements 1989-1994: II, Results, validation, and comparisons, *J. Geophys. Res.*, 103, 16251-16273, 1998a.

## SURFACE ULTRAVIOLET RADIATION

- DeLand, M.T., and R.P. Cebula, Solar UV activity at solar cycle 21 and 22 minimum from NOAA-9 SBUV/2 data, *Sol. Phys.*, 177, 105-116, 1998b.
- DeLuisi, J.J., and J. Barnett, An examination of the calibration stability of the US Robertson-Berger meter network (abstract), *EOS Trans. Amer. Geophys. Union*, 79, (43), *Fall Meeting Suppl.*, 1992.
- Diaz, S.B., C.R. Booth, T.B. Lucas, and I. Smolskaia, Effects of ozone depletion on irradiances and biological doses over Ushuaia, in *Impact of UV-B Radiation on Pelagic Freshwater Ecosystems*, *Adv. Limnol.*, 43, edited by C.E. Williamson and H.E. Zagarese, pp. 115-122, E. Schweizerbart, Stuttgart, Germany, 1994.
- Diaz, S.B., J.E. Frederick, T.B. Lucas, C.R. Booth, and I. Smolskaia, Solar ultraviolet irradiance at Tierra del Fuego: Comparison of measurements and calculations over a full annual cycle, *Geophys. Res. Lett.*, 23, 355-358, 1996.
- Duguay, C.R., An approach to the estimation of surface net radiation in mountain areas using remote sensing and digital terrain data, *Theor. Appl. Climatol.*, 52, 55-68, 1995.
- Eck, T.F., P.K. Bhartia, P.H. Hwang, and L.L. Stowe, Reflectivity of Earth's surface and clouds in ultraviolet from satellite observations, *J. Geophys. Res.*, 92, 4287-4296, 1987.
- Eck, T.F., P.K. Bhartia, and J.B. Kerr, Satellite estimation of spectral UVB irradiance using TOMS derived total ozone and UV reflectivity, *Geophys. Res. Lett.*, 22, 611-614, 1995.
- Estupinan, J.G., S. Raman, G.H. Crescenti, J.J. Streicher, and W.F. Barnard, The effects of clouds and haze on UV-B radiation, *J. Geophys. Res.*, 101, 16807-16816, 1996.
- Feister, U., and R. Grewe, Higher UV radiation inferred from low ozone levels at northern midlatitudes in 1992 and 1993, *Global Planet. Change*, 11, 25-34, 1995.
- Feister, U., R. Grewe, and K. Gericke, A method for correction of cosine errors in measurements of spectral UV irradiance, *Sol. Energy*, 60, 313-332, 1997.
- Fioletov, V.E., J.B. Kerr, and D.I. Wardle, The relationship between total ozone and spectral UV irradiance from Brewer spectrophotometer observations and its use for derivation of total ozone from UV measurements, *Geophys. Res. Lett.*, 24, 2705-2708, 1997.
- Fioletov, V.E., E. Griffioen, J.B. Kerr, D.I. Wardle, and O. Uchino, Influence of volcanic sulfur dioxide on spectral UV irradiance as measured by Brewer spectrophotometers, *Geophys. Res. Lett.*, 25, 1665-1668, 1998.
- Forster, P.M. de F., Modeling ultraviolet radiation at the Earth's surface: Part I, The sensitivity of ultraviolet irradiance to atmospheric changes, *J. Appl. Meteorol.*, 34, 2412-2425, 1995.
- Forster, P.M. de F., and K.P. Shine, A comparison of two radiation schemes for calculating ultraviolet radiation, *Quart. J. Roy. Meteorol. Soc.*, 121, 1113-1131, 1995.
- Forster, P.M. de F., K.P. Shine, and A.R. Webb, Modeling ultraviolet radiation at the Earth's surface: Part II, Model and instrument comparison, *J. Appl. Meteorol.*, 34, 2426-2439, 1995.
- Frederick, J.E., and C. Erlick, The attenuation of sunlight by high latitude clouds: Spectral dependence and its physical mechanisms, *J. Atmos. Sci.*, 54, 2813-2819, 1997.
- Frederick, J.E., and H.D. Steele, The transmission of sunlight through cloudy skies: An analysis based on standard meteorological information, *J. Appl. Meteorol.*, 34, 2755-2761, 1995.
- Frederick, J.E., A.E. Koob, A.D. Alberts, and E.C. Weatherhead, Empirical studies of tropospheric transmission in the ultraviolet: Broadband measurements, *J. Appl. Meteorol.*, 32, 1883-1892, 1993.
- Frederick, J.E., S.B. Diaz, I. Smolskaia, W. Esposito, T. Lucas, and C.R. Booth, Ultraviolet solar radiation in the high latitudes of South America, *Photochem. Photobiol.*, 60, 356-362, 1994.
- Gardiner, B.G., A.R. Webb, A.F. Bais, M. Blumthaler, I. Dirmhirn, P. Forster, D. Gillotay, K. Henriksen, and M. Huber, European intercomparison of ultraviolet spectroradiometers, *Environ. Technol.*, 14, 25-43, 1993.
- Geogdzhayev, I.V., T.V. Kondranin, N.E. Chubarova, and A.N. Rublev, Comparison of UV measurements and modelling under broken cloudiness, paper presented at the *International Radiation Symposium*, University of Alaska, Fairbanks, 19-24 August 1996.
- Geogdzhayev, I.V., T.V. Kondranin, A.N. Rublev, and N.E. Chubarova, UV radiation transfer through broken cloud fields: Modeling and comparison with measurements, *Izv. Atmos. Oceanic Phys.*, 33, 680-686, 1997.

- Grant, W.B., Global stratospheric ozone and UV-B radiation, *Science*, 242, 1111-1112, 1988.
- Grant, R.H., and G.M. Heisler, Obscured overcast sky radiance distributions for ultraviolet and photosynthetically active radiation, *J. Appl. Meteorol.*, 36, 1336-1345, 1997.
- Grant, R.H., G.M. Heisler, and W. Gao, Clear sky radiance distributions in ultraviolet wavelength bands, *Theor. Appl. Climatol.*, 371, 1-13, 1996.
- Grant, R.H., G.M. Heisler, and W. Gao, Ultraviolet sky radiance distributions of translucent overcast skies, *Theor. Appl. Climatol.*, 58, 129-139, 1997.
- Green, A.E.S., The penetration of ultraviolet radiation to the ground, *Physiol. Plant.*, 58, 351-359, 1983.
- Grenfell, T.C., S.G. Warren, and P.C. Mullen, Reflection of solar radiation by the Antarctic snow surface at ultraviolet, visible, and near-infrared wavelengths, *J. Geophys. Res.*, 99, 18669-18684, 1994.
- Gurney, K.R., Evidence for increasing ultraviolet irradiance at Point Barrow, Alaska, *Geophys. Res. Lett.*, 25, 903-906, 1998.
- Herman, B.M., and S.R. Browning, A numerical solution to the equation of radiative transfer, *J. Atmos. Sci.*, 22, 559-566, 1965.
- Herman, B.M., W. Asous, and S.R. Browning, A semi-analytic technique to integrate the radiative transfer equation over optical depth, *J. Atmos. Sci.*, 37, 1828-1838, 1980.
- Herman, B.M., T.R. Caudill, D.E. Flittner, K.J. Thome, and A. Ben-David, Comparison of the Gauss-Seidel spherical polarized radiative transfer code with other radiative transfer codes, *Appl. Opt.*, 34, 4563-4572, 1996.
- Herman, J.R., and E. Celarier, Earth surface reflectivity climatology at 340 nm to 380 nm from TOMS data, *J. Geophys. Res.*, 102, 28003-28011, 1997.
- Herman, J.R., and D. Larko, Low ozone amounts during 1992-1993 from Nimbus-7 and Meteor-3/TOMS, *J. Geophys. Res.*, 99, 3438-3496, 1994.
- Herman, J.R., P.K. Bhartia, J. Kiemke, Z. Ahmad, and D. Larko, UV-B increases (1979-1992) from decreases in total ozone, *Geophys. Res. Lett.*, 23, 2117-2120, 1996.
- Herman, J.R., P.K. Bhartia, O. Torres, C. Hsu, C. Seftor, and E. Celarier, Global distribution of UV-absorbing aerosols from Nimbus-7/TOMS data, *J. Geophys. Res.*, 102, 16911-16922, 1997.
- Hicks, B.B., J.J. DeLuisi, and D.R. Matt, The NOAA Integrated Surface Irradiance Study (ISIS): A new surface radiation monitoring program, *Bull. Amer. Meteorol. Soc.*, 77, 2857-2864, 1996.
- Hofmann, D.J., S.J. Oltmans, J.A. Lathrop, J.M. Harris, and H. Vömel, Record low ozone over Mauna Loa Observatory, Hawaii, during the winter of 1994-1995, *Geophys. Res. Lett.*, 23, 1533-1536, 1996.
- Huber, M., M. Blumthaler, and W. Ambach, Total atmospheric ozone determined from spectral measurements of direct solar UV irradiance, *Geophys. Res. Lett.*, 22, 53-56, 1995.
- Ireland, W., and R. Sacher, The angular distribution of solar ultraviolet, visible and near-infrared radiation from cloudless skies, *Photochem. Photobiol.*, 63, 483-486, 1996.
- Ito, T., Y. Sakoda, T. Uekubo, H. Naganuma, M. Fukuda, and M. Hayashi, Scientific application of UV-B observations from JMA network, in *Proceedings of the 13<sup>th</sup> University of Occupational and Environmental Health (UOEH) International Symposium and the 2<sup>nd</sup> Pan Pacific Cooperative Symposium on Human Health and Ecosystems*, Kitakyushu, Japan, 13-15 October 1993, edited by Y. Kodama and S.D. Lee, pp. 107-125, 1994.
- Justus, C.G., and B.B. Murphey, Temporal trends in surface irradiance at ultraviolet wavelengths, *J. Geophys. Res.*, 99, 1389-1394, 1994.
- Kerr, J.B., Observed dependencies of atmospheric UV radiation and trends, in *Solar Ultraviolet Radiation: Modelling, Measurements, and Effects*, NATO ASI Series I, Vol. 52, edited by C.S. Zerefos and A.F. Bais, pp. 259-266, Springer-Verlag, Berlin, 1997.
- Kerr, J.B., Diurnal variation of column ozone at Toronto and Edmonton, in *Atmospheric Ozone: Proceedings of the XVIII Quadrennial Ozone Symposium*, edited by R.D. Bojkov and G. Visconti, pp. 53-56, Parco Scientifico e Tecnologico d'Abruzzo, L'Aquila, Italy, 1998.
- Kerr, J.B., and C.T. McElroy, Evidence for large upward trends of ultraviolet-B radiation linked to ozone depletion, *Science*, 262, 1032-1034, 1993.
- Kerr, J.B., and C.T. McElroy, Total ozone measurements made with the Brewer ozone spectrophotometer during STOIC 1989, *J. Geophys. Res.*, 100, 9225-9230, 1995.

## SURFACE ULTRAVIOLET RADIATION

- Kirchhoff, V.W.J.H., F. Zamorano, and C. Casiccia, UV-B enhancements at Punta Arenas, Chile, *J. Photochem. Photobiol. B: Biol.*, 38, 174-177, 1997.
- Kjeldstad, B., B. Johnsen, and T. Koskela (eds.), *The Nordic Intercomparison of Ultraviolet and Total Ozone Instruments at Izaña, October 1996*, Meteorological Publication 36, Finnish Meteorological Institute, Helsinki, 1997.
- Koepke, P., A. Bais, D. Balis, M. Buchwitz, H. De Backer, X. de Cabo, P. Eckert, P. Eriksen, D. Gillotay, A. Heikkila, T. Koskela, B. Lapeta, Z. Litynska, J. Lorente, B. Mayer, A. Renaud, A. Ruggaber, G. Schauburger, G. Seckmeyer, P. Seifert, A. Schmalwieser, H. Schwander, K. Vanicek, and M. Weber, Comparison of models used for UV-index calculations, *J. Photochem. Photobiol. B: Biol.*, in press, 1998.
- Kohler, U., Recalibration of the Hohenpeissenberg Dobson spectrophotometer 104 presuming effective absorption coefficients, *J. Atmos. Chem.*, 4, 359-373, 1986.
- Koskela, T. (ed.), *The Nordic Intercomparison of Ultraviolet and Total Ozone Instruments at Izaña from 24 October to 5 November 1993: Final Report*, Meteorological Publications, Finnish Meteorological Institute, Helsinki, 1994.
- Krotkov, N.A., P.K. Bhartia, J.R. Herman, V. Fioletov, and J. Kerr, Satellite estimation of spectral surface UV irradiance in the presence of tropospheric aerosols: 1, Cloud-free case, *J. Geophys. Res.*, 103, 8779-8793, 1998.
- Krzyscin, J.W., UV controlling factors and trends derived from the ground-based measurements taken at Belsk, Poland, 1976-1994, *J. Geophys. Res.*, 101, 16797-16805, 1996.
- Kylling, A., A. Albold, and G. Seckmeyer, Transmittance of a cloud is wavelength-dependent in the UV-range: Physical interpretation, *Geophys. Res. Lett.*, 24, 397-400, 1997.
- Kylling, A., A.F. Bais, M. Blumthaler, J. Schreder, and C.S. Zerefos, The effect of aerosols on solar UV irradiances during the PAUR campaign, *J. Geophys. Res.*, 103, 26051-26060, 1998.
- Lean, J.L., G.J. Rottman, H.L. Kyle, T.N. Woods, J.R. Hickey, and L.C. Puga, Detection and parameterization of variations in solar mid- and near-ultraviolet radiation (200-400 nm), *J. Geophys. Res.*, 102, 29939-29956, 1997.
- Lenoble, J., Modeling of the influence of snow reflectance on UV irradiance for cloudless sky, *Appl. Opt.*, 37, 2441-2447, 1998.
- Leszczynski, K., K. Jokela, L. Ylianttila, R. Visuri, and M. Blumthaler, *Report of the WMO/STUK Intercomparison of Erythemally-Weighted Solar UV Radiometers (Spring/Summer 1995, Helsinki, Finland)*, Global Atmosphere Watch Report No. 112, 90 pp., World Meteorological Organization, Geneva, 1997.
- Leszczynski, K., K. Jokela, L. Ylianttila, R. Visuri, and M. Blumthaler, Erythemally weighted radiometers in solar UV monitoring: Results from the WMO/STUK intercomparison, *Photochem. Photobiol.*, 67, 212-221, 1998.
- Liepert, B., P. Fabian, and H. Groassl, Solar radiation in Germany—observed trends and an assessment of their causes: Part 1, Regional approach, *Contrib. Atmos. Phys.*, 67, 15-29, 1994.
- Liley, J.B., and R.L. McKenzie, Time-dependent wavelength non-linearities in spectrometers for solar UV monitoring, in *IRS'96: Current Problems in Atmospheric Radiation*, edited by W.L. Smith and K. Stamnes, Deepak, Hampton, Va., 1997.
- Loeb, N.G., and R. Davis, Observational evidence of plane parallel modeling biases: Apparent dependence of cloud optical depth on solar zenith angle, *J. Geophys. Res.*, 101, 1621-1634, 1996.
- Long, C.S., *Ultraviolet Index Verification Report: Indicators of Surface Ultraviolet Radiation Observation Characteristics*, NOAA, National Centers for Environmental Prediction, Washington, D.C., 1996.
- Long, C.S., A.J. Miller, H.T. Lee, J.D. Wild, R.C. Przywarty, and D. Hufford, Ultraviolet index forecasts issued by the National Weather Service, *Bull. Amer. Meteorol. Soc.*, 77, 729-748, 1996.
- Lubin, D., and E.H. Jensen, Effects of clouds and stratospheric ozone depletion on ultraviolet radiation trends, *Nature*, 377, 710-713, 1995.
- Lubin, D., E.H. Jensen, and H.P. Gies, Global surface ultraviolet climatology from TOMS and ERBE data, *J. Geophys. Res.*, 103, 26061-26091, 1998.
- Madronich, S., Increases in biologically damaging UV-B radiation due to stratospheric ozone depletion: A brief review, *Arch. Hydrobiol.*, 43, 17-30, 1994.
- Madronich, S., and F.R. de Gruijl, Stratospheric ozone depletion between 1979 and 1992: Implication for biologically active ultraviolet-B radiation and non-melanoma skin cancer incidence, *Photochem. Photobiol.*, 59, 541-546, 1994.

- Madronich, S., R.L. McKenzie, M. Caldwell, and L.O. Björn, Changes in ultraviolet radiation reaching the Earth's surface, *Ambio.*, 24, 143-152, 1995.
- Marshak, A., A. Davis, R.F. Calahan, and W.J. Wiscomb, Nonlocal independent pixel approximation: Direct and inverse problems, *IEEE Trans. Geosci. Remote Sens.*, 36, 192-205, 1998.
- Mateer, C.L., On the information content of Umkehr observations, *J. Atmos. Sci.*, 22, 370-381, 1965.
- Mayer, B., and G. Seckmeyer, All-weather comparison between spectral and broadband (Robertson-Berger) UV measurements, *Photochem. Photobiol.*, 64, 792-799, 1996.
- Mayer, B., G. Seckmeyer, and A. Kylling, Systematic long-term comparison of spectral UV measurements and UVSPEC modeling results, *J. Geophys. Res.*, 102, 8755-8767, 1997.
- McElroy, C.T., A spectroradiometer for the measurement of direct and scattered solar irradiance from on-board the NASA ER-2 high-altitude research aircraft, *Geophys. Res. Lett.*, 22, 1361-1364, 1995.
- McKenzie, R.L., P.V. Johnston, M. Kotkamp, A. Bittar, and J.D. Hamlin, Solar ultraviolet spectroradiometry in New Zealand: Instrumentation and sample results from 1990, *Appl. Opt.*, 31, 6501-6509, 1992.
- McKenzie, R.L., M. Kotkamp, G. Seckmeyer, R. Erb, C.R. Roy, H.P. Gies, and S.J. Toomey, First southern hemisphere intercomparison of measured solar UV spectra, *Geophys. Res. Lett.*, 20, 2223-2226, 1993.
- McKenzie, R.L., M. Kotkamp, and W. Ireland, Upwelling UV spectral irradiances and surface albedo measurements at Lauder, New Zealand, *Geophys. Res. Lett.*, 23, 1757-1760, 1996.
- McKenzie, R.L., K. Paulin, and M. Kotkamp, Erythral UV irradiances at Lauder, New Zealand: Relationship between horizontal and normal incidence, *Photochem. Photobiol.*, 65, 683-689, 1997a.
- McKenzie, R.L., P.V. Johnston, and G. Seckmeyer, UV spectro-radiometry in the Network for the Detection of Stratospheric Change (NDSC), in *Solar Ultraviolet Radiation: Modelling, Measurements and Effects*, NATO ASI Series I, Vol. 52, edited by C.S. Zerefos and A.F. Bais, pp. 279-287, Springer-Verlag, Berlin, 1997b.
- McKinlay, A.F., and B.L. Diffey, A reference action spectra for ultraviolet induced erythema in human skin, in *Human Exposure to Ultraviolet Radiation: Risks and Regulations*, edited by W.R. Passchier and B.M.F. Bosnjakovich, pp. 83-87, Elsevier, Amsterdam, 1987.
- McPeters, R.D., S.M. Hollandsworth, L.E. Flynn, J.R. Herman, and C.J. Seftor, Long-term ozone trends derived from the 16-year combined Nimbus 7/ Meteor 3 TOMS version 7 record, *Geophys. Res. Lett.*, 23, 3699-3702, 1996.
- Meerkotter, R., B. Wissinger, and G. Seckmeyer, Surface UV from ERS 2/GOME and NOAA/AVHRR data: A case study, *J. Geophys. Res.*, 24, 1939-1942, 1997.
- Mims, F.M. III, and J.E. Frederick, Cumulus clouds and UV-B, *Nature*, 371, 291, 1994.
- Mims, F.M. III, J.W. Ladd, and R.A. Blaha, Increased solar ultraviolet-B associated with record low ozone over Texas, *Geophys. Res. Lett.*, 22, 227-230, 1995.
- Nack, M.L., and A.E.S. Green, Influence of clouds, haze, and smog on the middle ultraviolet reaching the ground, *Appl. Opt.*, 13, 2405-2415, 1974.
- Nemeth, P., Z. Toth, and Z. Nagy, Effect of weather conditions on UV-B radiation reaching the Earth's surface, *J. Photochem. Photobiol. B: Biol.*, 32, 177-181, 1996.
- Nezval, E.I., Statistical characteristics of the UV irradiance in Moscow, 1968-1992, *Meteorol. Hydrol.*, 8, 64-71, 1996.
- Olmo, F.J., and L. Alados-Arboledas, Pinatubo eruption effects on solar radiation at Almeira (36.83°N, 2.41°W), *Tellus*, 47B, 602-606, 1995.
- Piazena, H., The effect of altitude upon the solar UV-B and UV-A irradiance in the topical Chilean Andes, *Sol. Energy*, 57, 133-140, 1996.
- Ramaswamy, V., M.D. Schwarzkopf, and W.J. Randel, Fingerprint of ozone depletion in the spatial and temporal pattern of recent lower-stratospheric cooling, *Nature*, 382, 616-618, 1996.
- Rikus, L., Prediction of UV-B dosage at the surface, *Aust. Meteorol. Mag.*, 46, 211-222, 1997.
- Rossow, W.B., and L.C. Garder, Cloud detection using satellite measurements of infrared and visible radiances for ISCCP, *J. Climate*, 6, 2370-2393, 1993.
- Rottman, G.J., T.N. Woods, and T.P. Sporn, Solar Stellar Irradiance Comparison Experiment 1: 1, Instrument design and operation, *J. Geophys. Res.*, 98, 10667-10677, 1993.
- Ryan, K.G., G.J. Smith, D.A. Rhoades, and R.B. Coppell, Erythral ultraviolet insolation in New Zealand at solar zenith angles of 30° and 45°, *Photochem. Photobiol.*, 63, 628-632, 1996.

## SURFACE ULTRAVIOLET RADIATION

- Sabziparvar, A.A., P.M. de F. Forster, and K.P. Shine, Changes in ultraviolet radiation due to stratospheric and tropospheric ozone changes since pre-industrial times, *J. Geophys. Res.*, *103*, 26107-26113, 1998.
- Schafer, J.S., V.K. Saxena, B.N. Wenny, W. Barnard, and J.J. DeLuisi, Observed influence of clouds on ultraviolet-B radiation, *Geophys. Res. Lett.*, *23*, 2625-2628, 1996.
- Schmid, B., and C. Wehrli, Comparison of Sun photometer calibration by use of the Langley technique and the standard lamp, *Appl. Opt.*, *21*, 4500-4512, 1995.
- Schmid, B., P.R. Spyak, S.F. Biggar, C. Wehrli, J. Sekler, T. Ingold, C. Mätzler, and N. Kämpfer, Evaluation of the applicability of solar and lamp radiometric calibrations of a precision sun photometer operating between 300 and 1025 nm, *Appl. Opt.*, *37*, 3923-3941, 1998.
- Schwander, H., P. Koepke, and A. Ruggaber, Uncertainties in modeled UV irradiances due to limited accuracy and availability of input data, *J. Geophys. Res.*, *102*, 9419-9429, 1997.
- Scotto, J., G. Cotton, F. Urbach, D. Berger, and T. Fears, Biologically effective ultraviolet radiation-surface measurements in the United States, 1974 to 1985, *Science*, *239*, 762-764, 1988.
- Seckmeyer, G., and G. Bernhard, Cosine error correction of spectral UV irradiances, *Proc. Soc. Photo-Opt. Instrum. Eng.*, *2049*, 140-151, 1993.
- Seckmeyer, G., and R.L. McKenzie, Increased ultraviolet radiation in New Zealand (45°S) relative to Germany (48°N), *Nature*, *359*, 135-137, 1992.
- Seckmeyer, G., S. Thiel, M. Blumthaler, P. Fabian, S. Gerber, A. Gugg-Helminger, D.P. Häder, M. Huber, C. Kettner, U. Köhler, P. Köpke, H. Maier, J. Schäfer, P. Suppan, E. Tamm, and E. Thomalla, Intercomparison of spectral UV-radiation measurement systems, *Appl. Opt.*, *33*, 7805-7812, 1994a.
- Seckmeyer, G., B. Mayer, R. Erb, and G. Bernhard, UV-B in Germany higher in 1993 than in 1992, *Geophys. Res. Lett.*, *21*, 577-580, 1994b.
- Seckmeyer, G., B. Mayer, G. Bernhard, R.L. McKenzie, P.V. Johnston, M. Kotkamp, C.R. Bluth, T. Lucas, T. Mestechkina, C.R. Roy, H.P. Gies, and D. Tomlinson, Geographical differences in the UV measured by intercompared spectroradiometers, *Geophys. Res. Lett.*, *22*, 1889-1892, 1995.
- Seckmeyer, G., R. Erb, and A. Albold, Transmittance of a cloud is wavelength-dependent in the UV-range, *Geophys. Res. Lett.*, *23*, 2753-2755, 1996.
- Seckmeyer, G., B. Mayer, G. Bernhard, R. Erb, A. Albold, H. Jäger, and W.R. Stockwell, New maximum UV irradiance levels observed in Central Europe, *Atmos. Environ.*, *31*, 2971-2976, 1997.
- Setlow, R.B., The wavelengths in sunlight effective in producing skin cancer: A theoretical analysis, *Proc. Natl. Acad. Sci., U.S.A.*, *71*, 3363-3366, 1974.
- Shetter, R.E., and M. Müller, Photolysis frequency measurements using actinic flux spectroradiometry during the PEM-Tropics Mission: Instrumentation description and some results, *J. Geophys. Res.*, in press, 1998.
- Slaper, H., H.A.J.M. Reinen, M. Blumthaler, M. Huber, and F. Kuik, Comparing ground-level spectrally resolved solar UV measurements using various instruments: A technique resolving effects of wavelength shift and slit width, *Geophys. Res. Lett.*, *22*, 2721-2724, 1995.
- Staehelin, J., and W. Schmid, Trend analysis of tropospheric ozone concentrations utilizing the 20-year data set of ozone balloon soundings over Payerne (Switzerland), *Atmos. Environ.*, *25A*, 1739-1749, 1991.
- Stamnes, K., S.C. Tsay, W. Wiscombe, and K. Jayaweera, Numerically stable algorithm for discrete-ordinate-method radiative transfer in multiple scattering and emitting layered media, *Appl. Opt.*, *27*, 2502-2509, 1988.
- Stolarski, R.S., P. Bloomfield, R.D. McPeters, and J.R. Herman, Total ozone trends deduced from Nimbus 7 TOMS data, *Geophys. Res. Lett.*, *6*, 1015-1018, 1991.
- Taalas, P., J. Damski, E. Kyrö, M. Ginzberg, and G. Talamoni, Effect of stratospheric ozone variations on UV radiation and on tropospheric ozone at high latitudes, *J. Geophys. Res.*, *102*, 1533-1539, 1997.
- Thompson, A., E.A. Early, J. DeLuisi, P. Disterhoff, D. Wardle, J. Kerr, J. Rives, Y. Sun, T. Lucas, T. Mestichina, and P. Neale, The 1994 North American interagency intercomparison of ultraviolet monitoring spectroradiometers, *J. Res. Natl. Inst. Stand. Technol.*, *102*, 279-322, 1997.
- Torres, O., P.K. Bhartia, J.R. Herman, Z. Ahmad, and J. Gleason, Derivation of aerosol properties from satellite measurements of backscattered ultraviolet radiation: Theoretical basis, *J. Geophys. Res.*, *103*, 17099-17110, 1998.

- Tsitas, S.R., and Y.L. Yung, The effect of volcanic aerosols on ultraviolet radiation in Antarctica, *Geophys. Res. Lett.*, *23*, 157-160, 1996.
- UNEP (United Nations Environment Programme), *Environmental Effects of Stratospheric Ozone Depletion: 1991 Update*, edited by J.C. van der Leun, M. Tevini, and R.C. Worrest, Nairobi, Kenya, 1991.
- UNEP (United Nations Environment Programme), *Environmental Effects of Ozone Depletion: 1994 Update*, edited by J.C. van der Leun, X. Tang, and M. Tevini, Nairobi, Kenya, 1994.
- UNEP (United Nations Environment Programme), *Environmental Effects of Ozone Depletion: 1998*, Panel Report pursuant to Article 6 of the Montreal Protocol on Substances that Deplete the Ozone Layer, in press, 1998.
- Varotsos, C., and K.Y. Kondratyev, On the relationship between total ozone and solar ultraviolet radiation at St. Petersburg, Russia, *Geophys. Res. Lett.*, *22*, 3481-3484, 1995.
- Varotsos, C.A., G.J. Chronopoulos, S. Katsikis, and N.K. Sakellariou, Further evidence of the role of air pollution on solar ultraviolet radiation reaching the ground, *Int. J. Remote Sens.*, *16*, 1883-1886, 1995.
- Vaughan, G., H.K. Roscoe, L.M. Bartlett, F.M. O'Connor, A. Sarkissian, M.V. Roozendaal, J.C. Lambert, P.C. Simon, and K. Karlsen, An intercomparison of ground-based UV-visible sensors of ozone and NO<sub>2</sub>, *J. Geophys. Res.*, *102*, 1411-1422, 1997.
- Walker, J.H., R.D. Saunders, J.K. Jackson, and K.D. Mielenz, Results of a CCPR intercomparison of spectral irradiance measurements by National Laboratories, *J. Res. Natl. Inst. Stand. Technol.*, *96*, 647-668, 1991.
- Wang, P., and J.P. Lenoble, Comparison between measurements and modeling of UV-B irradiance for clear sky: A case study, *Appl. Opt.*, *33*, 3964-3971, 1994.
- Wardle, D.I., J.B. Kerr, C.T. McElroy, and D.R. Francis, *Ozone Science: Canadian Perspective on the Changing Ozone Layer*, 119 pp., Environment Canada, Toronto, 1997.
- Weatherhead, E.C., and A.R. Webb, International response to the challenge of measuring solar ultraviolet radiation, *Radiat. Prot. Dosim.*, *72*, 223-229, 1997.
- Weatherhead, E.C., G.C. Tiao, G.C. Reinsel, J.E. Frederick, J.J. DeLuisi, D.S. Choi, and W.K. Tam, Analysis of long-term behavior of ultraviolet radiation measured by Robertson-Berger meters at 14 sites in the United States, *J. Geophys. Res.*, *102*, 8737-8754, 1997.
- Webb, A.R. (ed.), *Advances in Solar Ultraviolet Spectroradiometry*, Air Pollution Research Report 63, 238 pp., European Commission, Luxembourg, 1997.
- Webb, A.R., B.G. Gardiner, M. Blumthaler, P. Forster, M. Huber, and P.J. Kirsch, A laboratory investigation of two ultraviolet spectroradiometers, *Photochem. Photobiol.*, *60*, 84-90, 1994.
- Weih, P., and A.R. Webb, Accuracy of spectral UV model calculations: 1, Consideration of uncertainties in input parameters, *J. Geophys. Res.*, *102*, 1541-1550, 1997a.
- Weih, P., and A.R. Webb, Accuracy of spectral UV model calculations: 2, Comparison of UV calculations with measurements, *J. Geophys. Res.*, *102*, 1551-1560, 1997b.
- Wendler, G., and T. Quackenbush, UV radiation in the southern seas in early spring 1993, *Theor. Appl. Climatol.*, *53*, 221-230, 1996.
- Wilson, S.R., and B.W. Forgan, In situ calibration technique for UV spectral radiometers, *Appl. Opt.*, *34*, 5475-5484, 1995.
- Woods, T.N., D.K. Prinz, G.J. Rottman, J. London, P.C. Crane, R.P. Cebula, E. Hilsenrath, G.E. Brueckner, M.D. Andrews, O.R. White, M.E. VanHoosier, L.E. Floyd, L.C. Herring, B.G. Knapp, C.K. Pankratz, and P.A. Reiser, Validation of the UARS solar ultraviolet irradiances: Comparison with the ATLAS 1 and 2 measurements, *J. Geophys. Res.*, *101*, 9541-9569, 1996.
- WMO (World Meteorological Organization), *Scientific Assessment of Ozone Depletion: 1991*, Global Ozone Research and Monitoring Project—Report No. 25, Geneva, 1992.
- WMO (World Meteorological Organization), Report of the WMO meeting of experts on UV-B measurements, data quality, and standardization of UV indices, Report 95, Les Diablerets, Switzerland, 1994.
- WMO (World Meteorological Organization), *Scientific Assessment of Ozone Depletion: 1994*, Global Ozone Research and Monitoring Project—Report No. 37, Geneva, 1995.

## SURFACE ULTRAVIOLET RADIATION

- Zeng, J., R. McKenzie, K. Stamnes, M. Wineland, and J. Rosen, Measured UV spectra compared with discrete ordinate method simulations, *J. Geophys. Res.*, *99*, 23019-23030, 1994.
- Zerefos, C.S., K. Tourpali, and A.G. Bais, Further studies on possible volcanic signal to the ozone layer, *J. Geophys. Res.*, *99*, 25741-25746, 1994.
- Zerefos, C.S., A.F. Bais, C. Meleti, and I.C. Ziomas, A note on the recent increase of solar UV-B radiation over northern middle latitudes, *Geophys. Res. Lett.*, *22*, 1245-1248, 1995a.
- Zerefos, C.S., C. Meleti, A.F. Bais, and A. Lambros, The recent UVB variability over southeastern Europe, *J. Photochem. Photobiol. B: Biol.*, *31*, 15-19, 1995b.
- Zerefos, C.S., D.S. Balis, A.F. Bais, D. Gillotay, P.C. Simon, B. Mayer, and G. Seckmeyer, Variability of UV-B at four stations in Europe, *Geophys. Res. Lett.*, *24*, 1363-1366, 1997.
- Ziemke, J.R., S. Chandra, R.D. McPeters, and P.A. Newman, Dynamical proxies of column ozone with applications to global trend models, *J. Geophys. Res.*, *102*, 6117-6129, 1997.
- Ziemke, J.R., J.R. Herman, J.L. Stanford, and P.K. Bhartia, Total ozone/UV-B monitoring and forecasting: Impact of clouds and the horizontal resolution of satellite retrievals, *J. Geophys. Res.*, *103*, 3865-3871, 1998.

# Appendix

## Internet Addresses for UV Sites

### Internet Sites with General UV Information

---

<a href="http://www.biospherical.com/nsf/index.html">http://www.biospherical.com/nsf/index.html</a>	NSF UV Sites
<a href="http://uvb.asrc.cestm.albany.edu/">http://uvb.asrc.cestm.albany.edu/</a>	USDA
<a href="http://insider.nrel.colostate.edu:8080/UVB/UVB.html">http://insider.nrel.colostate.edu:8080/UVB/UVB.html</a>	Colorado State University
<a href="http://uvb.nrel.colostate.edu/uvb">http://uvb.nrel.colostate.edu/uvb</a>	USDA
<a href="http://www.niwa.cri.nz/lauder">http://www.niwa.cri.nz/lauder</a>	NIWA, New Zealand
<a href="http://www.noaa.gov/uvb/fctsh.html">http://www.noaa.gov/uvb/fctsh.html</a>	NOAA UV index
<a href="http://www.epa.gov/ozone/uvindex/uvcalc.html">http://www.epa.gov/ozone/uvindex/uvcalc.html</a>	NOAA UV index
<a href="http://www.atdd.noaa.gov/isis/isis_frame.htm">http://www.atdd.noaa.gov/isis/isis_frame.htm</a>	NOAA
<a href="http://www.epa.gov/ozone/othlinks.html#uvindex">http://www.epa.gov/ozone/othlinks.html#uvindex</a>	U.S. EPA
<a href="http://sedac.ciesin.org/ozone">http://sedac.ciesin.org/ozone</a>	CIESIN UV and Ozone
<a href="http://wwwsolar.nrl.navy.mil/susim_atlas_data.html">http://wwwsolar.nrl.navy.mil/susim_atlas_data.html</a>	Solar Radiation: SUSIM
<a href="http://maia.colorado.edu/solstice">http://maia.colorado.edu/solstice</a>	Solar Radiation: SOLSTICE
<a href="http://www-uars.gsfc.nasa.gov/cdrom_main.html">http://www-uars.gsfc.nasa.gov/cdrom_main.html</a>	Solar Radiation: SOLSTICE
<a href="http://wrdc-mgo.nrel.gov">http://wrdc-mgo.nrel.gov</a>	World Radiation Centre
<a href="http://www.ozone.fmi.fi/SUVDAMA/kuvaus.html">http://www.ozone.fmi.fi/SUVDAMA/kuvaus.html</a>	SUVDAMA Project
<a href="http://www.itek.norut.no/~olae/fastrt">http://www.itek.norut.no/~olae/fastrt</a>	UV Exposure Calculations
<a href="http://www.tor.ec.gc.ca/woudc">http://www.tor.ec.gc.ca/woudc</a>	WOUDC Canada
<a href="http://jwocky.gsfc.nasa.gov">http://jwocky.gsfc.nasa.gov</a>	TOMS Homepage
<a href="http://www.ozone.fmi.fi/">http://www.ozone.fmi.fi/</a>	Finnish Meteorological Institute

### Internet Sites with UV Index Information

---

<a href="http://www.bom.gov.au/bmrc/medr/uvi.html">http://www.bom.gov.au/bmrc/medr/uvi.html</a>	Australia	(UV index)
<a href="http://www.smhi.se/uvindex/en/uvprog.htm">http://www.smhi.se/uvindex/en/uvprog.htm</a>	Sweden	(UV index)
<a href="http://nic.fb4.noaa.gov/products/stratosphere/uv_index">http://nic.fb4.noaa.gov/products/stratosphere/uv_index</a>	United States	(UV index)
<a href="http://www.ec.gc.ca/ozone/tocuvyou.htm">http://www.ec.gc.ca/ozone/tocuvyou.htm</a>	Canada	(UV index)
<a href="http://www.ozone.fmi.fi/o3group/o3home.html">http://www.ozone.fmi.fi/o3group/o3home.html</a>	Finland	(UV index)
<a href="http://www.niwa.cri.nz/lauder">http://www.niwa.cri.nz/lauder</a>	New Zealand	(UV index)
<a href="http://www-med-physik.vu-wien.ac.at/uv/uv_home.htm">http://www-med-physik.vu-wien.ac.at/uv/uv_home.htm</a>	Austria	(UV index)
<a href="http://www.chmi.cz/meteo/ozon/hk.html">http://www.chmi.cz/meteo/ozon/hk.html</a>	Czech Republic	(UV index)

## SURFACE ULTRAVIOLET RADIATION

### Internet Sites with UV Information, by Country

---

Argentina	<a href="http://www.conae.gov.ar/caratula.html">http://www.conae.gov.ar/caratula.html</a>
Australia	<a href="http://www.bom.gov.au/info/about_uv.html">http://www.bom.gov.au/info/about_uv.html</a>
Austria	<a href="http://www-med-physik.vu-wien.ac.at/uv/uv_online.htm">http://www-med-physik.vu-wien.ac.at/uv/uv_online.htm</a>
Belgium	<a href="http://www.meteo.oma.be">http://www.meteo.oma.be</a>
Canada	<a href="http://www.ec.gc.ca/ozone/tocuvyou.htm">http://www.ec.gc.ca/ozone/tocuvyou.htm</a>
Czech Republic	<a href="http://www.chmi.cz/meteo/ozon/o3uvb.html">http://www.chmi.cz/meteo/ozon/o3uvb.html</a>
Finland	<a href="http://www.ozone.fmi.fi/o3group/o3home.html">http://www.ozone.fmi.fi/o3group/o3home.html</a>
France	<a href="http://www.club-internet.fr/securite-solaire/index.htm">http://www.club-internet.fr/securite-solaire/index.htm</a>
Germany	<a href="http://www.dwd.de/services/gfmm/gfmm_home.html">http://www.dwd.de/services/gfmm/gfmm_home.html</a>
Greece	<a href="http://www.athena.auth.gr/lap/">http://www.athena.auth.gr/lap/</a>
Japan	<a href="http://www.shiseido.co.jp/e/e9708uvi/html">http://www.shiseido.co.jp/e/e9708uvi/html</a>
New Zealand	<a href="http://www.niwa.cri.nz/lauder">http://www.niwa.cri.nz/lauder</a>
Spain	<a href="http://www.infomet.fcr.es">http://www.infomet.fcr.es</a>
	<a href="http://www.solysalud.org/sys/indiceUV/indiceuv.html">http://www.solysalud.org/sys/indiceUV/indiceuv.html</a>
Sweden	<a href="http://www.smhi.se/egmain/index.htm">http://www.smhi.se/egmain/index.htm</a>
Taiwan	<a href="http://www.envi.org.tw/Foundation6/English/">http://www.envi.org.tw/Foundation6/English/</a>
United States	<a href="http://nic.fb4.noaa.gov/products/stratosphere/uv_index/index.html">http://nic.fb4.noaa.gov/products/stratosphere/uv_index/index.html</a>

### Internet Sites for International UV Projects

---

COST-713	<a href="http://159.213.57.69/uvweb/wwwcost.html">http://159.213.57.69/uvweb/wwwcost.html</a>
SUVDAMA	<a href="http://www.ozone.fmi.fi/SUVDAMA/">http://www.ozone.fmi.fi/SUVDAMA/</a>
WMO-WOUDC	<a href="http://www.tor.ec.gc.ca/woudc/woudc.html">http://www.tor.ec.gc.ca/woudc/woudc.html</a>